Technical Report CHL-98-9
April 1998

US Army Corps of Engineers
Waterways Experiment Station

Application of a Two-Dimensional Model of Hydrodynamics to the Lower Approach of the New Kentucky Lock, Tennessee River, Kentucky

Numerical Model Investigation

by Richard L. Stockstill, John E. Hite, Jr.

Prepared for U.S. Army Engineer District, Nashville

The contents of this report are not to be used for advertising, publication, or promotional purposes. Citation of trade names does not constitute an official endorsement or approval of the use of such commercial products.

The findings of this report are not to be construed as an official Department of the Army position, unless so designated by other authorized documents.

PRINTED ON RECYCLED PAPER

Technical Report CHL-98-9
April 1998

Application of a Two-Dimensional Model of Hydrodynamics to the Lower Approach of the New Kentucky Lock, Tennessee River, Kentucky

Numerical Model Investigation

by Richard L. Stockstill, John E. Hite, Jr.

U.S. Army Corps of Engineers
Waterways Experiment Station
3909 Halls Ferry Road
Vicksburg, MS 39180-6199

Final report

Prepared for U.S. Army Engineer District, Nashville
Nashville, TN 37202-1070

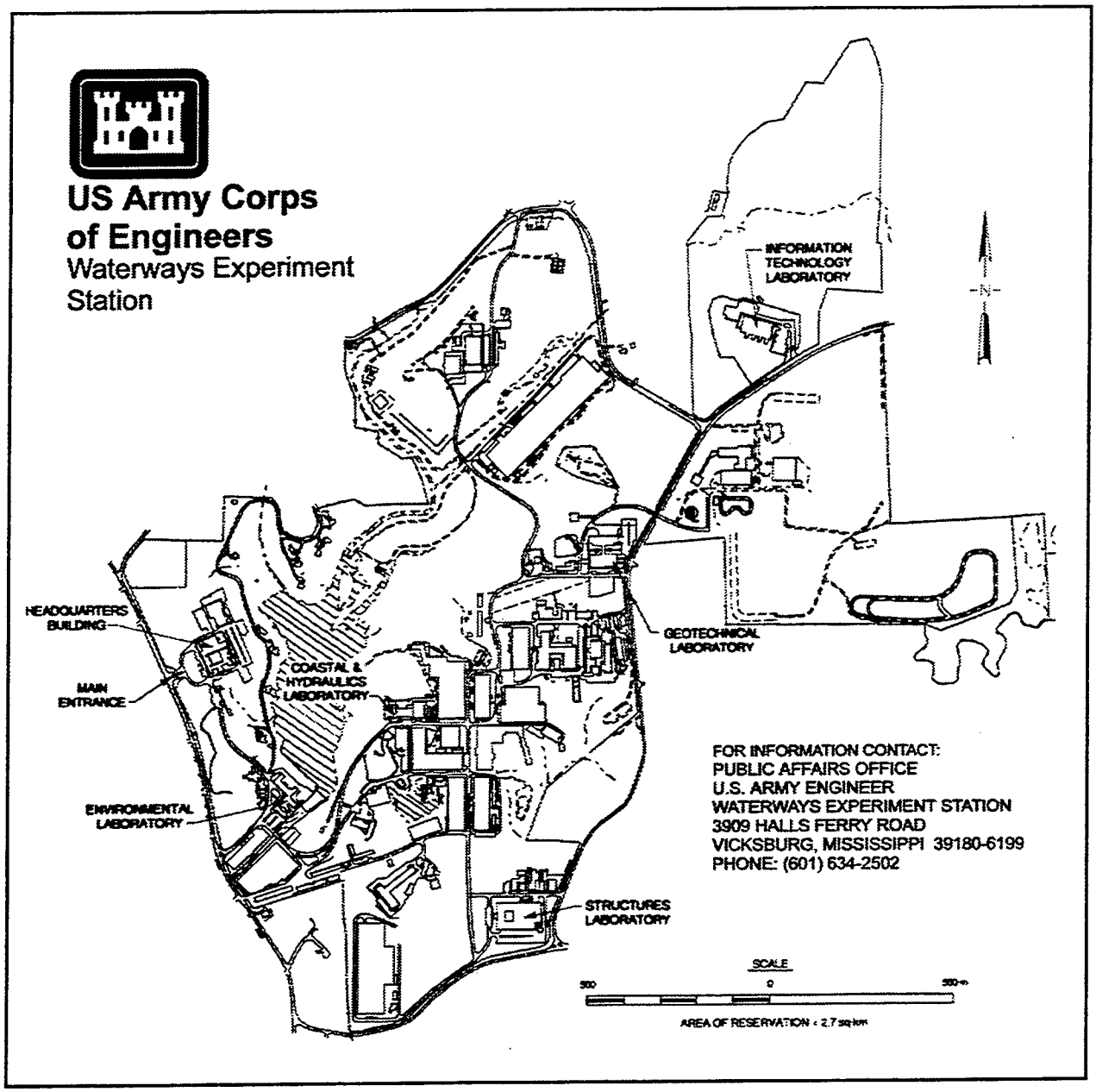

Waterways Experiment Station Cataloging-in-Publication Data

Stockstill, Richard L.

Application of a two-dimensional model of hydrodynamics to the lower approach of the New Kentucky Lock, Tennessee River, Kentucky : numerical model investigation / by Richard L. Stockstill, John E. Hite, Jr. ; prepared for U.S. Army Engineer District, Nashville.

144 p. : ill. ; 28 cm. — (Technical report ; CHL-98-9)

Includes bibliographic references.

1. Finite element method — Evaluation. 2. Locks (Hydraulic engineering) — Kentucky —Models. 3. Tennessee River. 4. Unsteady flow (fluid dynamics) — Evaluation. I. Hite, John E. II. United States. Army. Corps of Engineers. Nashville District. III. U.S. Army Engineer Waterways Experiment Station. IV. Coastal and Hydraulics Laboratory (U.S. Army Engineer Waterways Experiment Station) V. Title. VI. Series: Technical report (U.S. Army Engineer Waterways Experiment Station) ; CHL-98-9.

TA7 W34 no.CHL-98-9

Contents

Preface

The two-dimensional numerical modeling of the flow conditions in the proposed Kentucky Lock was performed for the U.S. Army Engineer District, Nashville (LRN). This study was authorized by the U.S. Army Engineer Division, Great Lakes and Ohio River, on 13 January 1997. Mr. Donald Getty, LRN, directed this study.

This work was conducted in the Coastal and Hydraulics Laboratory (CHL) of the U.S. Army Engineer Waterways Experiment Station (WES) during the period March 1997 to October 1997 under the direction of Dr. J. R. Houston, Director, CHL; Mr. Charles C. Calhoun, Assistant Director, CHL; and Dr. P. G. Combs, Chief, Rivers and Structures Division, CHL.

Extension of the HIVEL2D (two-dimensional hydrodynamic numerical) model was completed by Dr. R. L. Stockstill, Spillways and Channels Branch, Rivers and Structures Division, CHL. Simulation runs and analyses of results were conducted by Dr. J. E. Hite, Jr., Leader of the Locks and Conduits Group, Rivers and Structures Division, and Dr. Stockstill under the supervision of Mr. B. P. Fletcher, Chief, Spillways and Channels Branch. Mr. S. Cornell, Spillways and Channels Branch, also assisted with the simulations and postprocessing of the model results. Dr. R. C. Berger, Estuaries and Hydroscience Division, CHL, provided technical assistance and peer review. The report was written by Drs. Hite and Stockstill.

At the time of publication of this report, Director of WES was Dr. Robert W. Whalin. Commander was COL Robin R. Cababa, CE.

Conversion Factors, Non-SI to SI Units of Measurement

Non-SI units of measurement used in this report can be converted to SI units as follows:

Multiply	By	To Obtain
cubic feet	0.02831685	cubic meters
cubic yards	0.7645549	cubic meters
feet	0.3048	meters
miles (U.S. statute)	1.609347	kilometers
tons (force)	8.896443	kilonewtons

1 Introduction

Background

The existing Kentucky Lock is located on the Tennessee River approximately 20 miles[1] southeast of Paducah, KY (Figure 1). The project consists of a gated spillway to regulate riverflows, a powerhouse for hydroelectric power generation, and a 600-ft-long navigation lock for moving industrial tow traffic and recreational boats through the project. The existing lock is operating at capacity, and an additional 1,200-ft-long by 110-ft-wide lock is projected to be necessary to satisfy future capacity requirements. The new lock will be located landward of the existing lock with the upstream pintles (cross-stream axis of the miter gates) located just over 100 ft downstream from the upstream pintles of the existing lock.

The new lock features a through-the-sill intake that carries flow to a multiport filling and emptying system. One proposed lock discharge plan uses an interlaced lateral system located downstream of the lower miter gate pintle as shown in Figure 2. Another alternative being investigated for the discharge system is a landside channel that discharges downstream of the lower approach guide wall as shown in Figure 3. A final decision on the discharge system will be made after all alternatives are evaluated.

Purpose and Scope

The initial investigation was performed to evaluate the flow conditions in the lower lock approach for different excavation plans in the approach channel with the interlaced lateral discharge system. These flow conditions must be known to determine the effect these flows have on tows in the lower approach area. Adverse flow conditions (large streamwise and cross-stream water-surface gradients) in the lower approach may prohibit tows from mooring in this area during lock discharges. The flow conditions selected for evaluation were a

[1] A table of factors for converting non-SI units of measurement to SI units is found on page vi.

headwater el[1] of 357, a tailwater el of 304.2, and emptying valve opening times of 1.5 min and 11.7 min. This flow is considered the 50 percent duration condition, and the valve speeds represent fast and slow valve operations, respectively.

Two excavation plans were evaluated with the interlaced lateral discharge design: the minimum excavation plan and the moderate excavation plan. The invert elevation of the lower approach channel with the minimum excavation plan was 289, and with the moderate excavation plan was 284.

A subsequent investigation of a landside discharge channel was performed after evaluation of the interlaced lateral discharge system. The U.S. Army Engineer District, Nashville, requested that the U.S. Army Engineer Waterways Experiment Station (WES) evaluate the flow conditions in the lower lock approach with a headwater el of 359 and tailwater el of 302 and 314 with an emptying valve operation of 1.5 min. Also, flow conditions were evaluated with a headwater el of 359, a tailwater el of 302, and an emptying valve operation of 6 min.

The landside and interlaced lateral discharge alternatives were evaluated by comparing water-surface differentials at selected locations. The hawser forces a tow and barge arrangement will experience are directly related to the water-surface slope on which the vessel rests. The particular locations for the interlaced lateral discharge alternative were near the bow and stern of a 3 × 3 barge arrangement and a 3 × 5 barge arrangement both having their upstream end moored at sta 17+00. Flow conditions resulting from the landside discharge alternative were also evaluated at sta 15+00 and 27+00, which would be representative of a 3 × 6 barge arrangement with the upstream end moored at sta 15+00.

Approach

The two-dimensional (2D), depth-averaged flow model, HIVEL2D, was used to model the unsteady velocities and water-surface elevations in the lower lock approach resulting from lock emptying operations. The HIVEL2D model was chosen for this study because it is designed to provide numerically stable solutions for advection-dominated flow containing large gradients in the flow variables. Large gradients in depths and velocities are present in the vicinity of lock outlets during emptying operations. The flow conditions in these areas can vary from no flow to peak discharges of about 22,000 cfs in less than 2 min. The HIVEL2D code was modified to allow specification of time-dependent inflow boundary conditions.

A plan view of the geometry and topography in the lower lock approach with the interlaced lateral discharge alternative and the minimum excavation plan is

[1] All elevations (el) and stages cited herein are in feet referred to the National Geodetic Vertical Datum (NGVD).

shown in Figure 4. The mesh used for the hydrodynamic computations with the initial simulations is shown in Figure 5. The computational mesh used for the simulations with the landside discharge channel is shown in Figure 6.

2 Description of Model

Governing Equations

Fluid motion is modeled using the 2D unsteady shallow-water equations. The shallow-water (or long-wave) equations are a result of the vertical integration of the equations of mass and momentum conservation for incompressible flow under the hydrostatic pressure assumption. This assumption implies that vertical accelerations are negligible compared with the horizontal accelerations and the acceleration due to gravity. The vertical accelerations are small when the characteristic wavelength is long relative to the depth, which is why these equations are referred to as long-wave or shallow-water equations.

The dependent variables of the fluid motion are defined by the flow depth h, the x-direction component of unit discharge p, and the y-direction component of unit discharge q. These variables are functions of the independent variables x and y, the two space directions, and time t. If the free-surface stresses are neglected, the shallow-water equations are given as (Abbott 1979):

$$\frac{\partial \boldsymbol{U}}{\partial t} + \frac{\partial \boldsymbol{F}}{\partial x} + \frac{\partial \boldsymbol{G}}{\partial y} + \boldsymbol{H} = \boldsymbol{0} \tag{1}$$

where

$$\boldsymbol{U} = \begin{Bmatrix} h \\ p \\ q \end{Bmatrix} \tag{2}$$

$$\boldsymbol{F} = \begin{Bmatrix} p \\ \frac{p^2}{h} + \frac{1}{2}gh^2 - h\frac{\sigma_{xx}}{\rho} \\ \frac{pq}{h} - h\frac{\sigma_{yx}}{\rho} \end{Bmatrix} \tag{3}$$

$$G = \begin{Bmatrix} q \\ \frac{pq}{h} - h\frac{\sigma_{xy}}{\rho} \\ \frac{q^2}{h} + \frac{1}{2}gh^2 - h\frac{\sigma_{yy}}{\rho} \end{Bmatrix} \quad (4)$$

and

$$H = \begin{Bmatrix} 0 \\ gh\frac{\partial z_0}{\partial x} + n^2 g\frac{p\sqrt{p^2+q^2}}{C_0 h^{7/3}} \\ gh\frac{\partial z_0}{\partial y} + n^2 g\frac{q\sqrt{p^2+q^2}}{C_0 h^{7/3}} \end{Bmatrix} \quad (5)$$

where

g = acceleration due to gravity

ρ = fluid density

z_0 = channel bed elevation

n = Manning's roughness coefficient

C_0 = dimensional constant ($C_0 = 1$ for SI units and 2.208 for non-SI units)

$\sigma_{xx}, \sigma_{xy}, \sigma_{yx}, \sigma_{yy}$ = Reynolds stresses due to turbulence where the first subscript indicates the direction and the second indicates the face on which the stress acts

The Reynolds stresses are determined using the Boussinesq approach relating stress to the gradient in the mean currents:

$$\sigma_{xx} = 2\rho\nu_t\left(\frac{\partial u}{\partial x}\right) \quad (6)$$

$$\sigma_{yy} = 2\rho\nu_t\left(\frac{\partial v}{\partial y}\right) \quad (7)$$

and

$$\sigma_{xy} = \sigma_{yx} = \rho \nu_t \left(\frac{\partial u}{\partial y} + \frac{\partial v}{\partial x} \right) \tag{8}$$

where

ν_t = kinematic eddy viscosity, which varies spatially

$u = p/h$, the depth-averaged x-direction component of velocity

$v = q/h$, the depth-averaged y-direction component of velocity

Values of the eddy viscosity are determined empirically as a function of the local flow variables as (Rodi 1980; Chapman and Kuo 1985):

$$\nu_t = n \sqrt{8g} \frac{C}{C_0} h^{5/6} |V| \tag{9}$$

where

C = coefficient that varies between 0.1 and 1.0

$|V|$ = velocity vector magnitude = $(u^2 + v^2)^{1/2}$

Extensions to Include Unsteady Inflow

HIVEL2D version 1.07 (Stockstill and Berger 1994) was designed to serve as a tool to provide steady-state solutions of flow fields. Modeling flow conditions in the lower lock approach during lock emptying required the ability to simulate the time-dependent flow rates that represent the lock emptying hydrograph in the computational model. The time-dependent discharge from the interlaced laterals was the inflow used to drive the hydrodynamic model. Two methods were used to simulate the lock discharge. In the first method, the total discharge was applied as flux through an inflow boundary located just downstream of the discharge laterals. This meant that values of p and q at this inflow boundary were specified as functions of time. Since significant vertical accelerations are generated in the real system in the vicinity of the discharge laterals, there was concern that the horizontal momentum resulting from these specified boundary conditions was unrealistic. Therefore, a second method was developed to simulate the lock discharge.

In this method the mass flow rate resulting from the lateral discharge outlet area was specified as a point source of mass. The conservation of mass equation (first row vector in Equation 1) was extended to include a change in mass term on the right-hand side.

$$\frac{\partial h}{\partial t} + \frac{\partial p}{\partial x} + \frac{\partial q}{\partial y} = i \tag{10}$$

where i is a time-dependent scalar value having units of length per time. Values of i are determined such that

$$\int_{A_l} i(t)\, dA_l = Q(t) \tag{11}$$

where

$i(t)$ = time dependent source term

A_l = plan area of the interlaced lateral structure

$Q(t)$ = lock discharge from the emptying hydrograph

This method of representing the discharge hydrograph was considered an improvement over the first method because it did not impose horizontal momentum at the inflow boundary. Numerical model results revealed insignificant differences in the flow variables two computational elements away from the discharge laterals. Peak water-surface elevations computed with the point source method slightly lagged in time behind the peaks computed when horizontal momentum was applied at the inflow boundary. The two methods of mass input provided essentially the same results at locations away from the discharge laterals. The point source method better represented the real system since no horizontal momentum was assumed and currents were generated by the water-surface gradients across the area representing the discharge laterals and the remaining flow field.

Discretization

Because there are no general solutions of the continuous functions in the governing equations, they must be solved by numerical methods. Discrete values of the unknown variables are solved using a Petrov-Galerkin finite element representation of the equations. Details of the finite element formulation are presented in Stockstill and Berger (1994).

A finite difference expression is used for the temporal derivatives. The general expression for the temporal derivative of the unknowns, U_j, is:

$$\frac{\partial U_j}{\partial t} = \frac{\alpha}{\Delta t}\left(U_j^{k+1} - U_j^{k}\right) + \frac{(1-\alpha)}{\Delta t}\left(U_j^{k} - U_j^{k-1}\right) \tag{12}$$

where

α = temporal differencing weight

Δt = time-step size

j = node location

k = time-step

An α value of 1 results in a first-order backward differencing, and an α of 1.5 results in a second-order backward differencing approximation of the temporal derivative.

3 Model Applications

Application of the modified HIVEL2D model to the proposed lower approach required the construction of a numerical model computational mesh to represent the design geometry and the specification of boundary conditions and model parameters.

Geometry and Computational Mesh

Interlaced lateral discharge alternative computational mesh

Initially, the lower approach length to the new lock was modeled from the upstream end of the interlaced laterals (approximately sta 14+50) to 130 ft downstream from the end of the proposed guide wall (sta 31+00). The entire width of the lower approach was modeled down to sta 25+50; and from sta 25+50 to 31+00, a 700-ft width of the lower approach was modeled. Figure 4 shows details of the geometry of the lower lock approach. This initial mesh had 564 nodes and 609 elements. Grid resolution was more refined at alignment and grade changes.

Examination of model results with the initial mesh led to the conclusion that the downstream boundary condition had significant influence on the velocity distribution on the left bank at the downstream end of the approach channel. Therefore, the model limits were extended significantly to prevent the outflow boundary conditions from influencing the flow patterns at the end of the approach channel. The larger mesh, shown in Figure 5, included a 4,400-ft length of the Tennessee River. The entire width of the river was represented from the tailrace of the powerhouse and spillway to 4,700 ft downstream from the outlet. This mesh had 1012 nodes and 1529 elements. Resolution was increased where large gradients of the flow variables were expected.

Landside discharge channel alternative computational mesh

This alternative required a large computational domain so that the flow patterns were properly modeled near the vicinity of the discharge channel outlet.

This computational mesh had 1140 nodes and 1851 elements and was finely resolved at the discharge channel outlet to the river as shown in Figure 6.

Boundary Conditions

Interlaced lateral alternative boundary conditions

This study included simulation of two discharge hydrographs furnished by the Nashville District that represented emptying valve openings of 1.5 min and 11.7 min. The hydrographs for these valve operations are shown in Figure 7. Tables 1 and 2 provide the discharge and time data for these hydrographs.

Landside discharge channel alternative boundary conditions

Inflow boundary conditions for this study were time-histories of the flow rate at sta 26+20 of the landside discharge channel. The two hydrographs shown in Figure 8 represented an emptying valve time of 1.5 min with a headwater el of 359 and tailwater el of 302 and 314. Tables 3 and 4 provide the discharge and time data for these hydrographs. The third condition evaluated with the landside discharge channel alternative was a headwater el of 359, a tailwater el of 302, and a 6-min emptying valve. The hydrograph for these conditions is shown in Figure 9, and the discharge and time data are provided in Table 5. As with the interlaced lateral design, the hydrographs used as inflow boundary conditions for the landside discharge channel were furnished by the Nashville District.

Model Parameters

Model and flow parameters used in the simulations are provided in the following tabulation.

Model Condition	Value
α	1.25
β	0.25
C_o	2.208
C	0.5
n	0.02
g	32.2 ft/sec^2

Here, β, which can range in value from 0.0 to 0.5, is a weighting term used in the test function of the finite element formulation of the governing equations. Details of the model's finite element formulation are provided in Stockstill and

Berger (1994). β can be thought of as an upwinding parameter that provides the numerical stability needed for modeling advection-dominated flows that may have shocks such as hydraulic jumps. Actually, HIVEL2D allows the input of two values of β (Berger, Stockstill, and Ott 1995). Small values (i.e., 0.1 to 0.2) are more precise and have been successfully applied to regions of the flow field having smooth solutions. Therefore, the larger value (i.e., 0.5) is automatically applied only to the domain's roughest regions, which are generally shocks such as hydraulic jumps (Berger and Stockstill 1995; Stockstill, Berger, and Nece 1997). The computed flow field was not expected to contain any hydraulic jumps; therefore only one value of β was used, which was chosen as an average of values used for smooth and rough solutions.

Berger (1993), while investigating the modeling of dam breaks, found that a value of 1.25 for the temporal derivative weighting coefficient, α, provides accurate timing of problems involving rapidly varying flow. Choice of the turbulent eddy viscosity coefficient, C, was simply an average of the range over which this coefficient has been known to vary (0.1 to 1.0) . Solutions are relatively insensitive to the selection of this parameter since the Boussinesq stresses describe momentum dispersion, which has insignificant effects on the computed flow depths. Likewise the Manning coefficient n of 0.02 probably describes a channel that is slightly smoother than the rock-cut channel proposed for the Kentucky Lock, but water-surface differentials within the channel generated by the rapidly varying flow issuing from the lock outlets are dominated by wave characteristics and not bed drag.

4 Results

The flow conditions in the lower approach were evaluated by comparing the water-surface elevations at two selected locations. For example, with the interlaced lateral discharge alternative, the upstream location was 147.5 ft downstream from the downstream end of the interlaced lateral (sta 17+00) and 55 ft out from the guide wall (Figure 4). One of the downstream locations was 600 ft from the upstream location (sta 23+00) and also 55 ft out from the guide wall. In this example, these water surfaces would represent the water-surface slope in the lower approach to which a 3 × 3 barge arrangement moored 142.5 ft downstream from the interlaced laterals would be exposed. A tow and barges moored in this area and exposed to extreme water-surface slopes and high-velocity flows will experience large hawser forces.

Interlaced Lateral Discharge Alternative

Simulations with both excavation plans were conducted using a time-step of 4 sec. The total time modeled for each of the valve schedules was that given by the lock discharge hydrographs that served as inflow boundary conditions. Longer simulation times were not run because inflow boundary conditions were unknown beyond the times given by the hydrographs.

Minimum excavation plan

1.5-min valve, sta 17+00 and sta 23+00. The initial simulation was performed with the minimum excavation plan, headwater el of 357, tailwater el of 304.2, and an emptying valve opening time of 1.5 min. These headwater and tailwater conditions were performed for all simulations with the interlaced lateral discharge alternative. In future descriptions of flows with the interlaced laterals these conditions are assumed. A time-history of the water-surface elevation at sta 17+00 is shown in Figure 10. The maximum water surface was 305.7 (which was 1.5 ft higher than the tailwater) and occurred 112 sec after the valve began opening. The minimum water-surface elevation at sta 17+00, 55 ft out from the guide wall, was 302.7 and occurred 8.8 min after the emptying valve began opening.

The water-surface elevations increased in the lower approach as the positive wave produced by the lock discharge traveled downstream. For this discussion, "positive" was used to designate a wave surface higher than the initial steady-state surface. If the wave surface was lower than the steady-state surface, the wave was described as negative. A wave reflected at the upstream end (lock miter gates) by doubling in magnitude when it intercepted the wall. When a wave reached the abrupt expansion in the lower approach, it was "pinned" in height and therefore reflected as a negative wave. This produced a standing wave (the entire approach length rocked up and down in phase). The seiche frequency was determined by the geometry of the approach and the depth. Several projects (e.g., Shows and Franco 1981 and Oswalt, Ables, and Murphy 1972) experience oscillations within approach canals when the lock intakes or outlets are located in or near the channel.

A time-history of the water-surface elevation at the downstream location (sta 23+00, 55 ft out from the guide wall) is also shown in Figure 10. The maximum water surface is slightly lower (305.3) than that observed at sta 17+00 and the minimum water-surface elevation is slightly higher (303.3). A time-history of the water-surface differential between sta 17+00 and sta 23+00, 55 ft from the guide wall, is shown in Figure 11. The downstream differential (which is considered a positive water-surface slope) results from water surfaces at sta 17+00 being higher than those at sta 23+00 at the same time, and the upstream differential (a negative water-surface slope) results from water surfaces at sta 17+00 being lower than those at sta 23+00 at the same time. A positive water-surface slope would move an unmoored tow and barges downstream, and a negative water-surface slope would result in an upstream drift of a tow and barges. The maximum positive slope was 0.63 ft in 600 ft, and the maximum negative slope was 0.74 ft in 600 ft. Neglecting the forces due to drag and inertia, assuming that the barge train acts as a single rigid vessel, and neglecting the effect of the vessel blockage area of the approach channel, the force required to hold a vessel in place is a function of only the water-surface slope. Using standard barge dimensions of 195 ft by 35 ft, the longitudinal hawser force computed for a 3 × 3 barge arrangement with a 9-ft draft and a water-surface slope of -0.74 ft in 600 ft is 21.3 tons. Due to the negative slope, a tow and barge arrangement would tend to move toward the downstream miter gates. Realizing that these assumptions are not entirely correct, one can still obtain a relative sense of forces in the lower lock approach due to water-surface slopes.

A plan view of velocity vectors and water-surface contours is shown in Figure 12. These are the flow conditions that occur 92, 180, and 360 sec after the emptying valve began opening. The highest velocity computed for sta 17+00, 55 ft from the guide wall, occurred at 204 sec and was 5 ft/sec.

1.5-min valve, sta 17+00 and 27+00. Additional time-histories were plotted to evaluate the water-surface slopes between sta 17+00 and 27+00. These conditions are applicable to a 3 × 5 barge arrangement in the lower approach. The maximum water-surface differential was found to be -1.19 ft (Figure 11), which would result in a longitudinal hawser force of 34.2 tons directed toward the miter gates, for the assumptions previously mentioned.

11.7-min valve, sta 17+00 and 23+00. The next simulation was performed with minimum excavation and the slower, 11.7-min valve opening. Time-histories of water-surface elevation with the 11.7-min valve at sta 17+00 and 23+00, 55 ft from the guide wall, are shown in Figure 10. The maximum water-surface elevation was 304.6 and the minimum water-surface elevation was 303.8 at sta 17+00 as shown in Figure 10. The water-surface elevations at sta 23+00 are very similar to those at sta 17+00 as Figure 10 illustrates. These results indicate that with the slower valve opening, the water surface in the lower approach varies only slightly from the tailwater elevation. The maximum water-surface differential with the long valve time (11.7 min) was 0.10 ft as shown in Figure 11. If this differential is converted to a longitudinal hawser force as described previously, the computed hawser force for a 3 × 3 barge arrangement with the upstream end moored at sta 17+00 is 2.9 tons. Flow conditions in the lower lock approach were improved with the slower valve speed; however, lock emptying times will increase with the slower valve.

11.7-min valve, sta 17+00 and 27+00. Additional time-histories were obtained with the 11.7-min valve speed to evaluate the water-surface slopes between sta 17+00 and 27+00. The maximum water-surface differential was found to be -0.16 ft (Figure 11), which would result in a longitudinal hawser force of 4.6 tons with the assumptions stated previously.

Comparison of results with minimum excavation. A comparison of the water-surface differentials at sta 17+00 and 23+00, 55 ft from the guide wall, between the 1.5- and 11.7-min valve times is shown in Figure 11. The results clearly indicate that a slower valve time causes much less water-surface slope in the lower approach channel and would be more favorable for tows and barges trying to moor in this area. This is also apparent when comparing the results between sta 17+00 and 27+00 shown in Figure 11.

Moderate excavation plan

1.5-min valve, sta 17+00 and 23+00. The next simulation was performed with the moderate excavation plan and a 1.5-min opening schedule for the emptying valves. The moderate excavation plan, shown in Figure 13, consisted of excavating approximately 57,000 yd^3 in an area 1,500 ft long by 200 ft wide beginning just downstream from the interlaced laterals. The bed elevation in this area was generally 5 ft lower than that of the minimum excavation plan.

Time-histories of the water-surface elevations at sta 17+00 and 23+00 with the 1.5-min valve and the moderate excavation plan are shown in Figure 14. The maximum water-surface at sta 17+00 occurred 104 sec after the valve began opening and reached el 305.6, which is 1.4 ft higher than the tailwater. The minimum water-surface elevation at sta 17+00 was 302.9 and occurred approximately 8 min after the emptying valve began opening. The water-surface differential between these stations is shown in Figure 15. The maximum positive slope was 0.56 ft in 600 ft, and the maximum negative slope was 0.59 ft in 600 ft.

A negative slope of 0.59 ft in 600 ft converted to a hawser force as previously described gives an upstream longitudinal hawser force of 17.0 tons for a 3 × 3 barge arrangement with the upstream end moored at sta 17+00. This is only a slight reduction from the force of 21.3 tons computed for the 1.5-min valve and minimum excavation plan.

Velocity vectors and water-surface contours computed for the moderate excavation plan and a 1.5-min valve speed at 92, 180, and 360 sec after the valve began opening are shown in Figure 16. Velocities of up to 5 ft/sec were observed in the lower approach channel, but this magnitude of velocity was not as widespread as with the minimum excavation plan. Higher velocities (≥5 ft/sec) occurred in the vicinity of shallower depths, the left half (looking downstream) of the lower approach channel between sta 22+00 and 26+00. Here, the bed elevation was the same as with the minimum excavation plan.

1.5-min valve, sta 17+00 and 27+00. Additional time-histories were also plotted with the 1.5-min valve speed to evaluate the water-surface slopes between sta 17+00 and 27+00 with the moderate excavation plan. The maximum water-surface differential was found to be -0.99 ft (Figure 15), which would result in an upstream longitudinal hawser force of 28.5 tons with the assumptions stated previously.

11.7-min valve, sta 17+00 and 23+00. Time-histories of the water-surface elevations at sta 17+00 and 23+00 with the moderate excavation plan and the 11.7-min valve are shown in Figure 14. The water surface varied only slightly from the tailwater elevation, and the maximum positive and negative water-surface slopes shown in Figure 15 were 0.09 and 0.08 ft, respectively. These slopes were slightly less than those with the minimum excavation plan and slow valve and would result in low hawser forces. A positive slope of 0.09 ft in 600 ft would result in a downstream longitudinal hawser force of 2.6 tons.

11.7-min valve, sta 17+00 and 27+00. Time-histories of the water surface were also obtained with the 11.7-min valve speed with the moderate excavation plan. In particular, the water-surface slopes between sta 17+00 and 27+00 were examined. The maximum water-surface differential was found to be -0.14 ft (Figure 15), which would result in an upstream longitudinal hawser force of 4.0 tons with the assumptions stated previously.

Comparison of results with moderate excavation. Comparisons of the results with 1.5- and 11.7-min valve times given the moderate excavation plan are also shown in Figure 15. The faster valve speed (1.5 min) produced much larger water-surface slopes than the slower (11.7 min) valve, and these higher slopes would cause higher hawser forces for a tow and barges moored in the lower lock approach. The flow conditions in the lower approach were favorable with the 11.7-min valve, but slower emptying times would result from the slower valve.

Comparison of minimum and moderate excavation plans

A comparison of Figures 11 and 15 shows the difference between the water-surface differentials for the minimum and moderate excavation plans for the 1.5-min valve. The maximum positive and negative differentials are reduced slightly with the moderate excavation plan and result from the larger depths with this plan. However, this reduction is not enough to significantly reduce the hawser forces for a tow moored in the lower approach. A very slight reduction in the maximum and minimum water-surface differentials was also observed with the 11.7-min valve and moderate excavation plan as seen by comparing Figures 11 and 15. The water-surface differentials observed for the minimum and moderate excavation plans with the 11.7-min valve were essentially the same. Results from these simulations are provided in Table 6.

Landside Discharge Channel Alternative

The Nashville District requested that WES evaluate flow conditions in the lower lock approach with a landside channel that discharged the lock flow at the end of the landside guide wall. A plan view of the landside discharge channel is shown in Figure 3. The following flow conditions were evaluated for this discharge alternative:

Headwater El	Tailwater El	Valve Time, min
359	302	1.5
359	314	1.5
359	302	6.0

The discharge hydrographs for these emptying conditions at sta 26+20 in the landside channel were furnished by the Nashville District and are shown in Figures 8 and 9.

Simulations were made using 3-sec time-steps. As with the lateral discharge design, the total simulation times were limited by the total time provided on the inflow hydrographs. The computational mesh used for all simulations with the landside discharge alternative is shown in Figure 6. The mesh represented approximately one mile of topography downstream from the proposed lock and a 1,600-ft width of the river at the discharge outlet. Downstream from the discharge outlet, the mesh represented approximately a 1,250-ft width of the river.

Headwater el 359, tailwater el 302, 1.5-min valve, sta 17+00 and 23+00

The first simulation with the landside discharge channel alternative was performed with headwater el 359, tailwater el 302, and a 1.5-min emptying valve operation. Water-surface elevations in the lower lock approach were compared to evaluate the water-surface slopes. The locations chosen were similar to those locations used in the evaluation of the flow conditions with the interlaced lateral discharge system. The upstream location is at sta 17+00, the downstream location is at sta 23+00, and both are 55 ft out from the landside guide wall. The minimum excavation plan was used for the topography in the lower lock approach. Time-histories of the water-surface elevations at sta 17+00 and 23+00 are shown in Figure 17. The water-surface differential between these stations, shown in Figure 18, represents the water-surface slope between the two locations. The maximum differential occurred 160 sec after the hydrograph began and was 0.69 ft. A positive differential means the upstream water surface is higher than the downstream water surface, and a negative differential indicates the downstream water surface is higher. If one neglects the forces due to drag and assumes that the force on the barges results entirely from the water-surface slope, the longitudinal hawser force computed for a 3 × 3 barge arrangement with a 9-ft draft and a water-surface slope of 0.69 ft in 600 ft is 20.1 tons. The longitudinal hawser force computed for the minimum excavation plan, headwater el 357, tailwater el 304.2, and a 1.5-min valve operation with the interlaced lateral discharge alternative was 21.3 tons.

Velocity vectors and water-surface contours at 90, 180, and 360 sec after the valve began opening are shown in Figure 19. Large eddies in the river are formed by the high-velocity flow discharging into the river as shown in Figure 19b. Large water-surface gradients also occurring in the vicinity of these eddies are not a desirable hydraulic feature. Swirling high-velocity flow in the river could be a safety hazard for small craft as well as cause navigation difficulties for larger tows.

Headwater el 359, tailwater el 302, 1.5-min valve, sta 15+00 and 27+00

Flow conditions in the lower lock approach were also evaluated at sta 15+00 and 27+00 to determine the longitudinal water-surface slopes that a 3 × 6 barge arrangement would experience with the upstream end at sta 15+00. Time-histories of the water-surface elevations at these stations with headwater el 359, tailwater el 302, and a 1.5-min emptying valve are shown in Figure 20. A time-history of the water-surface differential between these stations is shown in Figure 21. The maximum water-surface differential was 1.32 ft and occurred 2.3 min after the valve began to open. For the assumptions already stated, this slope results in a downstream longitudinal hawser force of 37.9 tons.

Headwater el 359, tailwater el 314, 1.5-min valve, sta 17+00 and 23+00

The next simulation was performed with headwater el 359, tailwater el 314, and a 1.5-min valve operation. Time-histories of the water-surface elevations at the upstream and downstream stations with these conditions are shown in Figure 17. The maximum water-surface differential was 0.37 ft (Figure 18) and occurred 2.6 min after the emptying valve began to open. A water-surface slope of 0.37 ft per 600 ft for a 3 × 3 barge arrangement drafted to 9 ft with the assumptions stated gives a hawser force of 10.6 tons. This is almost one-half the force determined with tailwater el 302. Greater depths associated with a higher tailwater change the characteristics of the lower lock approach channel. These increased depths result in faster wave celerity $(gh)^{1/2}$ and shorter periods of water-surface oscillations within the channel. Although the magnitude of the oscillations did not differ significantly from those of a 1.5-min valve time and tailwater el 302 (Figure 17), the differentials between the stations within the channel were considerably less. The water-surface differential between the upstream and downstream stations and consequently the hawser forces are less.

Headwater el 359, tailwater el 314, 1.5-min valve, sta 15+00 and 27+00

Time-histories of the water-surface elevations at sta 15+00 and 27+00 with headwater el 359, tailwater el 314, and a 1.5-min emptying valve are shown in Figure 20. A time-history of the water-surface differential between these stations is shown in Figure 21. The maximum water-surface differential occurred 2.6 min after the valve began to open. This differential of 0.88 ft results in a downstream longitudinal hawser force of 25.3 tons using the assumptions mentioned previously.

Headwater el 359, tailwater el 302, 6.0-min valve, sta 17+00 and 23+00

A simulation was performed next with headwater el 359, tailwater el 302, and a 6-min emptying valve operation. The time-histories of water-surface elevation at sta 17+00 and 23+00 are shown in Figure 22. The water-surface differential between the stations is shown in Figure 18. The maximum water-surface differential was -0.11 ft and occurred at 11.3 min during the emptying cycle. This differential gives a hawser force of 2.6 tons. The negative differential indicates the downstream water surface was higher than the upstream water surface.

Headwater el 359, tailwater el 302, 6.0-min valve, sta 15+00 and 27+00

Time-histories of the water-surface elevations at sta 15+00 and 27+00 with headwater el 359, tailwater el 302, and a 6-min emptying valve are shown in Figure 23. The water-surface differential between these stations is plotted as a function of time in Figure 21. The maximum water-surface differential was 0.22 ft and occurred 3.6 min after the valve began to open. For the assumptions already stated, this slope results in a downstream longitudinal hawser force of 6.3 tons.

Comparison of landside discharge channel alternative results

The results from the three simulations are summarized in Table 7. These results indicate that the slower valve speed has a significant influence on the water-surface slopes in the lower lock approach as one would expect. The hawser forces computed based on longitudinal water-surface slope were reduced by almost an order of magnitude by slowing the valve opening time from 1.5 min to 6.0 min. The hawser forces were also reduced significantly with a 12-ft higher tailwater for the 1.5-min emptying valve operation. It is interesting to note that even though the landside channel discharges downstream from a tow moored along the landside guide wall, for five of the six simulations, the longitudinal hawser forces are in the downstream direction. This is a result of the water-surface oscillations caused by the long-period gravity wave generated from the lock discharging into the river. Maximum oscillations are present at the vertical barrier of the lock lower miter gates.

Because the maximum drawdown at the lower miter gates occurs relatively early in the emptying cycle, there should still be positive head on the miter gates. However, conditions of reverse head on the miter gates are possible if the oscillations remain after the lock chamber has emptied. Successful design of the miter gate mechanical components depends on accurate determinations of the pressures on the miter gates.

5 Summary and Conclusions

Two-dimensional (depth-averaged) simulations of the flow conditions in the lower lock approach for the proposed 1,200-ft lock at Kentucky Lock, Tennessee River, were performed to evaluate the interlaced lateral and landside channel discharge alternatives. Two bed configurations were evaluated with the interlaced lateral discharge alternative to determine the benefits of increased excavation in the lower approach channel. The simulations with the interlaced lateral discharge system were conducted for headwater el 357, tailwater el 304.2, and emptying valve opening times of 1.5 and 11.7 min. This headwater and tailwater combination represents the 50 percent duration conditions, and the valve times represent fast and slow valve operations. The simulations with the landside discharge channel were conducted with headwater el 359, tailwater el 302 and 314, and a 1.5-min emptying valve operation. An emptying valve opening time of 6 min was also simulated with headwater el 359 and tailwater el 302.

The flow conditions in the lower approach were evaluated by comparing water-surface differentials at selected locations. These locations were in the vicinity of the bow and stern of a 3 × 3 barge arrangement moored with the upstream end at sta 17+00 and a 3 × 5 barge arrangement with the upstream end moored at sta 17+00 for the interlaced lateral discharge alternative. With the landside discharge alternative, flow conditions were also evaluated at sta 15+00 and 27+00, which would be representative of a 3 × 6 barge arrangement with the upstream end moored at sta 15+00. The water-surface slope between the two stations is considered to be a major contributor to the hawser force the barges moored in this area would experience during lock emptying. In this type of analysis, the hawser forces the tow and barge arrangement will experience are directly related to the water-surface slope on which the vessel rests.

The simulation results with the interlaced lateral discharge system indicate that with the minimum excavation plan and the fast (1.5 min) valve, large longitudinal water-surface slopes exist in the lower approach. A 3 × 3 barge arrangement with the upstream end moored at sta 17+00 would experience hawser forces greater than 20 tons. A 3 × 5 barge arrangement with the upstream end moored at sta 17+00 would experience hawser forces greater than 34 tons. The water-surface slopes resulting from the 11.7-min valve and minimum excavation were greatly reduced from those observed with the fast valve. A 3 × 3

and a 3 × 5 barge arrangement moored with the upstream end at sta 17+00 would probably experience hawser forces less than 5 tons with the 11.7-min emptying valve. Of course, slow valve operations result in slower emptying times, which must be considered as well as the flow conditions inside the lock chamber and culverts to determine the overall effects from slow valve times.

The water-surface slopes computed for the 1.5- and 11.7-min valve speeds with the interlaced lateral discharge alternative and the moderate excavation plan were slightly less than those computed with the minimum excavation plan, as one would expect given the same boundary conditions. The surge produced by the lock discharge is essentially independent of the bed elevation, although the greater depths resulting from the moderate excavation would coincide with slower velocities. The seiching frequency within the approach channel is only slightly higher with the 5-ft increase in depth. The gravity wave celerity is increased by a factor of the square root of the moderate excavation depth (20.2 ft) to minimum excavation depth (15.2 ft) ratio. That is, the moderate excavation plan increases the celerity by a factor of $(20.2/15.2)^{1/2}$ or 1.15. This increase in celerity results in a reduction of the oscillation period (increased frequency) of the lower approach.

Relatively large slopes still occurred with the moderate excavation plan with the fast valve, and much smaller slopes occurred with the slow valve. The hawser forces computed for the moderate excavation plan were less than those computed with the minimum excavation plan, but not significantly less. The additional 5 ft of excavation in the moderate excavation plan does not provide enough reduction in hawser force to consider this plan. The differences observed between the two excavation plans indicate that a certain amount of excavation is probably beneficial. This amount should probably be based on the amount needed for tow and barge maneuverability in the lower approach including vessel squat, rather than on an amount needed to reduce hawser forces. Franco (1976) points out that if the channel is not deep enough, barges can hit the bottom of the canal during the wave troughs.

The results from the simulations with the landside discharge channel alternative support the results obtained with the interlaced lateral discharge alternative. A slower emptying valve reduces the water-surface slopes in the lower lock approach for the same headwater and tailwater combination. A higher tailwater elevation helps reduce the hawser forces, but the slower valve is where the most reduction in hawser force can be achieved. The results computed from the interlaced lateral discharge alternative and the landside discharge channel alternative are not directly comparable due to the different headwater and tailwater combinations requested by the Nashville District. However, for the same headwater and tailwater conditions, the interlaced lateral system would probably result in slightly higher hawser forces for tow and barge arrangements moored along the landside guide wall. A 3 × 6 barge arrangement with the upstream end moored at sta 17+00 would probably experience hawser forces over 40 tons with the interlaced laterals compared with forces greater than 37 tons for a 3 × 6 with the upstream end moored at sta 15+00 with the landside discharge channel alternative. This difference is relatively small, and does not justify

construction of the higher cost landside channel. The most effective lock outlet from a hydraulic engineer's viewpoint is one that is hydraulically efficient yet provides good energy dissipation and has minimal impact on navigation. Unfortunately, the economics involved for this type system usually eliminates it as an alternative. The performance of the outlet must then be adjusted to satisfy the economics. Discharging a lock immediately downstream from the lower miter gates with an interlaced lateral is generally less expensive, but requires extreme caution when operating the emptying valves. Slower valve operations and lock emptying times will be required for this type discharge system versus one that discharges away from the lower approach.

References

Abbott, M. B. (1979). *Computational hydraulics, elements of the theory of free surface flows.* Pitman Advanced Publishing Limited, London.

Berger, R. C. (1993). "A finite element scheme for shock capturing," Technical Report HL-93-12, U.S. Army Engineer Waterways Experiment Station, Vicksburg, MS.

Berger, R. C., and Stockstill, R. L. (1995). "Finite element model for high velocity channels," *Journal of Hydraulic Engineering*, ASCE, 121(10), 710-716.

Berger, R. C., Stockstill, R. L., and Ott, M. W. (1995). "HIVEL2D users' manual," Technical Report REMR-HY-13, U.S. Army Engineer Waterways Experiment Station, Vicksburg, MS.

Chapman, R. S., and Kuo, C. Y. (1985). "Application of the two-equation k-ϵ turbulence model to a two-dimensional steady, free surface flow problem with separation," *International Journal for Numerical Methods in Fluids* 5, 257-268.

Franco, J. J. (1976). "Development of navigation with locks and dams," Miscellaneous Paper H-76-15, U.S. Army Engineer Waterways Experiment Station, Vicksburg, MS.

Oswalt, N. R., Ables, J. H., and Murphy, T. E. (1972). "Navigation conditions and filling and emptying system, New Bankhead Lock, Black Warrior River, Alabama; Hydraulic model investigation," Technical Report H-72-6, U.S. Army Engineer Waterways Experiment Station, Vicksburg, MS.

Rodi, W. (1980). "Turbulence models and their application in hydraulics - a state of the art review," State-of-the-Art Paper, International Association for Hydraulic Research, Delft, The Netherlands.

Shows, L. J., and Franco, J. J. (1981). "Navigation conditions at McAlpine Locks and Dam, Ohio River; Hydraulic model investigation," Technical Report HL-81-7, U.S. Army Engineer Waterways Experiment Station, Vicksburg, MS.

Stockstill, R. L., and Berger, R. C. (1994). "HIVEL2D: A two-dimensional flow model for high-velocity channels," Technical Report REMR-HY-12, U.S. Army Engineer Waterways Experiment Station, Vicksburg, MS.

Stockstill, R. L., Berger, R. C., and Nece, R. E. (1997). "Two-dimensional flow model for trapezoidal high-velocity channels," *Journal of Hydraulic Engineering*, ASCE, 123(10), 844-852.

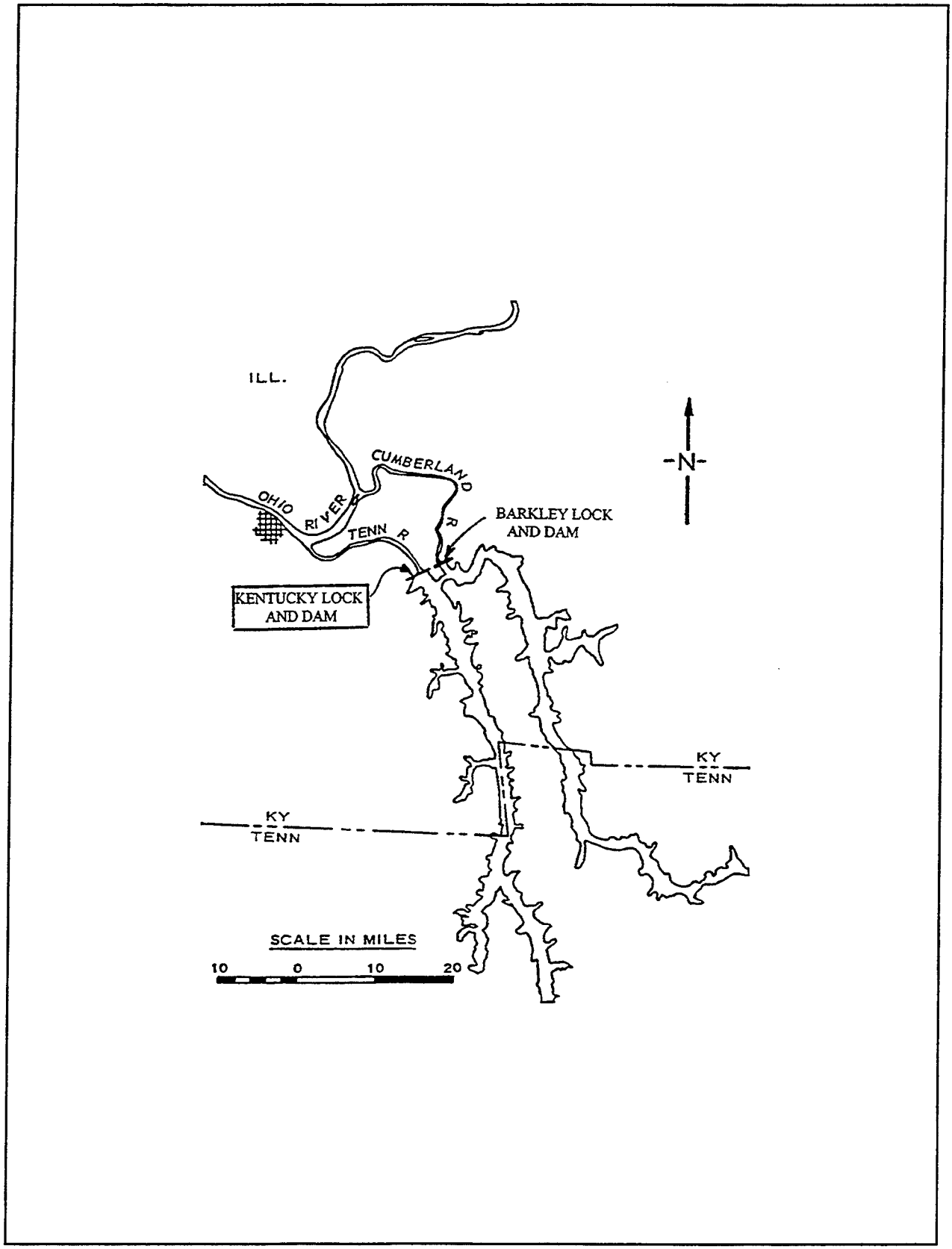

Figure 1. Vicinity map

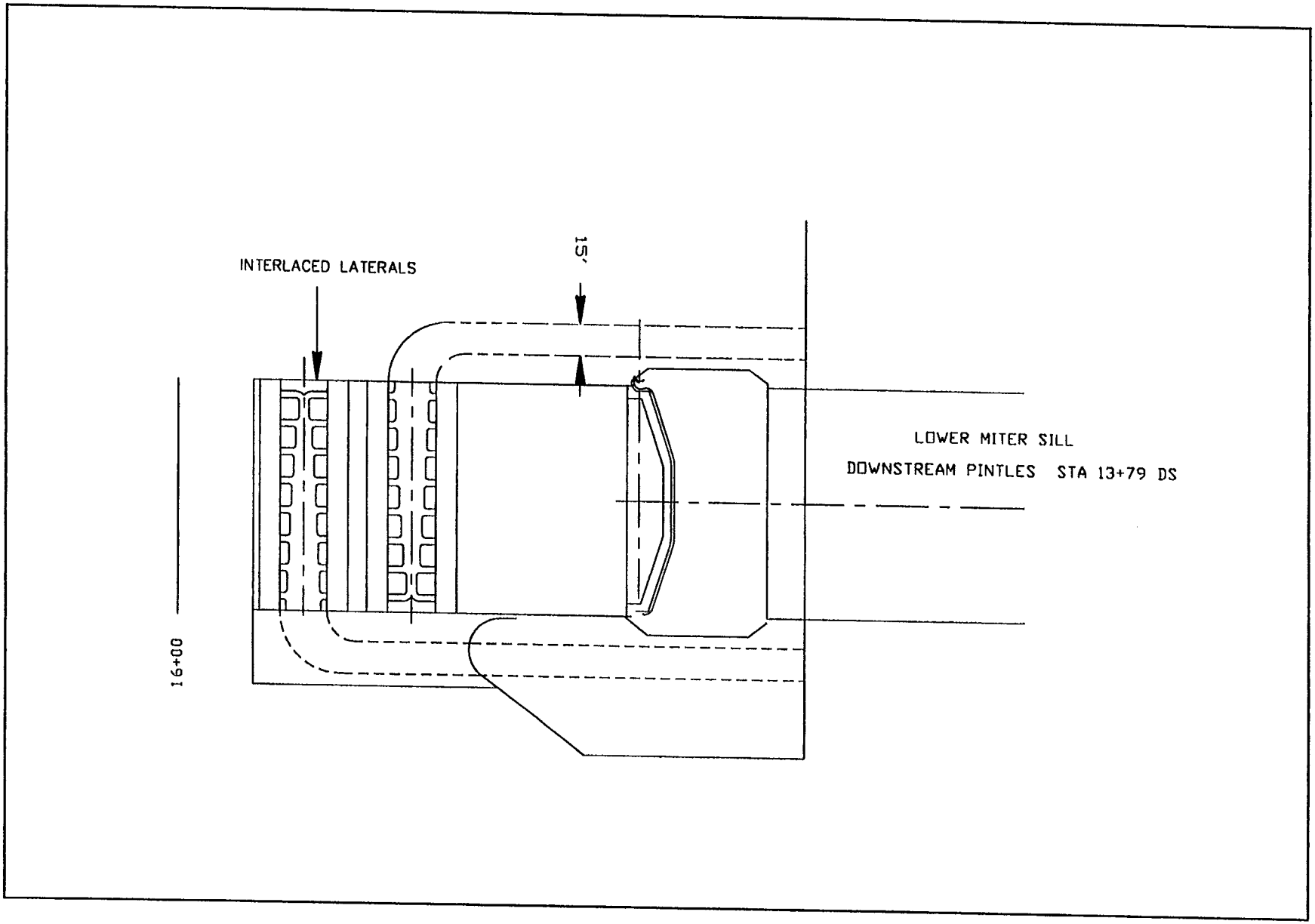

Figure 2. Interlaced lateral discharge system

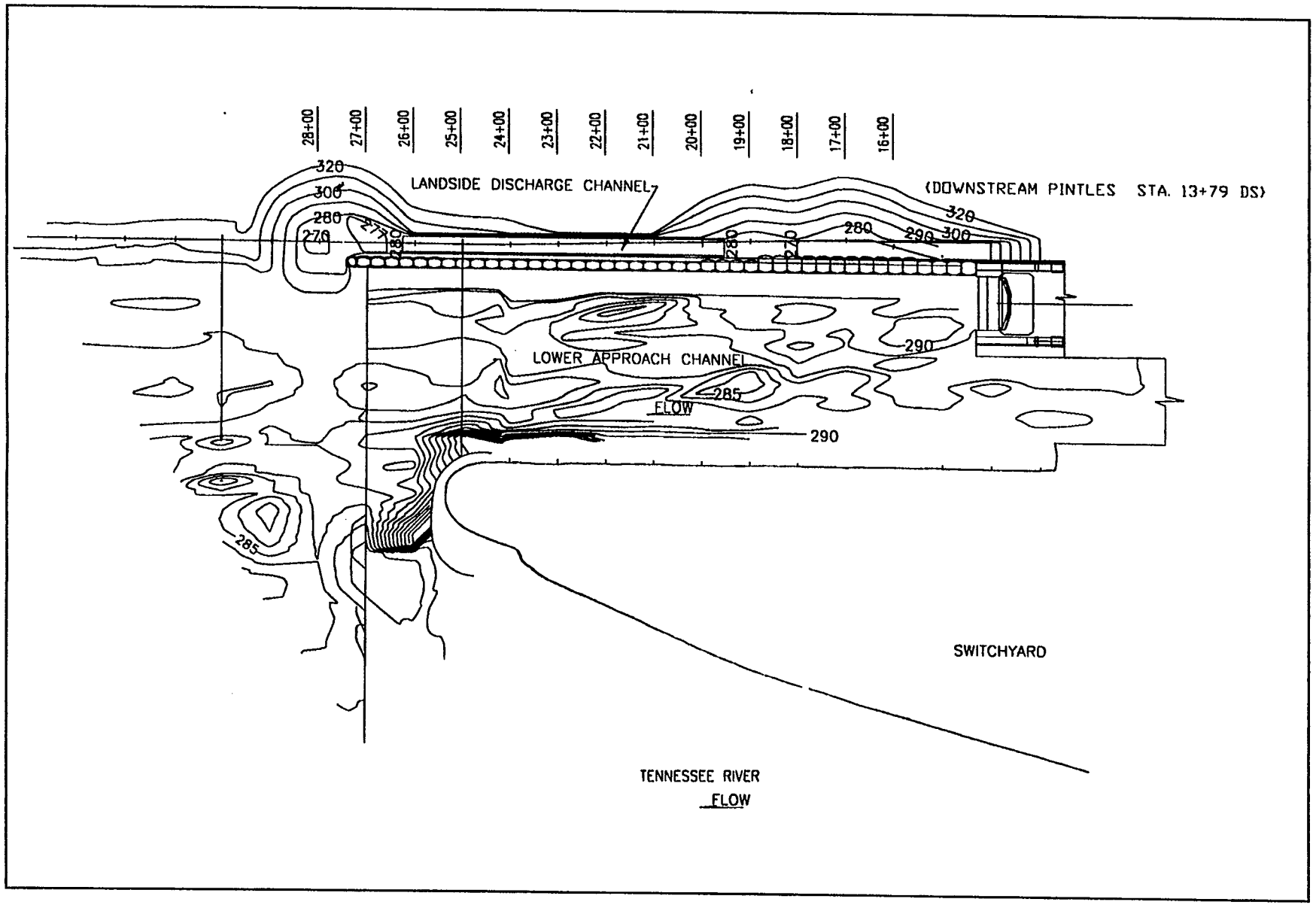

Figure 3. Landside discharge channel

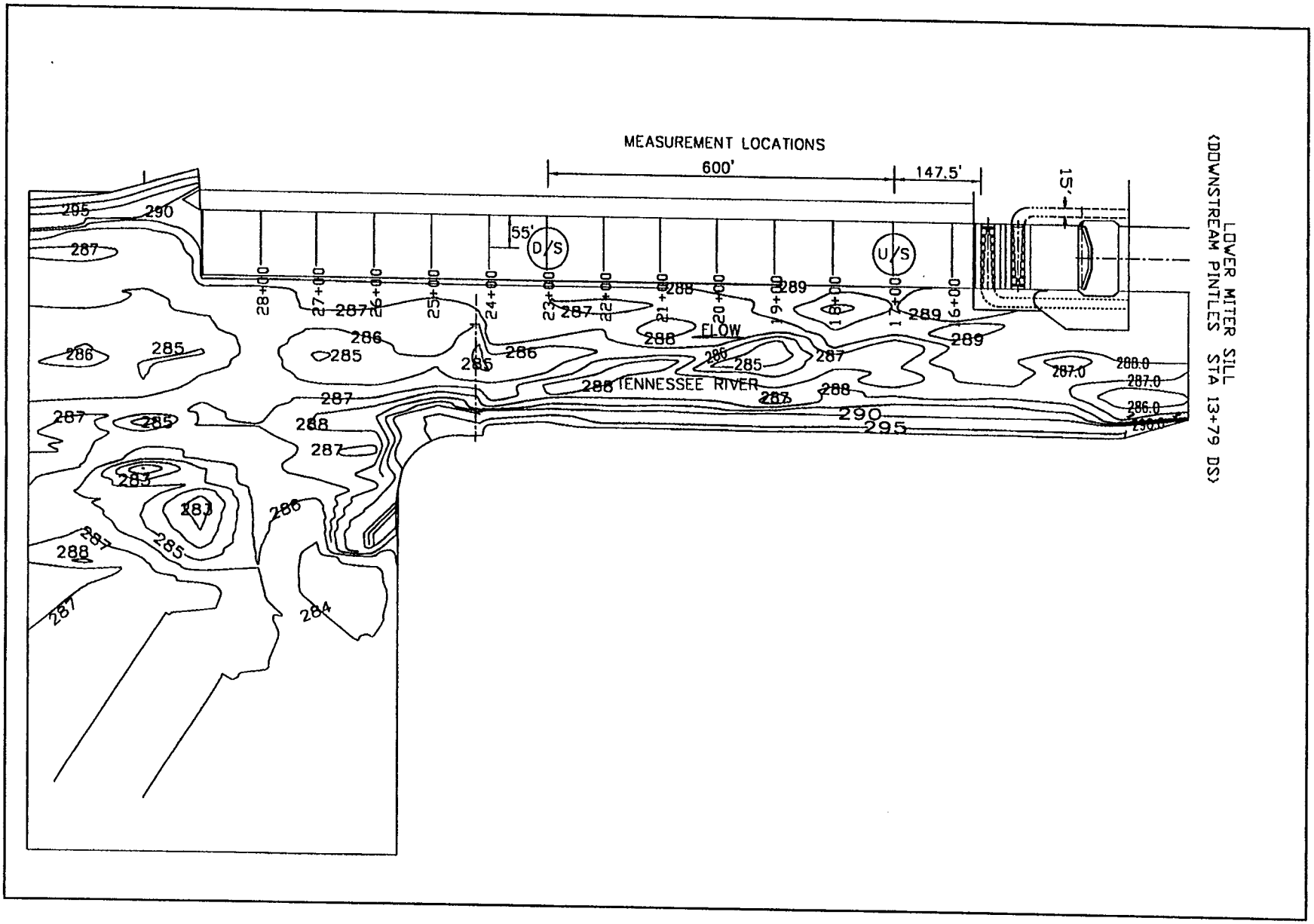

Figure 4. Plan view of lower lock approach, interlaced lateral discharge alternative and minimum excavation plan

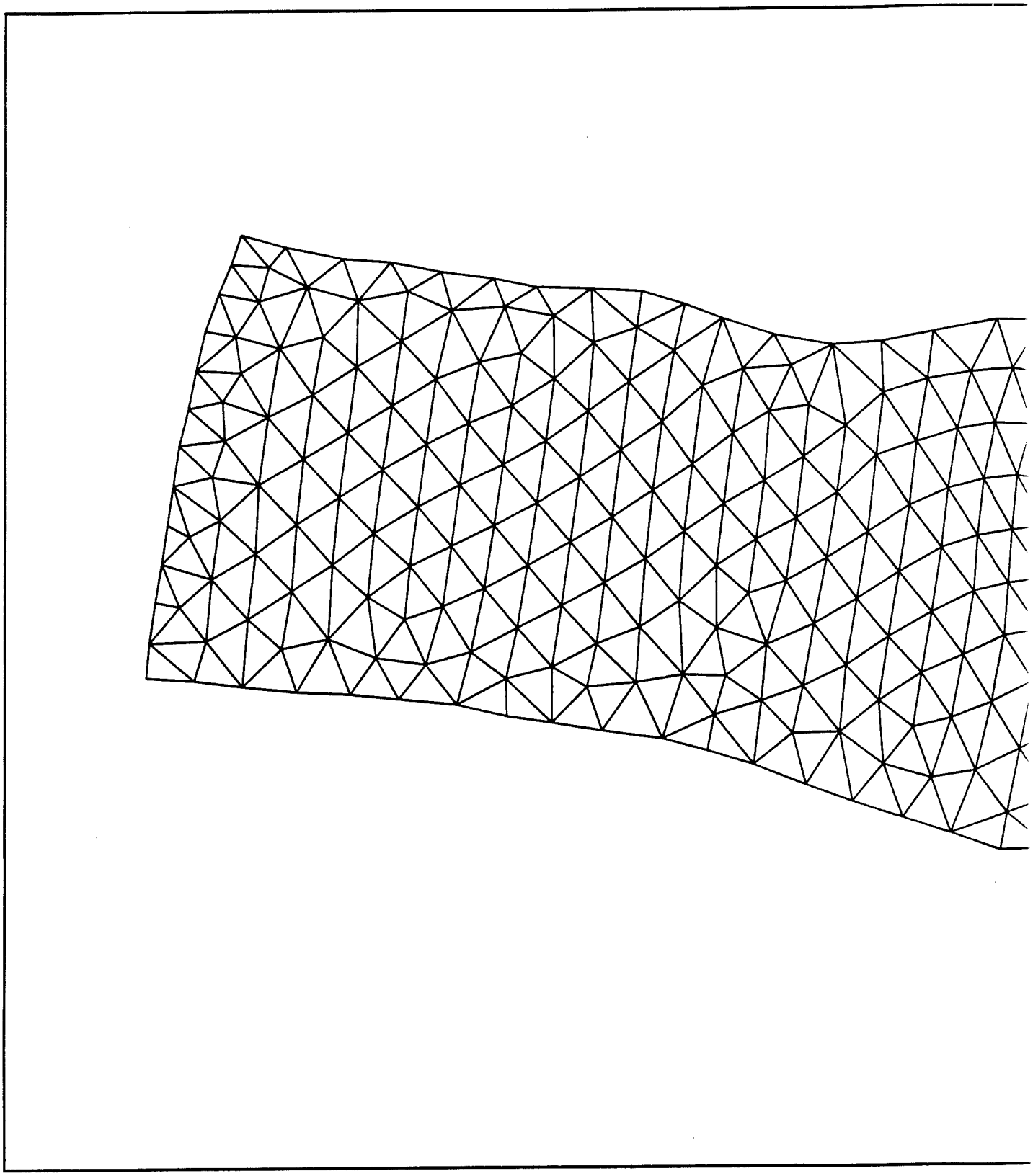

a. Overall view of mesh

Figure 5. Mesh used for hydrodynamic computations with interlaced lateral discharge alternative (continued)

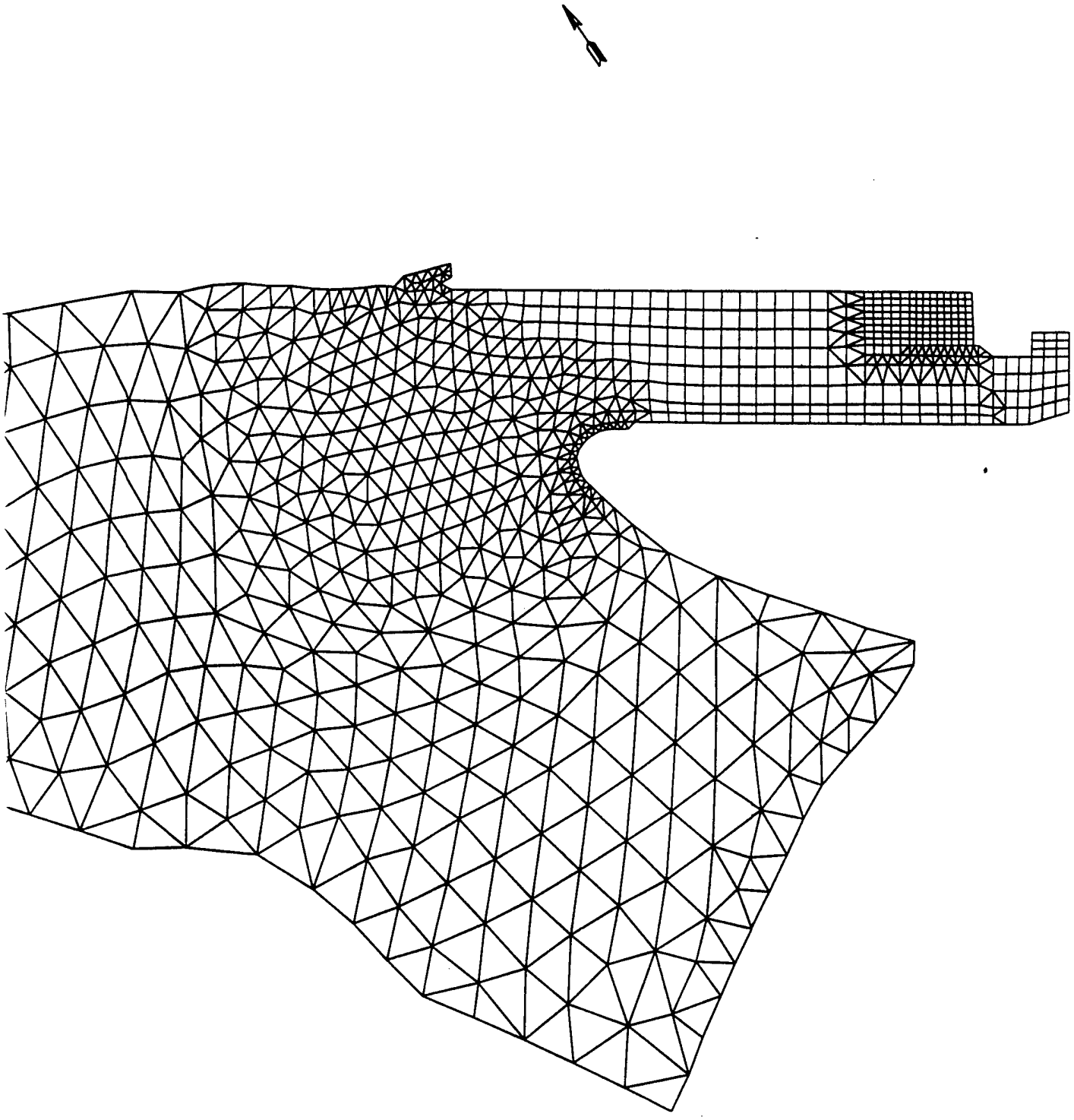

nued)

(2)

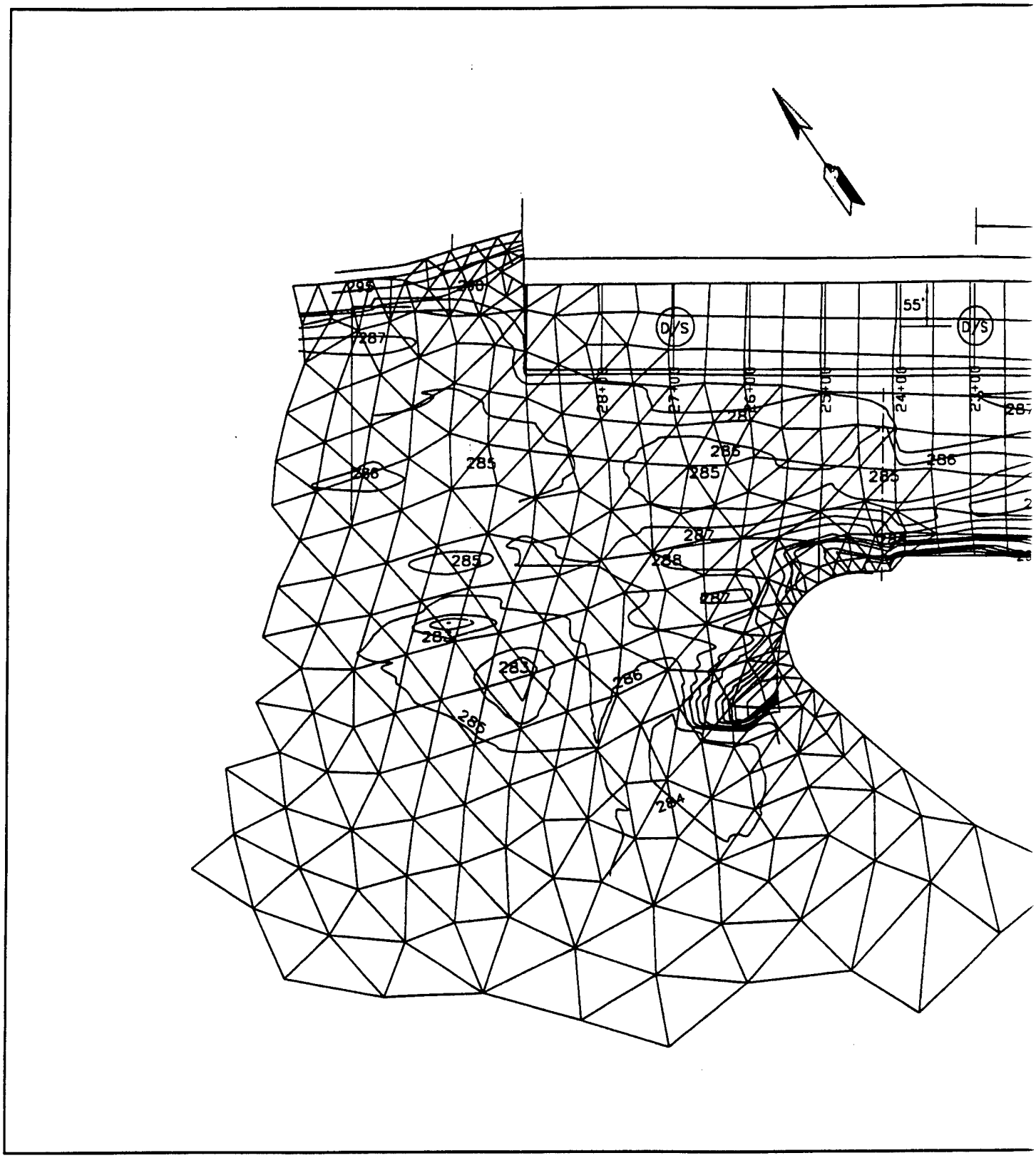

b. Close-up of lower approach

Figure 5. (Concluded)

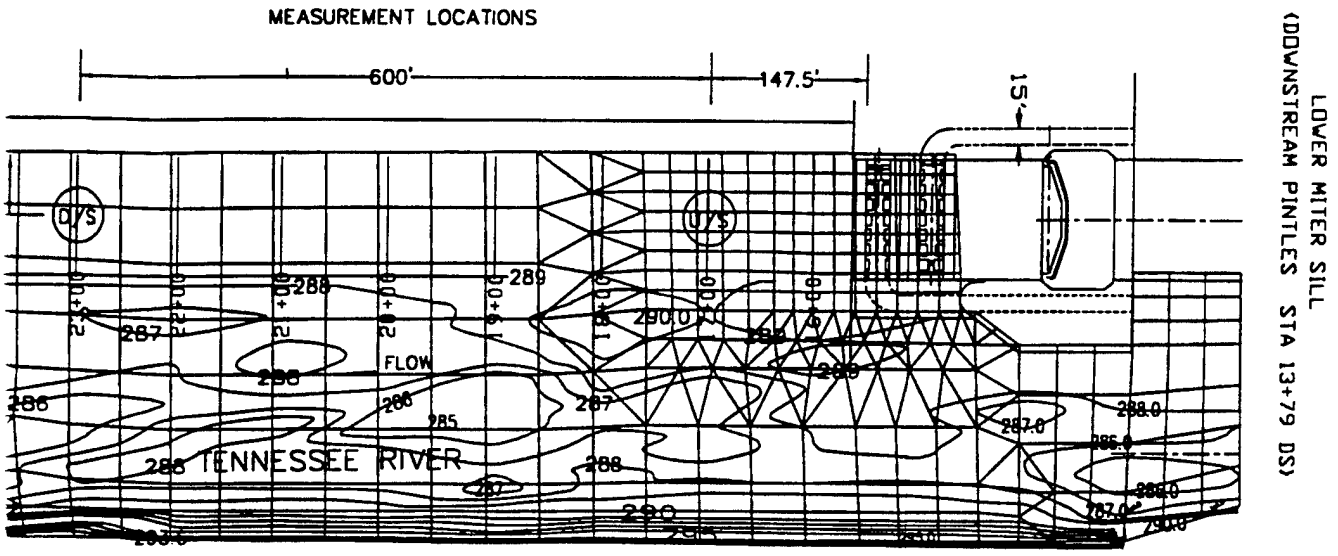
MEASUREMENT LOCATIONS
600'
147.5'
15'
U/S
U/S
288
289
290.0
287
286
FLOW
285
TENNESSEE RIVER
288
287
290
287.0
288.0
286.0
287.0
290.0
LOWER MITER SILL
(DOWNSTREAM PINTLES STA 13+79 DS)

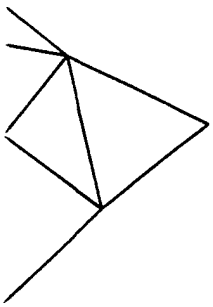

(2)

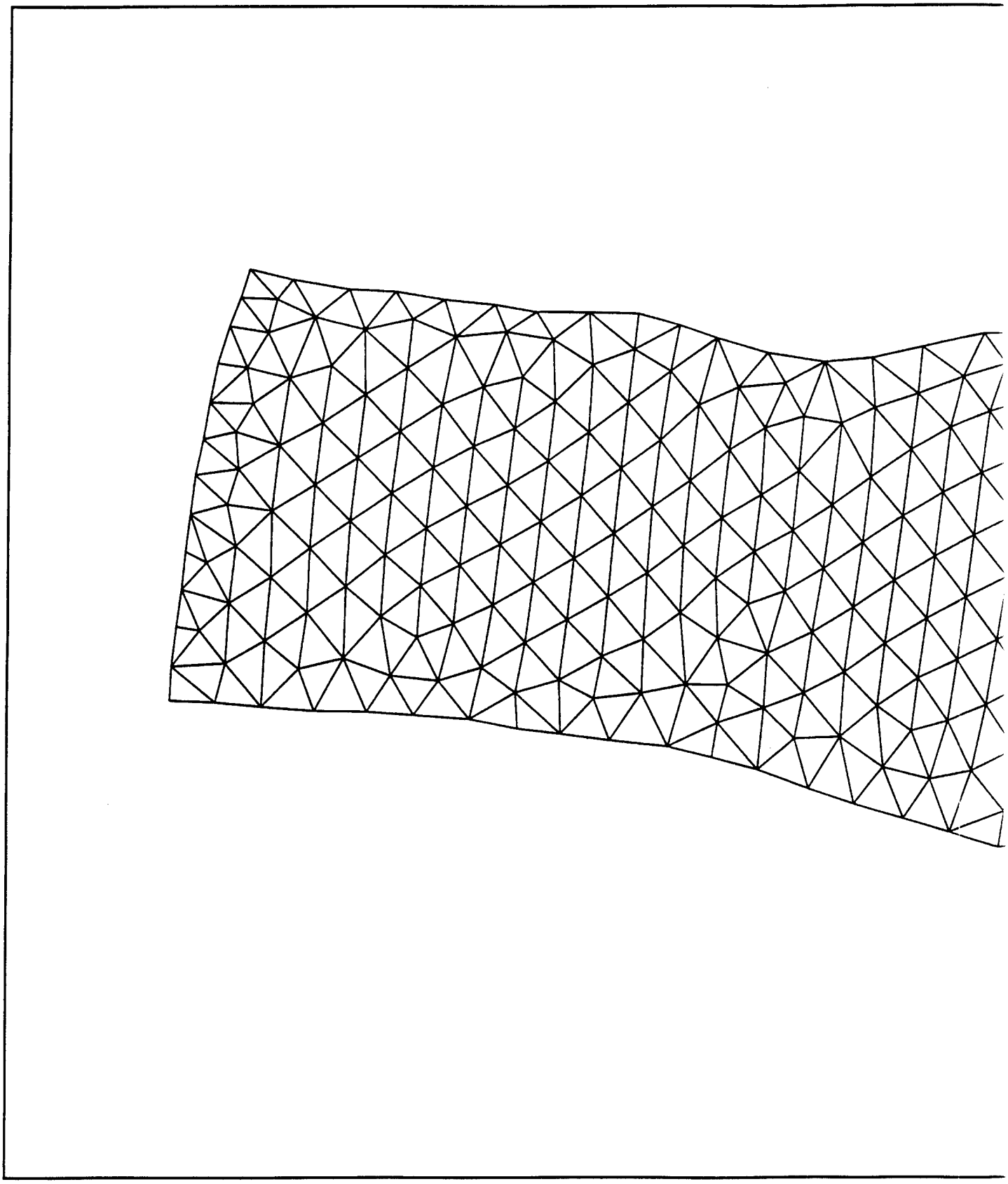

Figure 6. Computational mesh used for simulations with the landside discharge channel

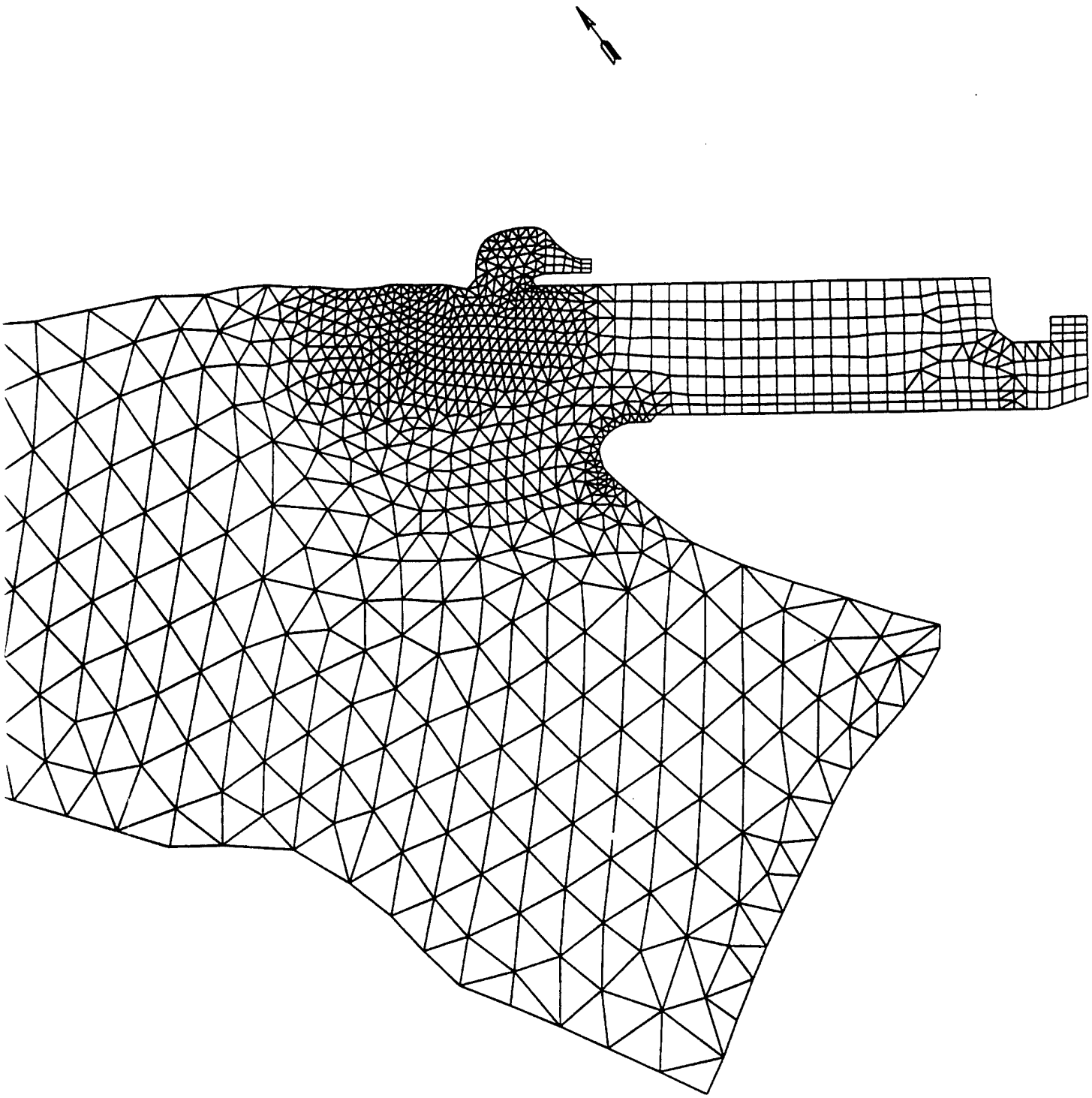

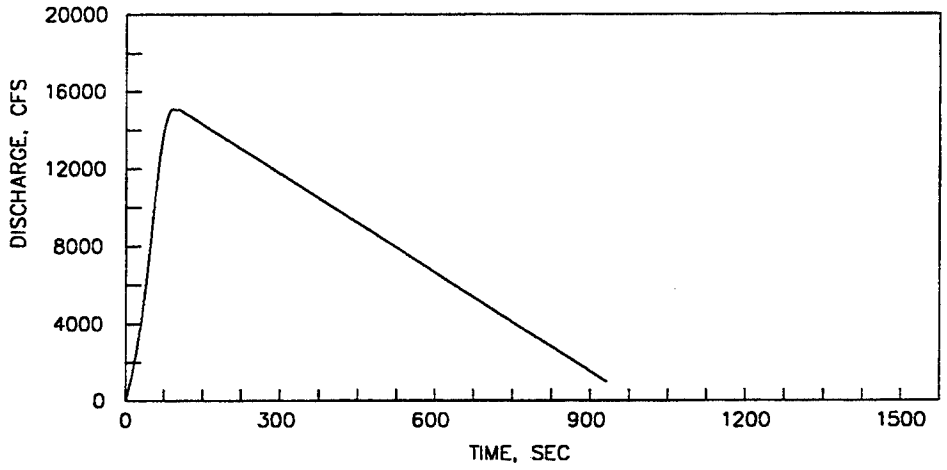

a. 1.5–min. valve opening

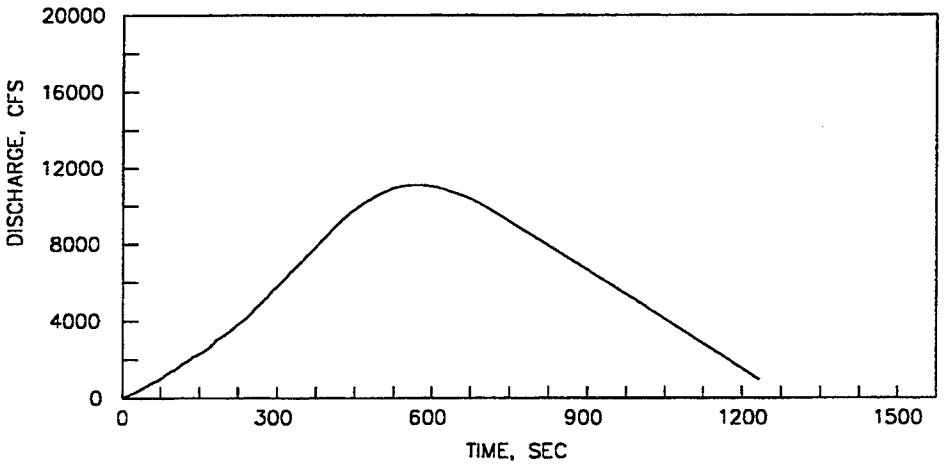

b. 11.7–min. valve opening

Figure 7. Emptying valve hydrographs, headwater el 357, tailwater el 304.2, interlaced lateral discharge alternative boundary conditions

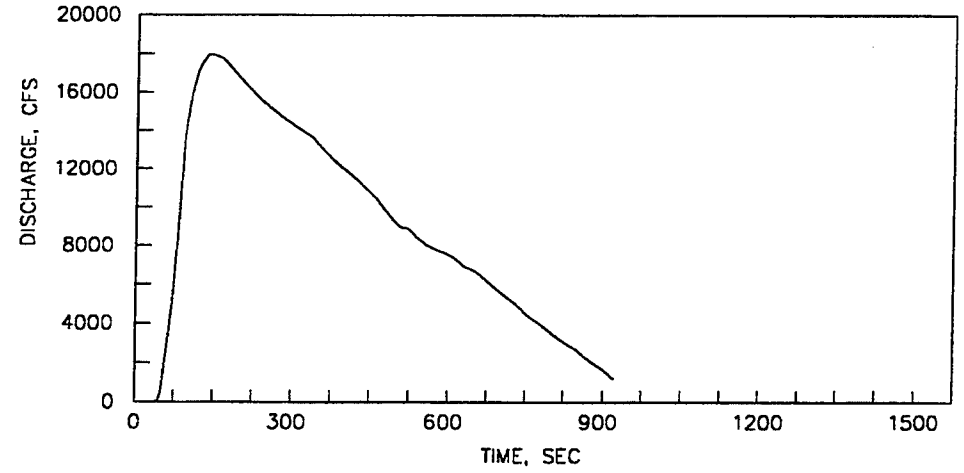

a. Tailwater el 302

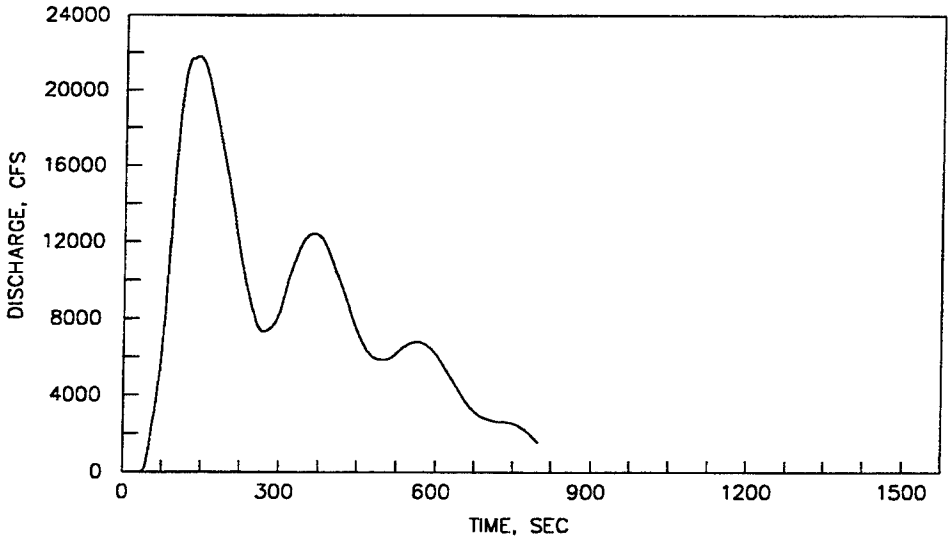

b. Tailwater el 314

Figure 8. Emptying valve hydrograph, sta 26+20, 1.5-min valve time, headwater el 359, landside discharge channel alternative

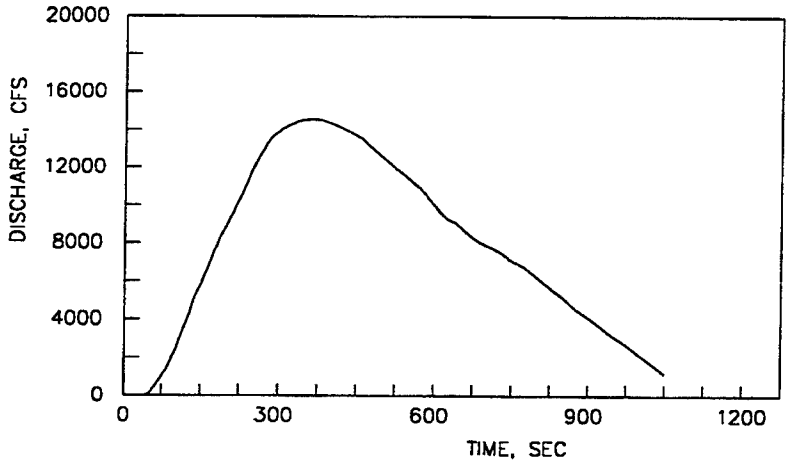

Figure 9. Emptying valve hydrograph, sta 26+20, 6-min valve, headwater el 359, landside discharge channel alternative

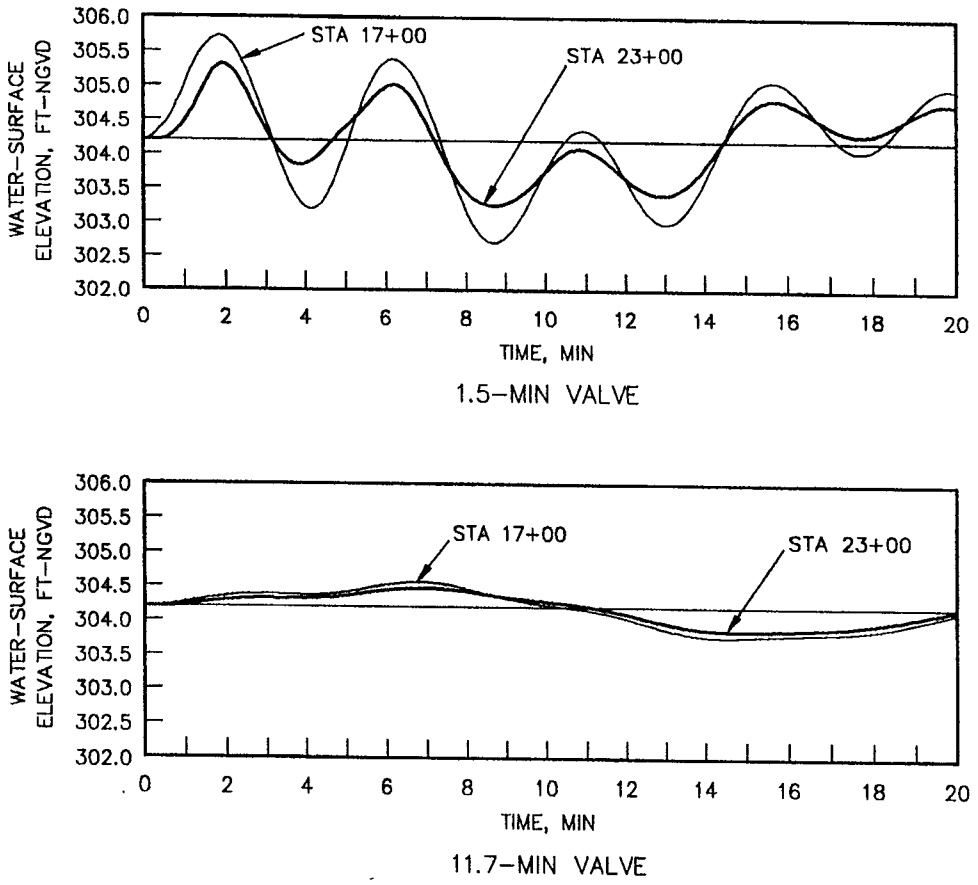

Figure 10. Water-surface elevations, tailwater el 304.2, minimum excavation plan, interlaced lateral discharge alternative

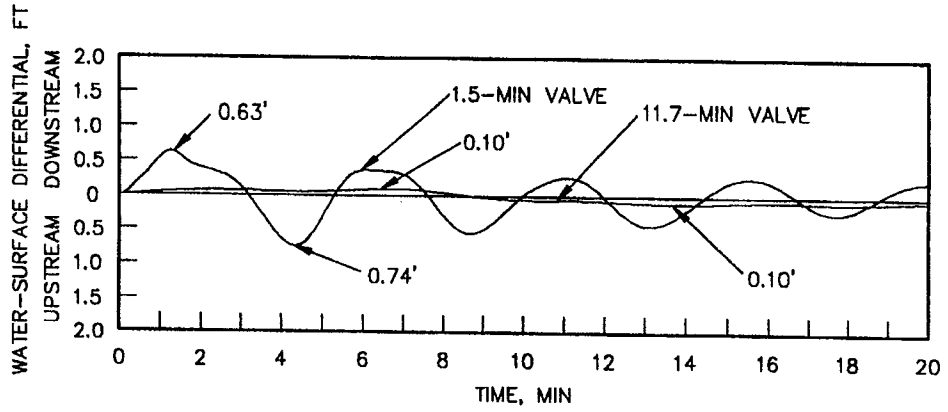

DIFFERENTIAL BETWEEN STA 17+00 AND STA 23+00

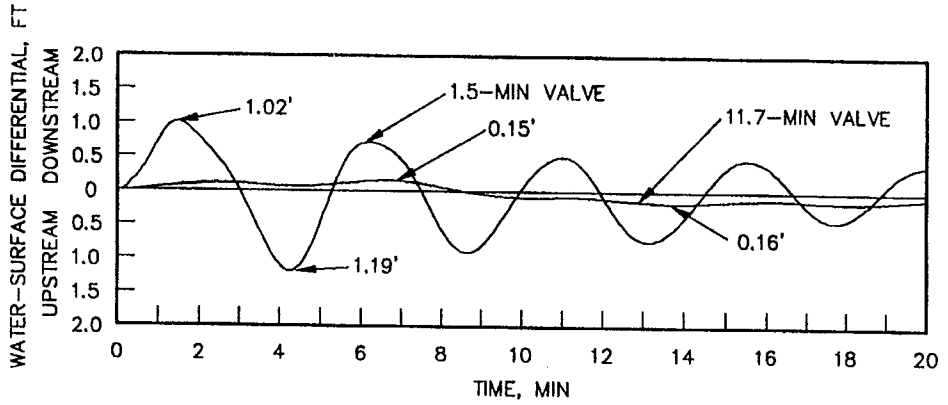

DIFFERENTIAL BETWEEN STA 17+00 AND STA 27+00

NOTE: DOWNSTREAM DIFFERENTIAL INDICATES HIGHER WATER SURFACE AT STA 17+00.

Figure 11. Water-surface differentials, lower pool el 304.2, minimum excavation plan, interlaced lateral discharge alternative

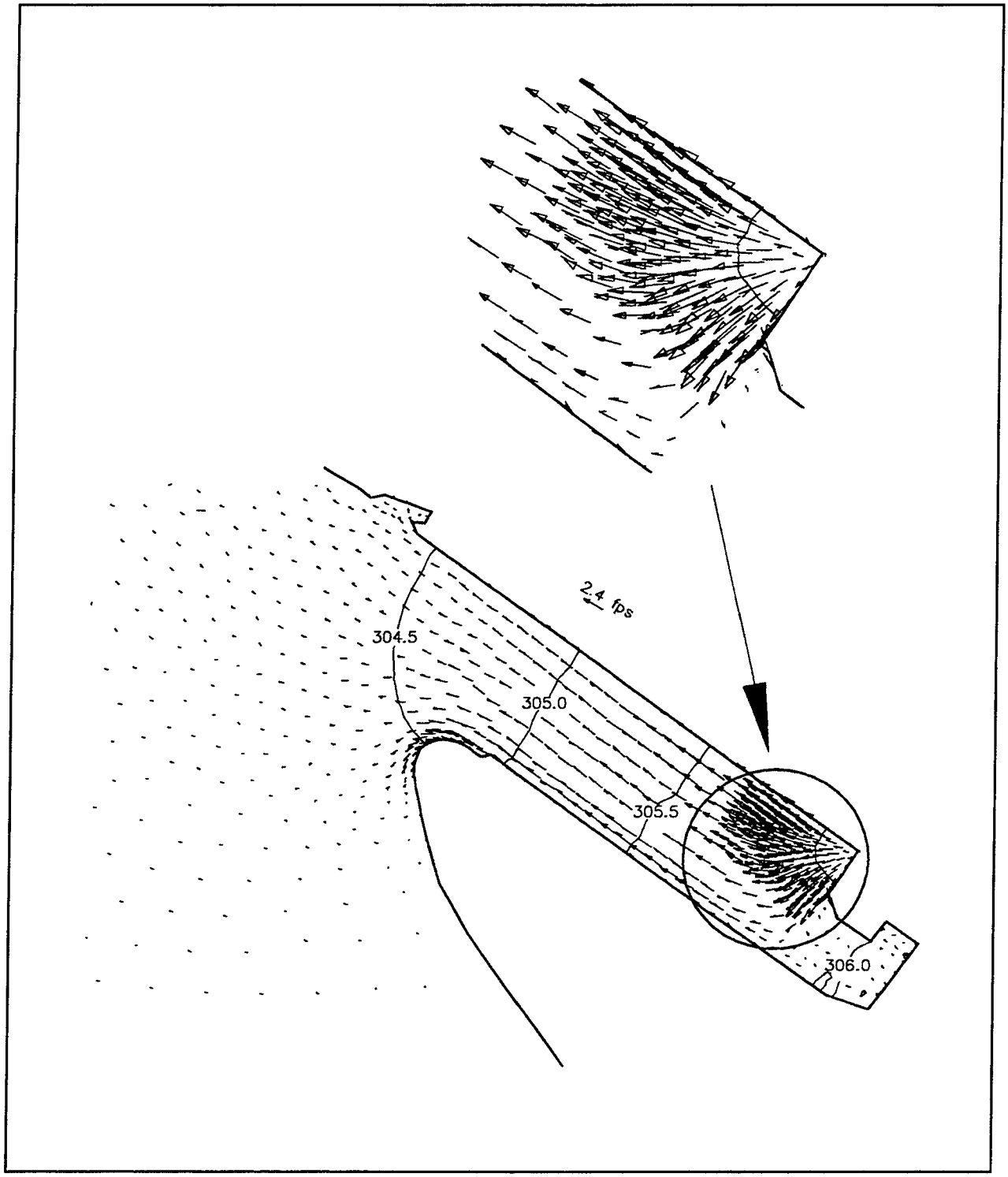

a. Conditions at 92 sec

Figure 12. Velocity vectors and water-surface contours during lock emptying, lower pool el 304.2, 1.5-min valve, minimum excavation plan, interlaced lateral discharge alternative (Sheet 1 of 3)

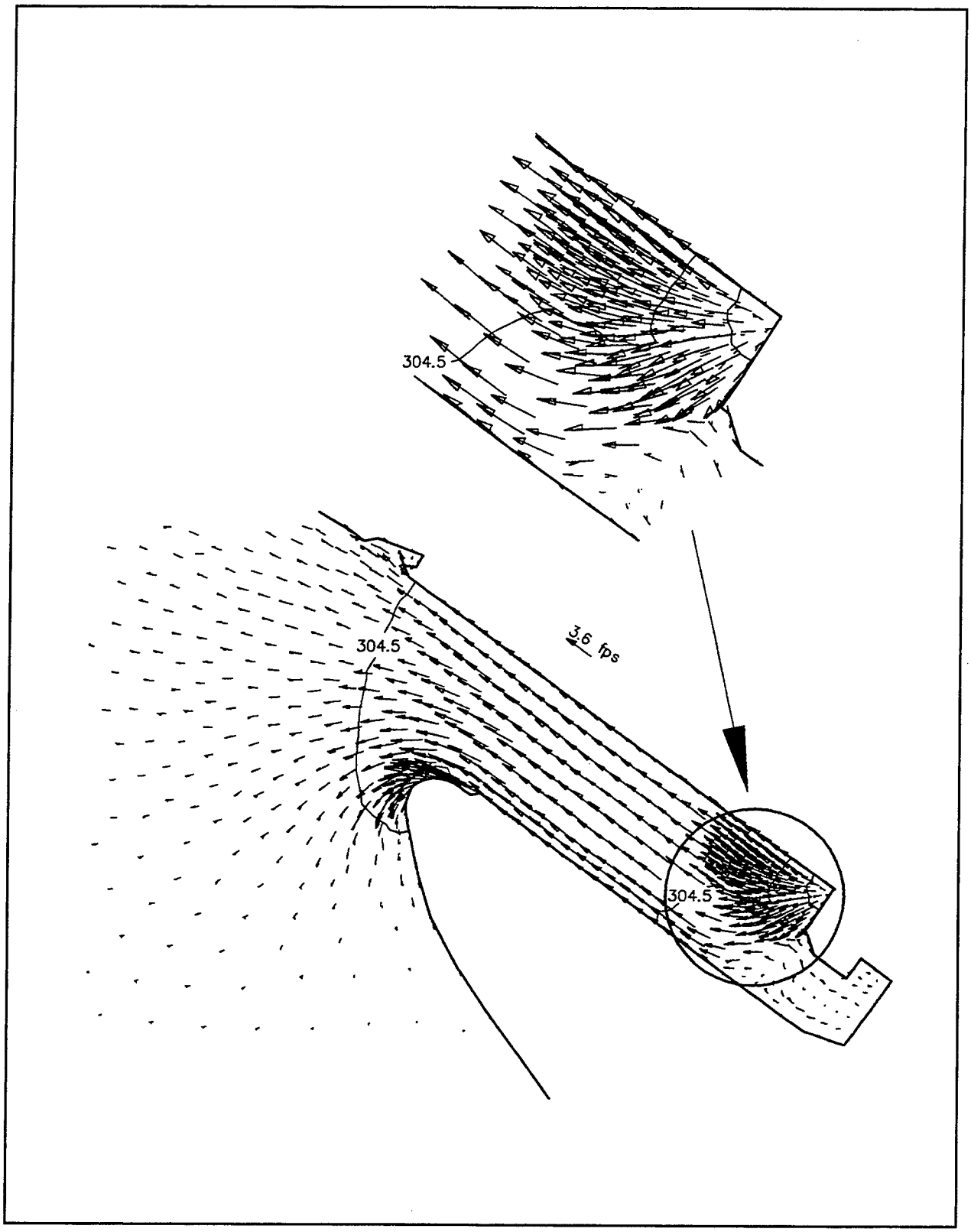

b. Conditions at 180 sec

Figure 12. (Sheet 2 of 3)

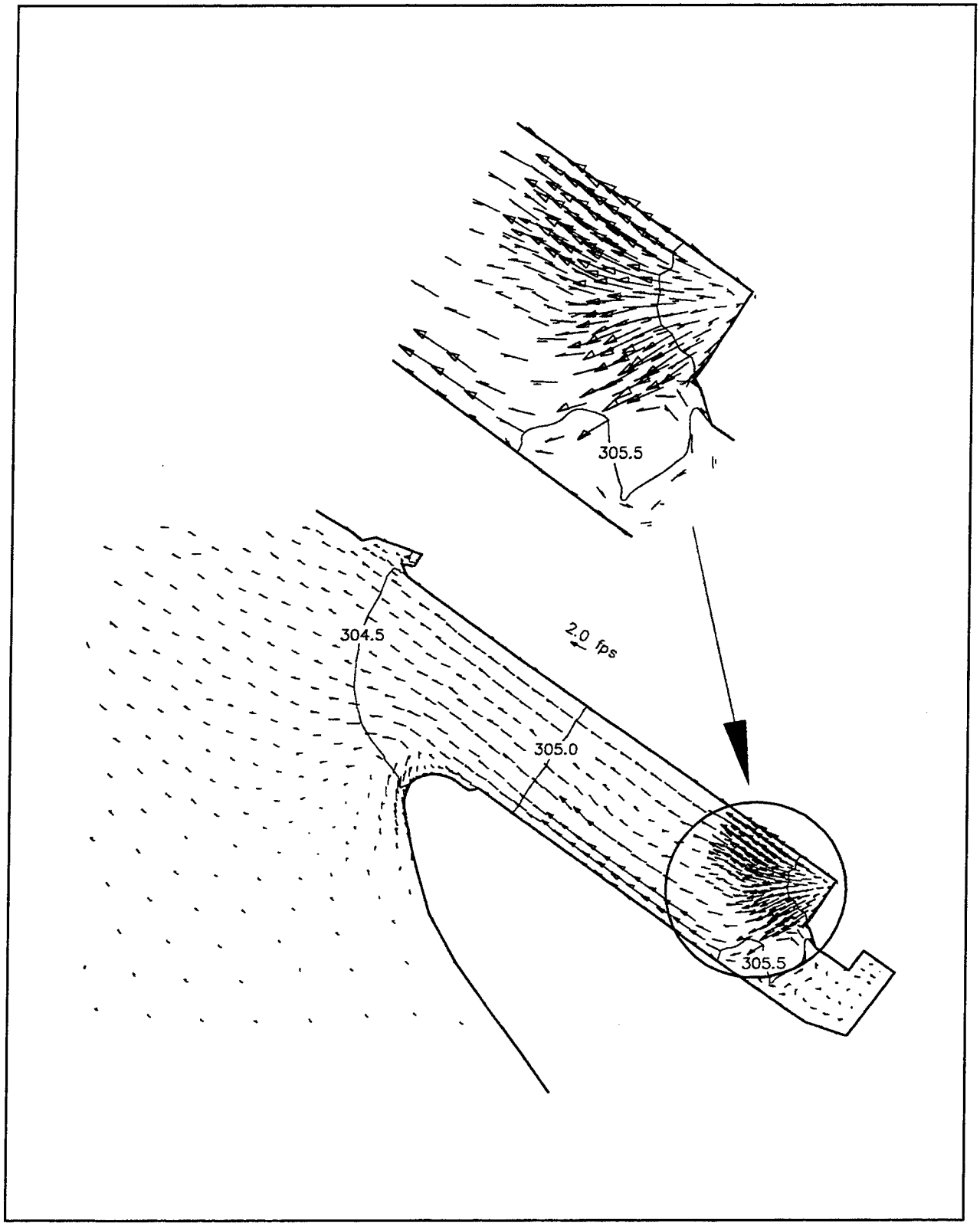

c. Conditions at 360 sec

Figure 12. (Sheet 3 of 3)

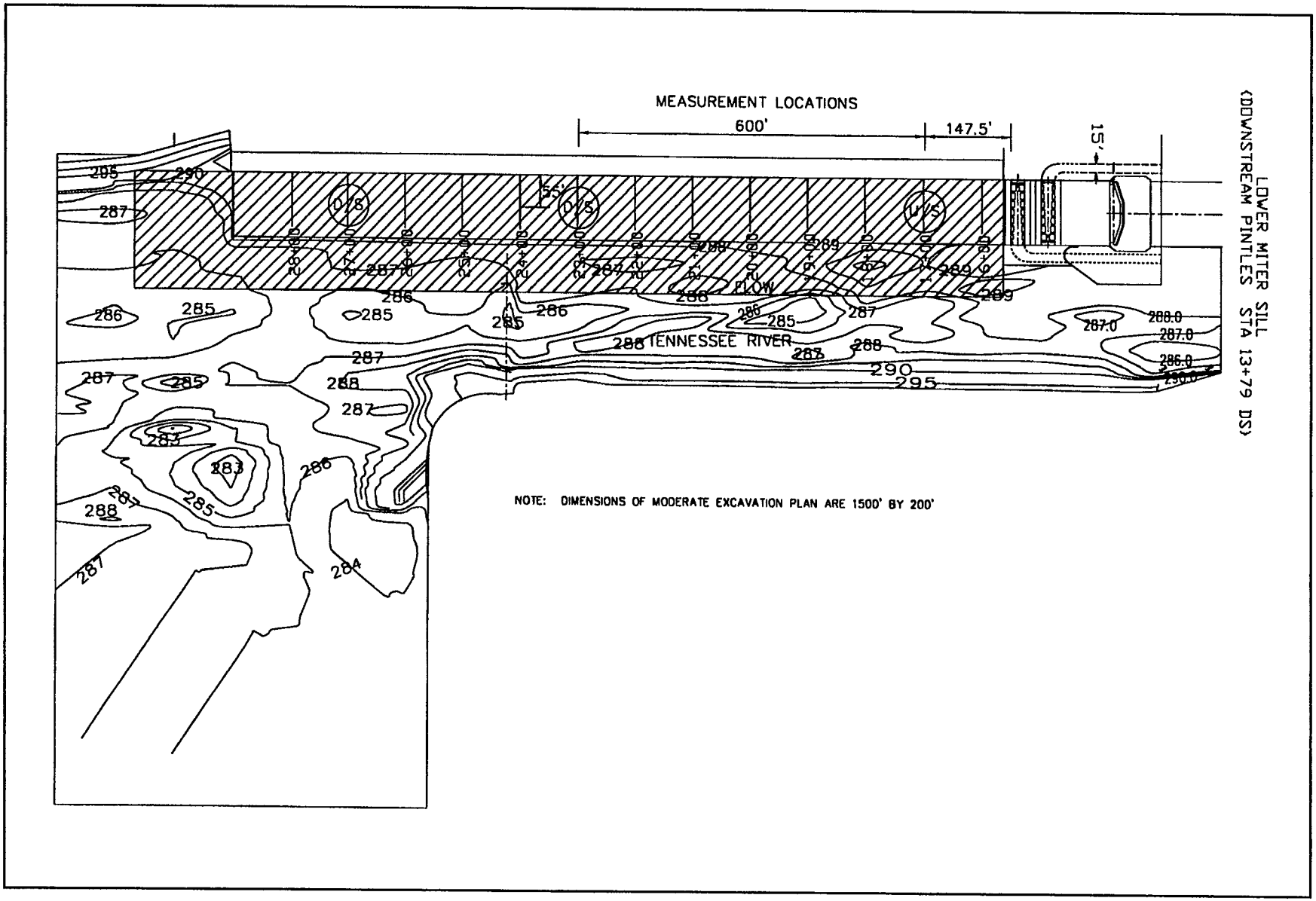

Figure 13. Moderate excavation plan, interlaced lateral discharge alternative

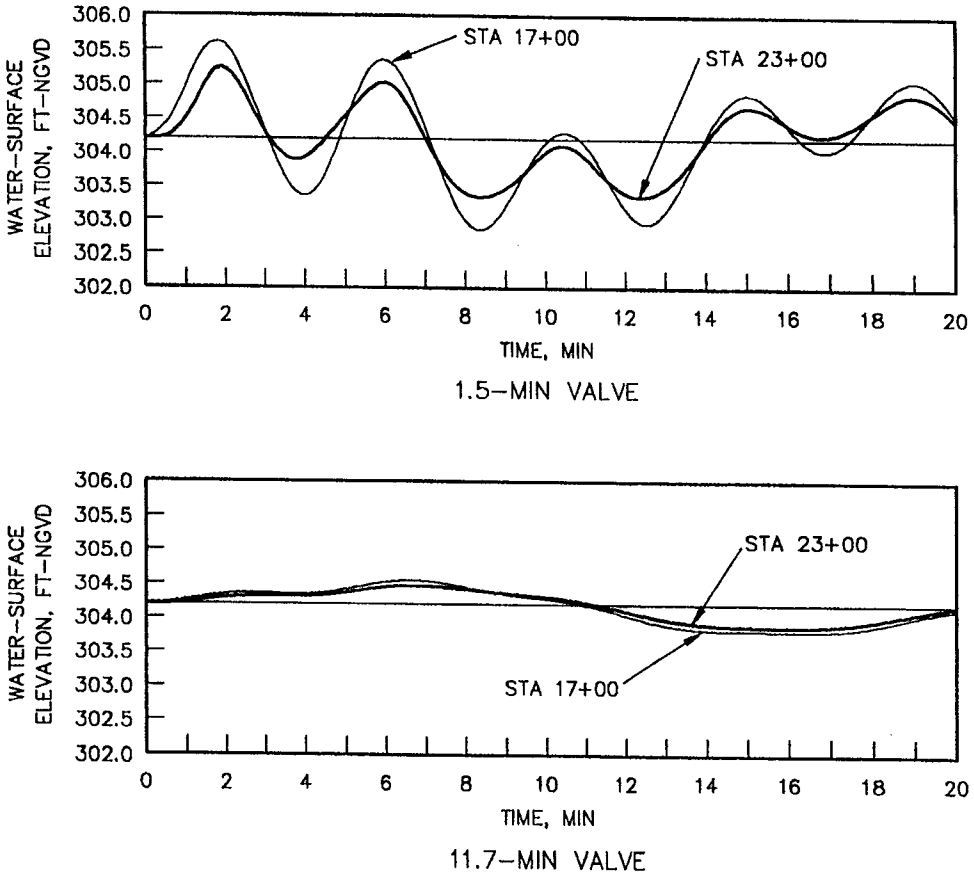

Figure 14. Water-surface elevations, 1.5-min valve, lower pool el 304.2, moderate excavation plan, interlaced lateral discharge alternative

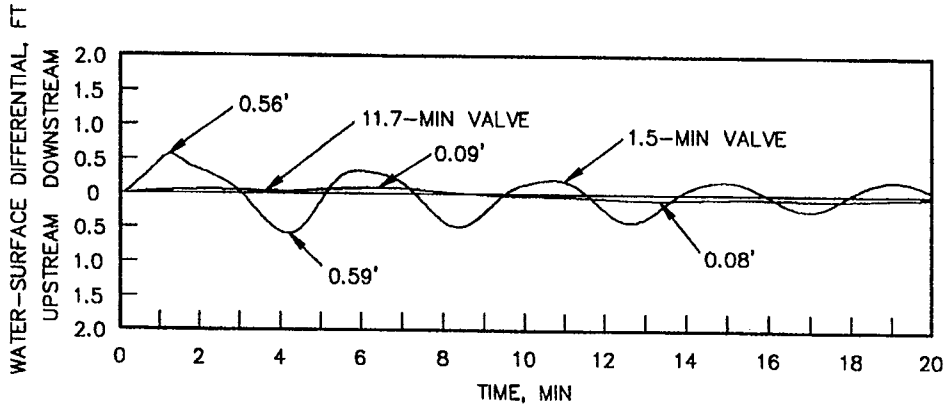

DIFFERENTIAL BETWEEN STA 17+00 AND STA 23+00

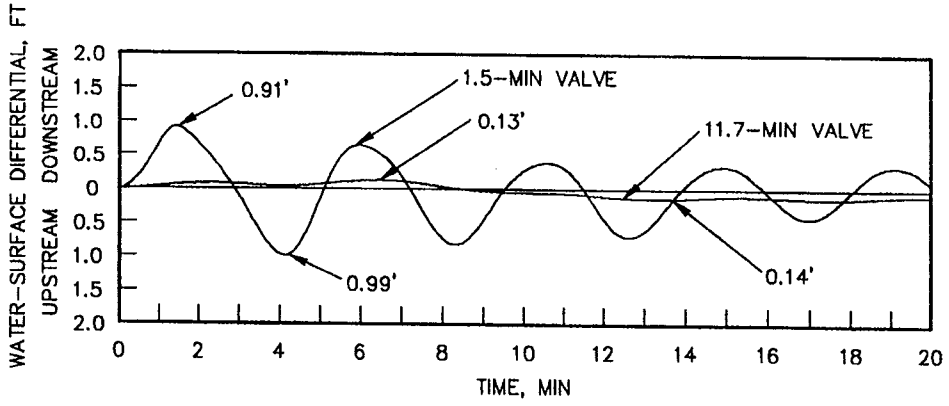

DIFFERENTIAL BETWEEN STA 17+00 AND STA 27+00

NOTE: DOWNSTREAM DIFFERENTIAL INDICATES HIGHER WATER SURFACE AT STA 17+00.

Figure 15. Water-surface differentials, lower pool el 304.2, moderate excavation plna, interlaced lateral discharge alternative

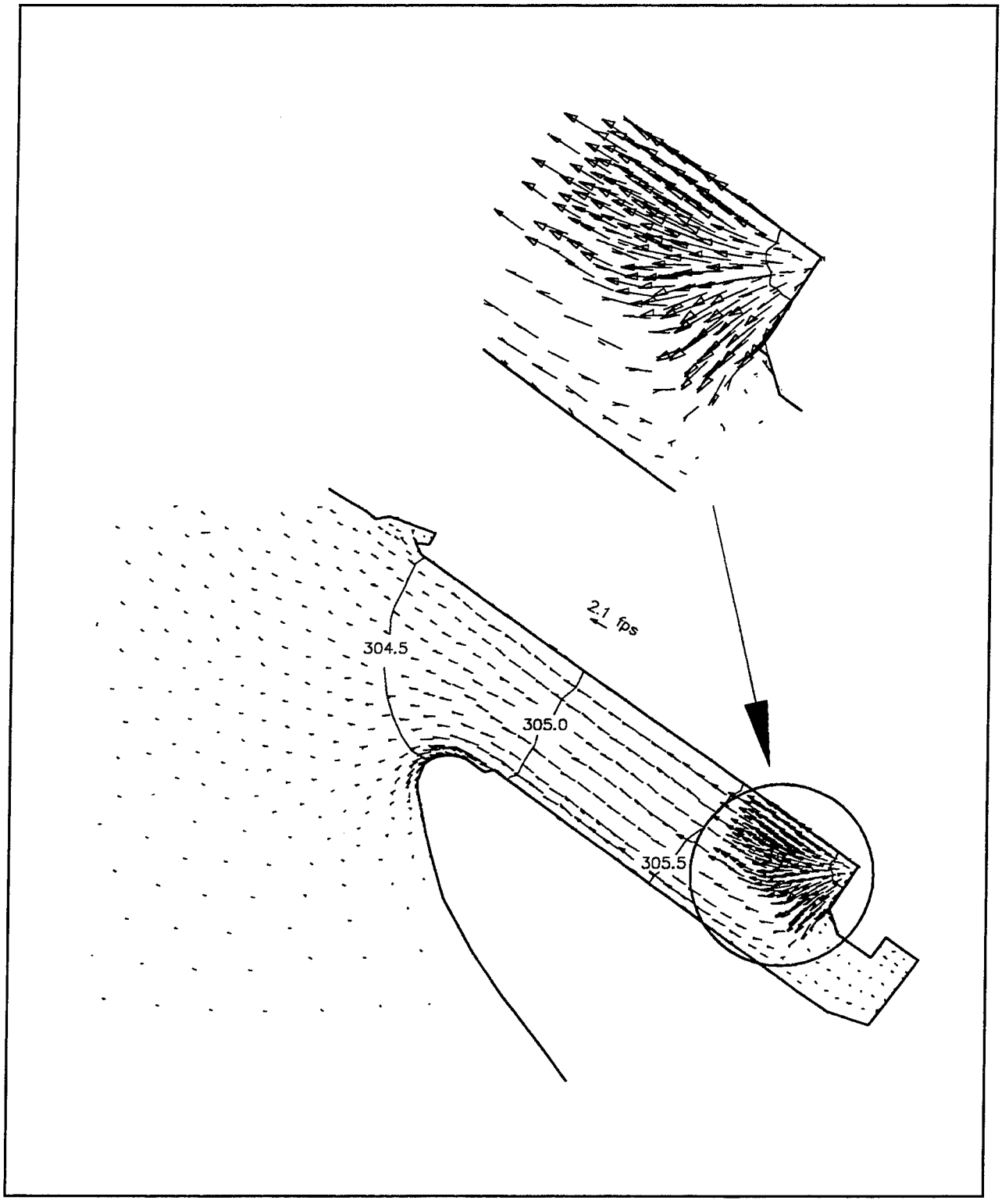

a. Conditions at 92 sec

Figure 16. Velocity vectors and water-surface contours during lock emptying, lower pool el 304.2, 1.5-min valve, moderate excavation plan, interlaced lateral discharge alternative (Sheet 1 of 3)

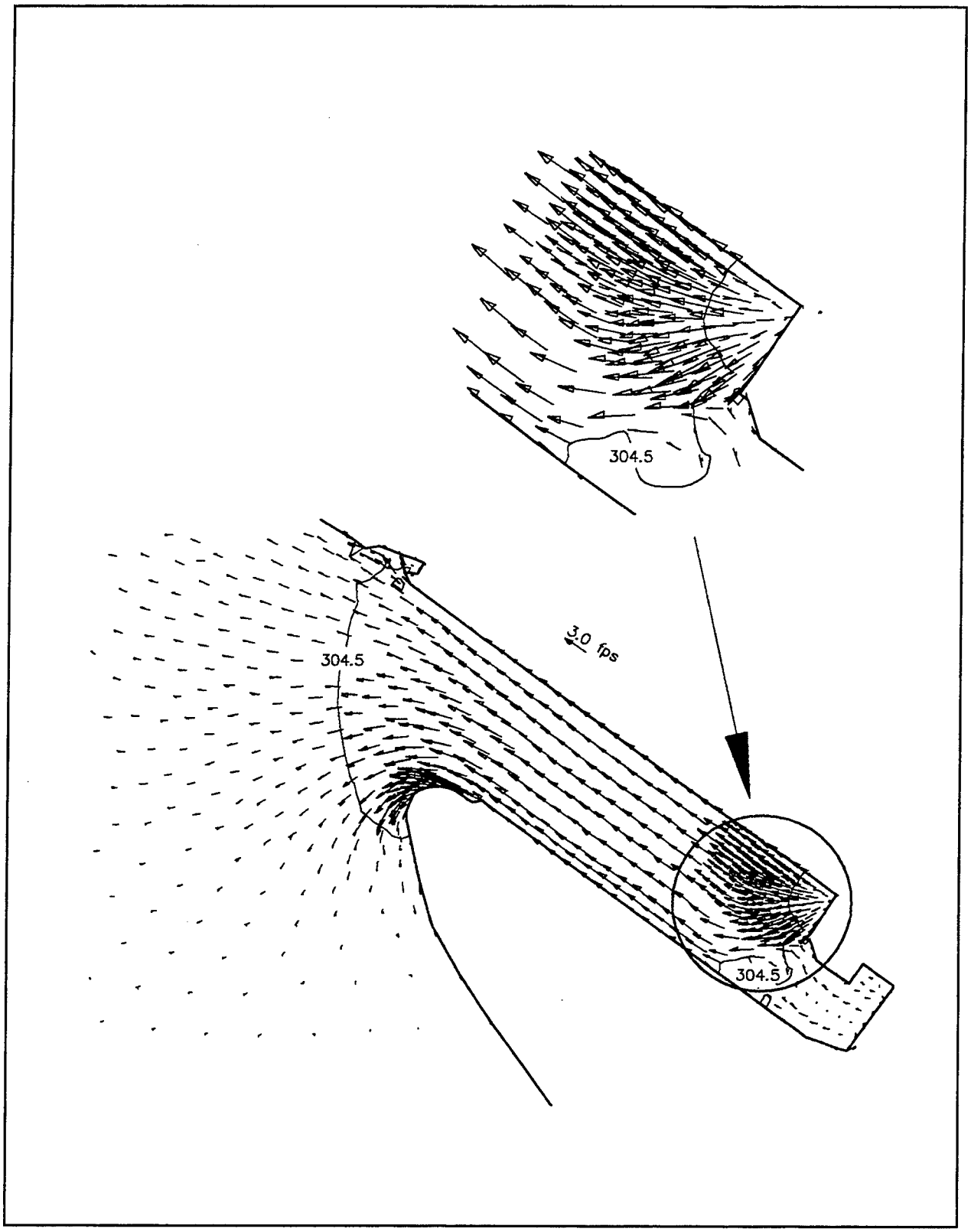

b. Conditions at 180 sec

Figure 16. (Sheet 2 of 3)

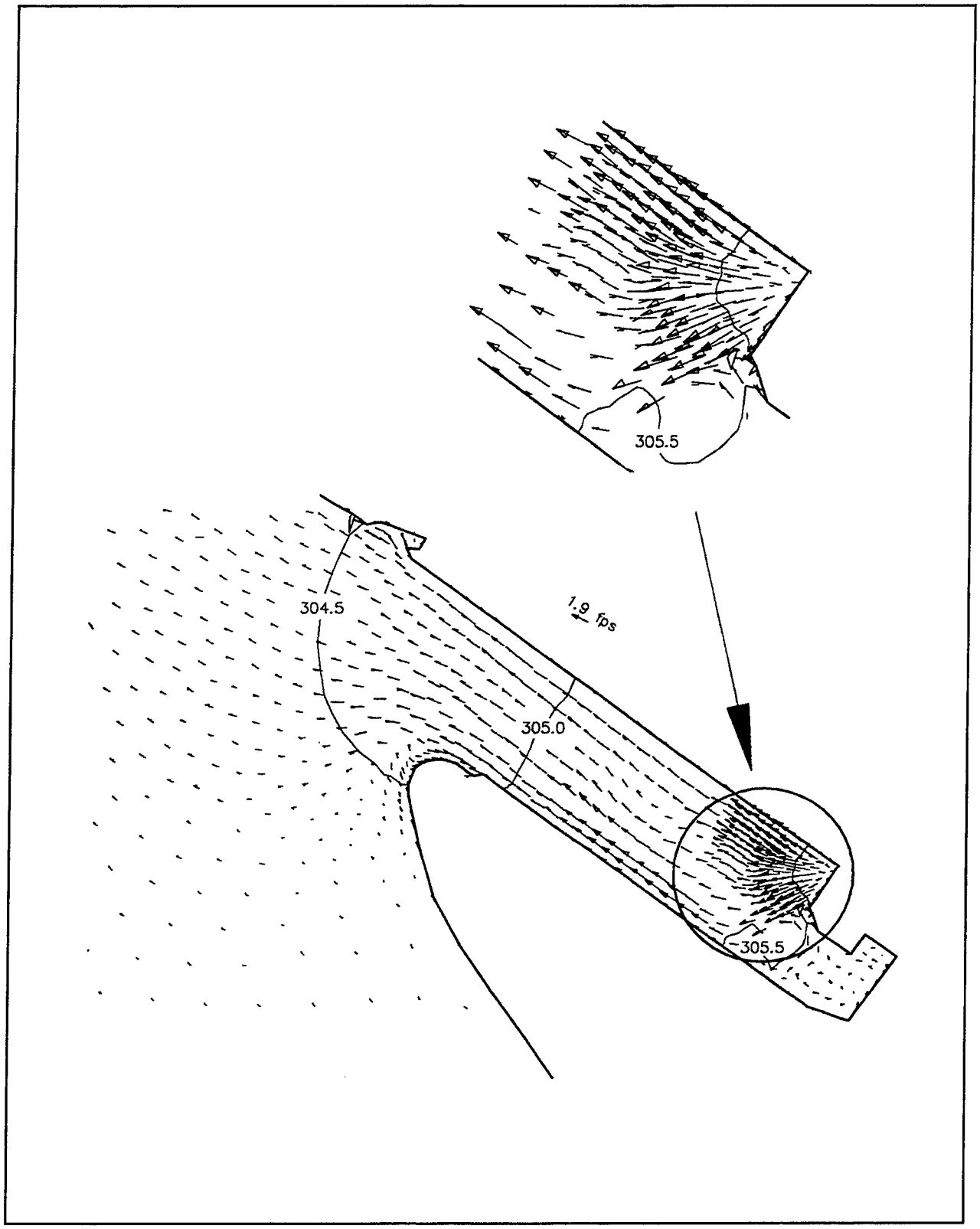

c. Conditions at 360 sec

Figure 16. (Sheet 3 of 3)

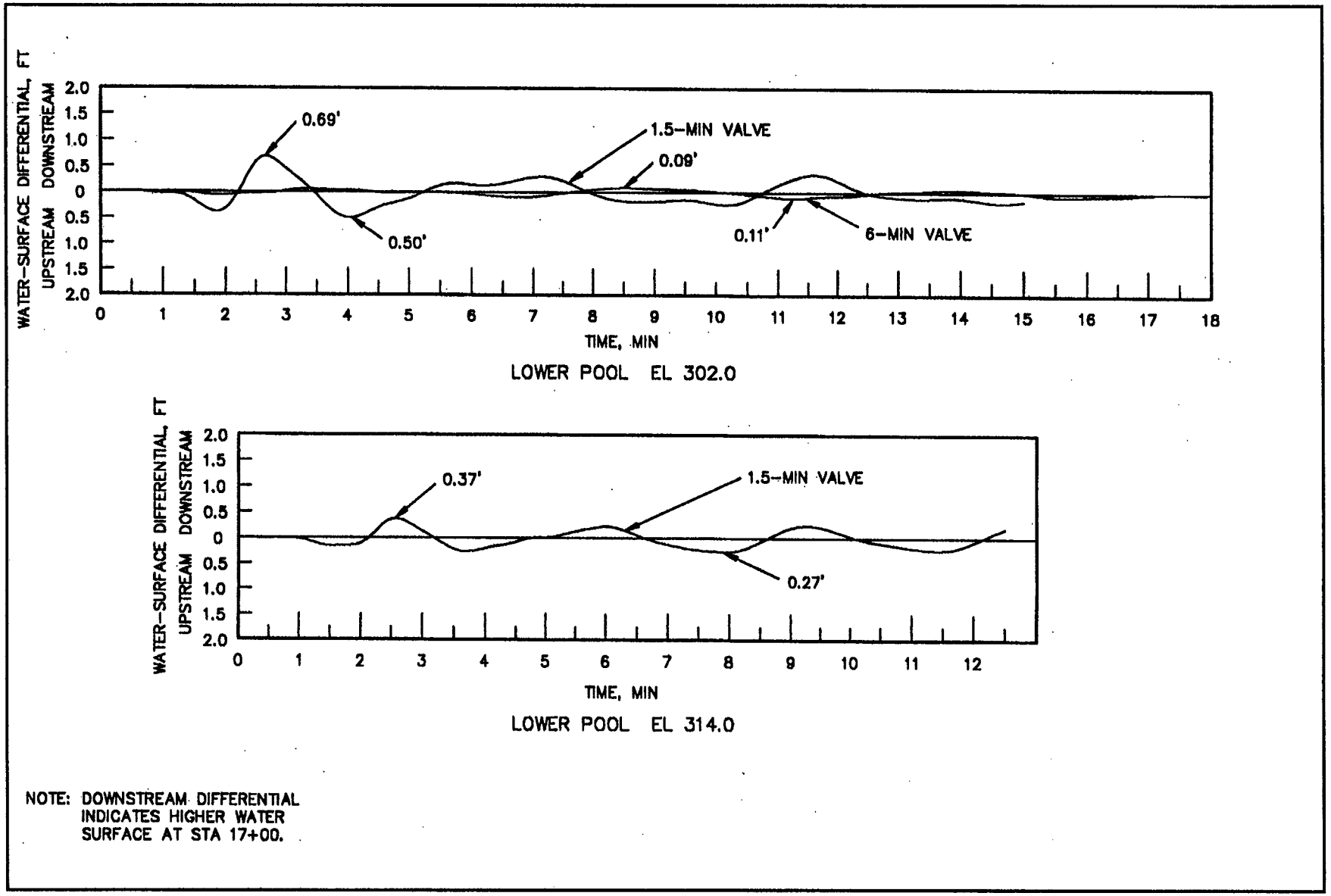

Figure 17. Water-surface elevations, sta 17+00 and 23+00, headwater el 359, 1.5-min valve, landside discharge channel alternative

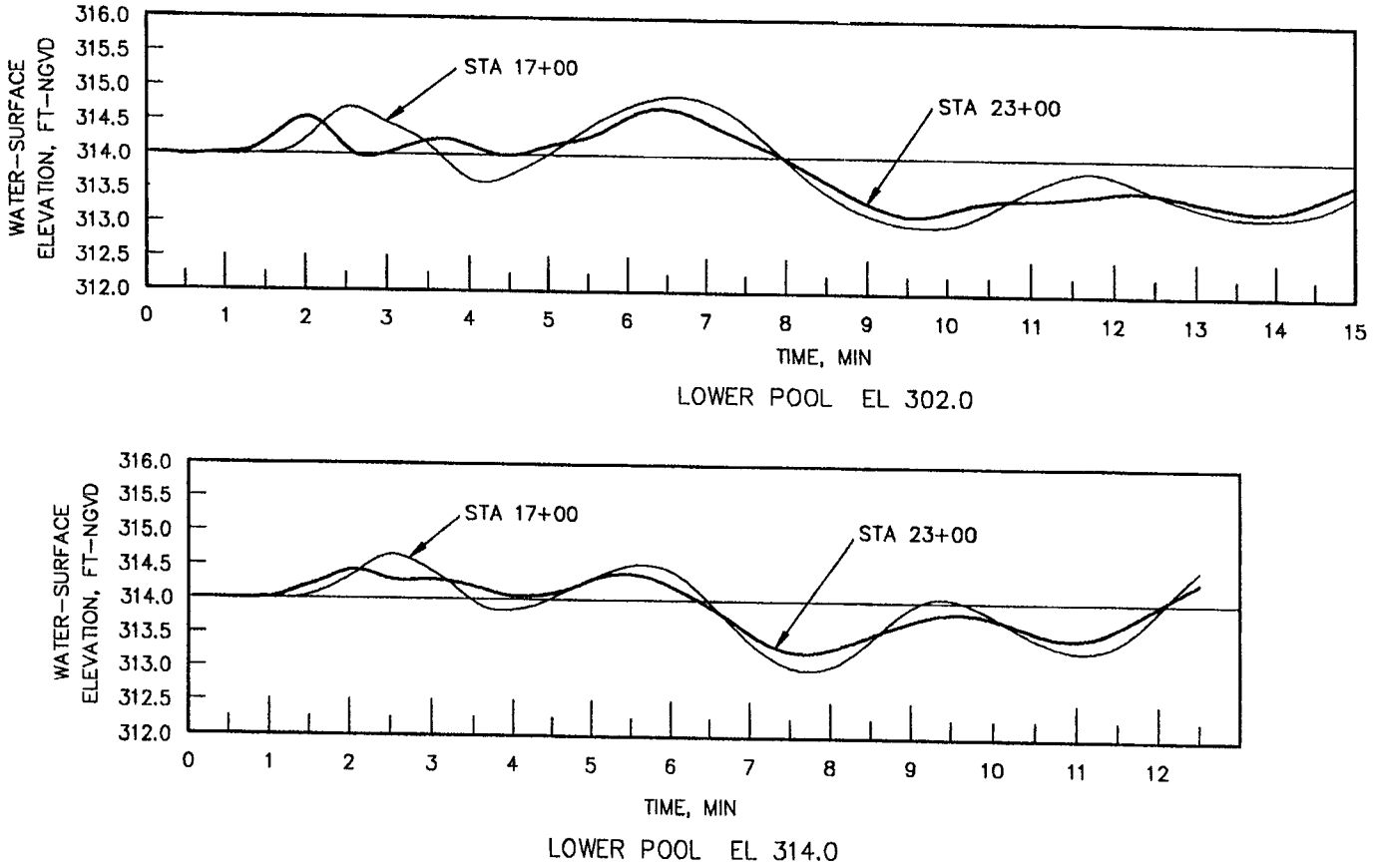

Figure 18. Water-surface differentials between sta 17+00 and 23+00, landside discharge channel alternative

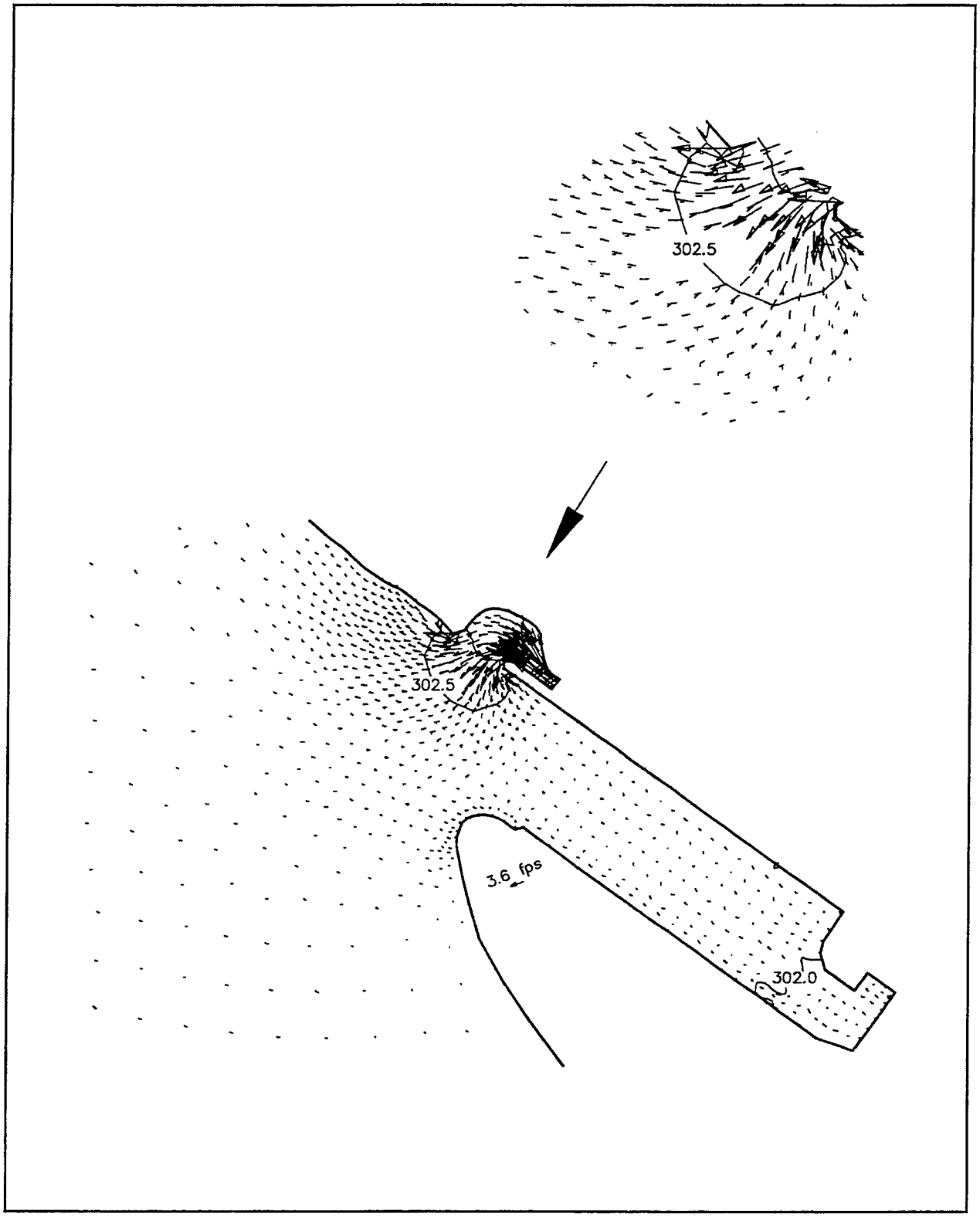

a. Conditions at 90 sec

Figure 19. Velocity vectors and water-surface contours during lock emptying, lower pool el 302, 1.5-min valve, landside discharge channel alternative (Sheet 1 of 3)

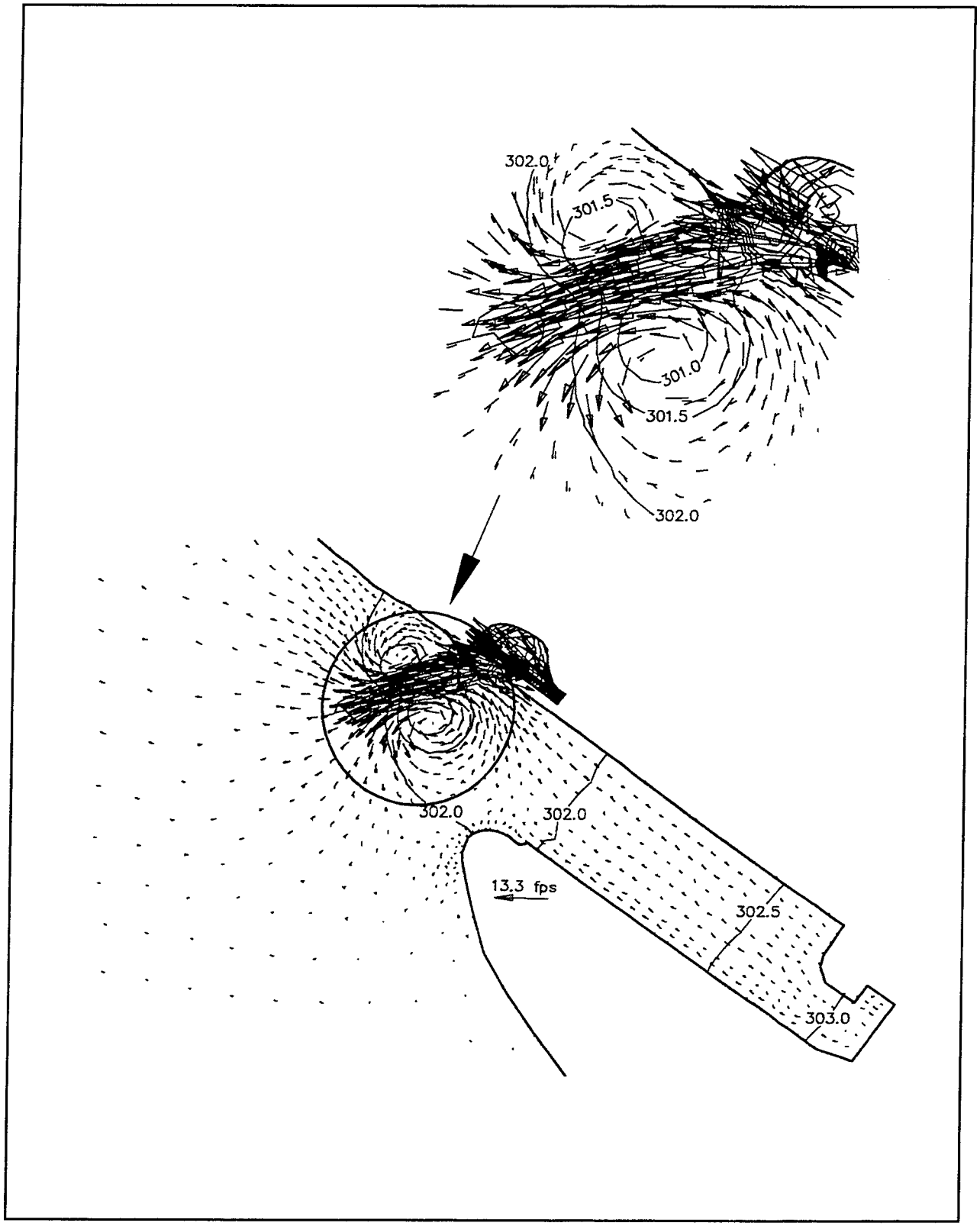

b. Conditions at 180 sec

Figure 19. (Sheet 2 of 3)

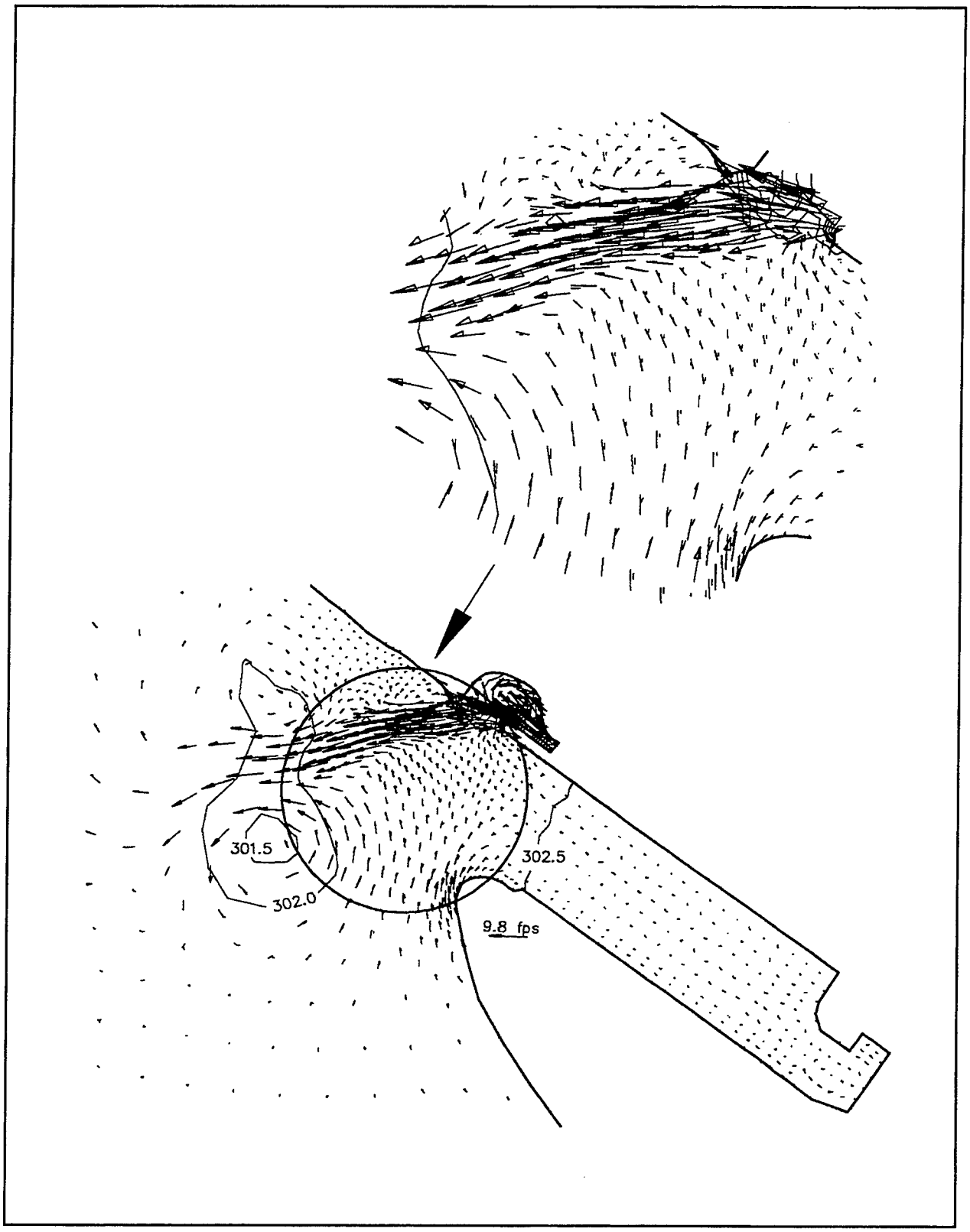

c. Conditions at 360 sec

Figure 19. (Sheet 3 of 3)

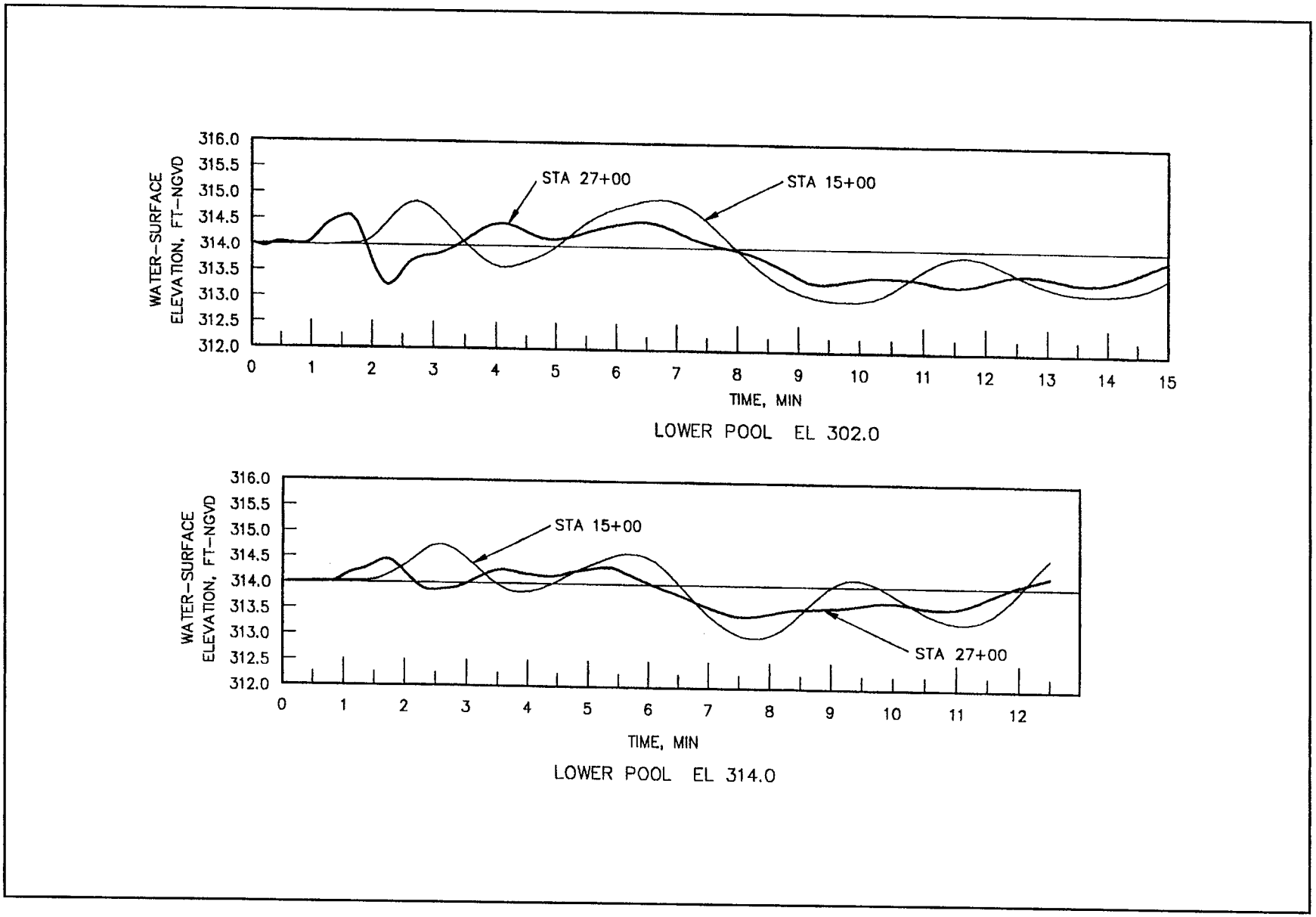

Figure 20. Water-surface elevations, headwater el 359, sta 15+00 and 27+00, 1.5-min valve, landside discharge channel alternative

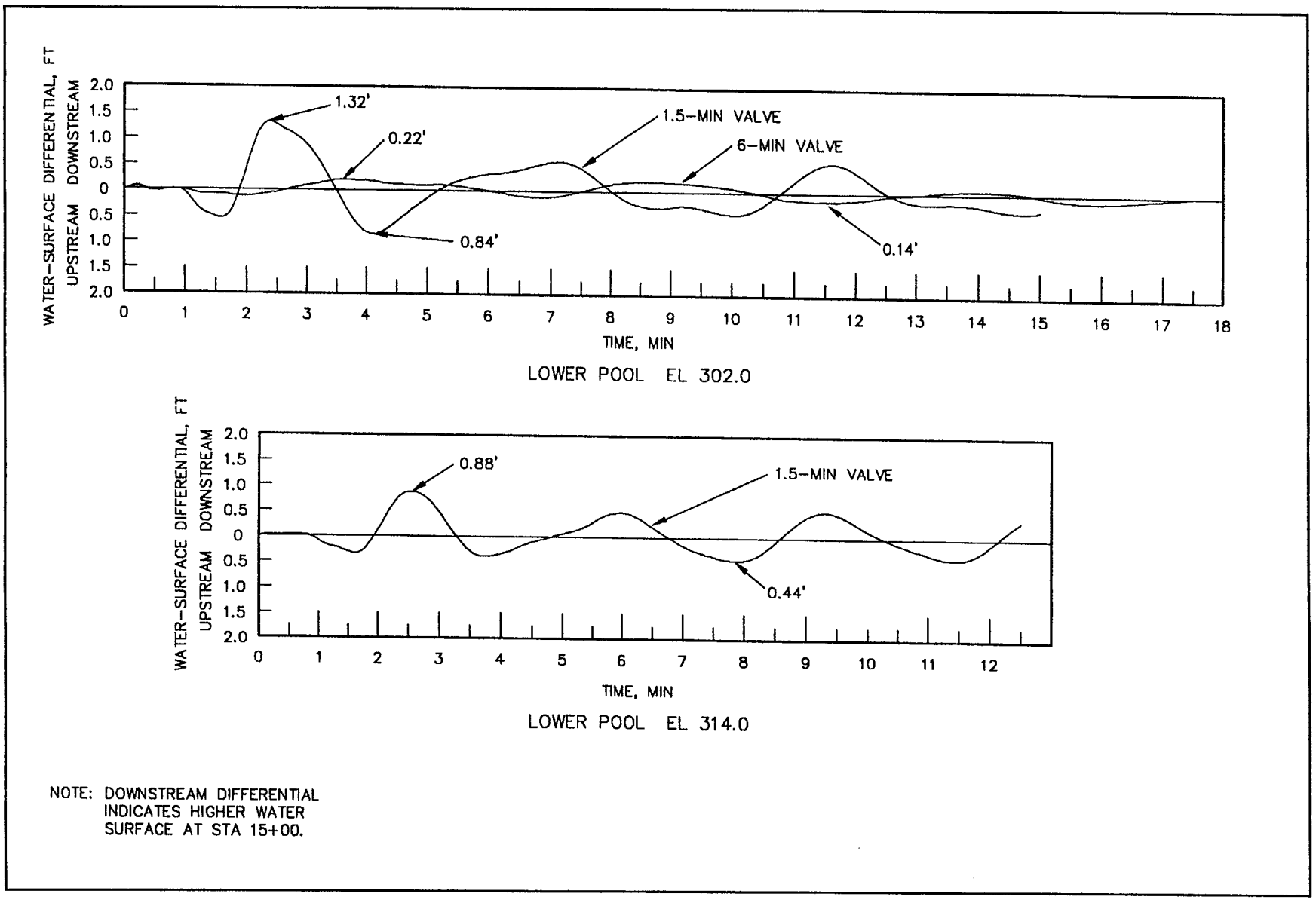

Figure 21. Water-surface differentials between sta 15+00 and 27+00, landside discharge channel alternative

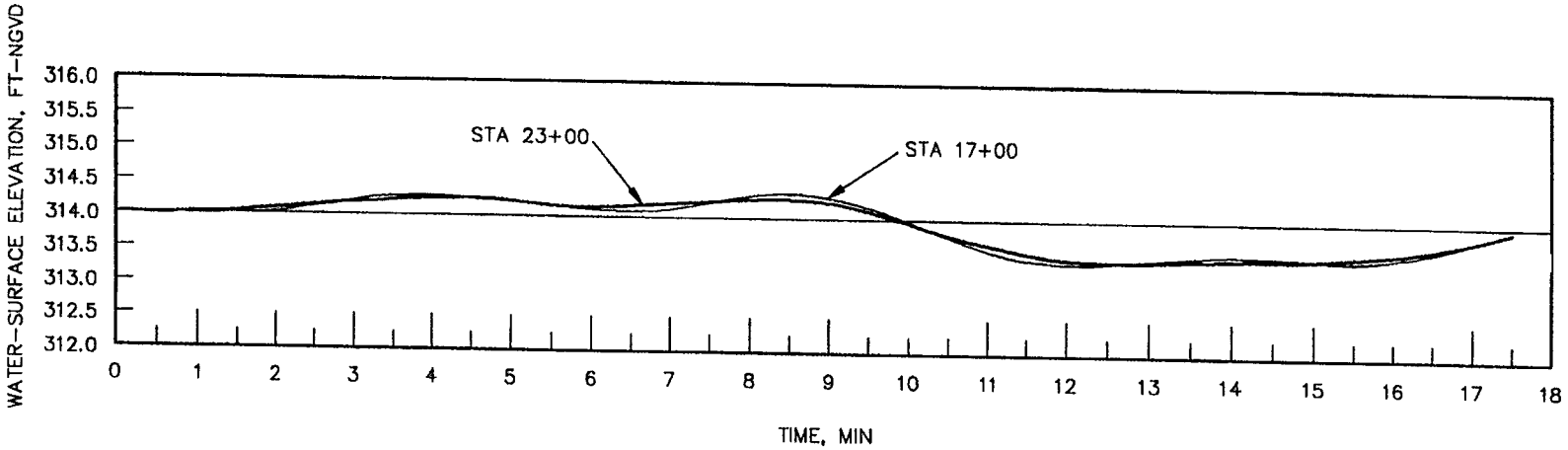

Figure 22. Water-surface elevations, sta 17+00 and 23+00, headwater el 359, tailwater el 302, 6-min valve, landside discharge channel alternative

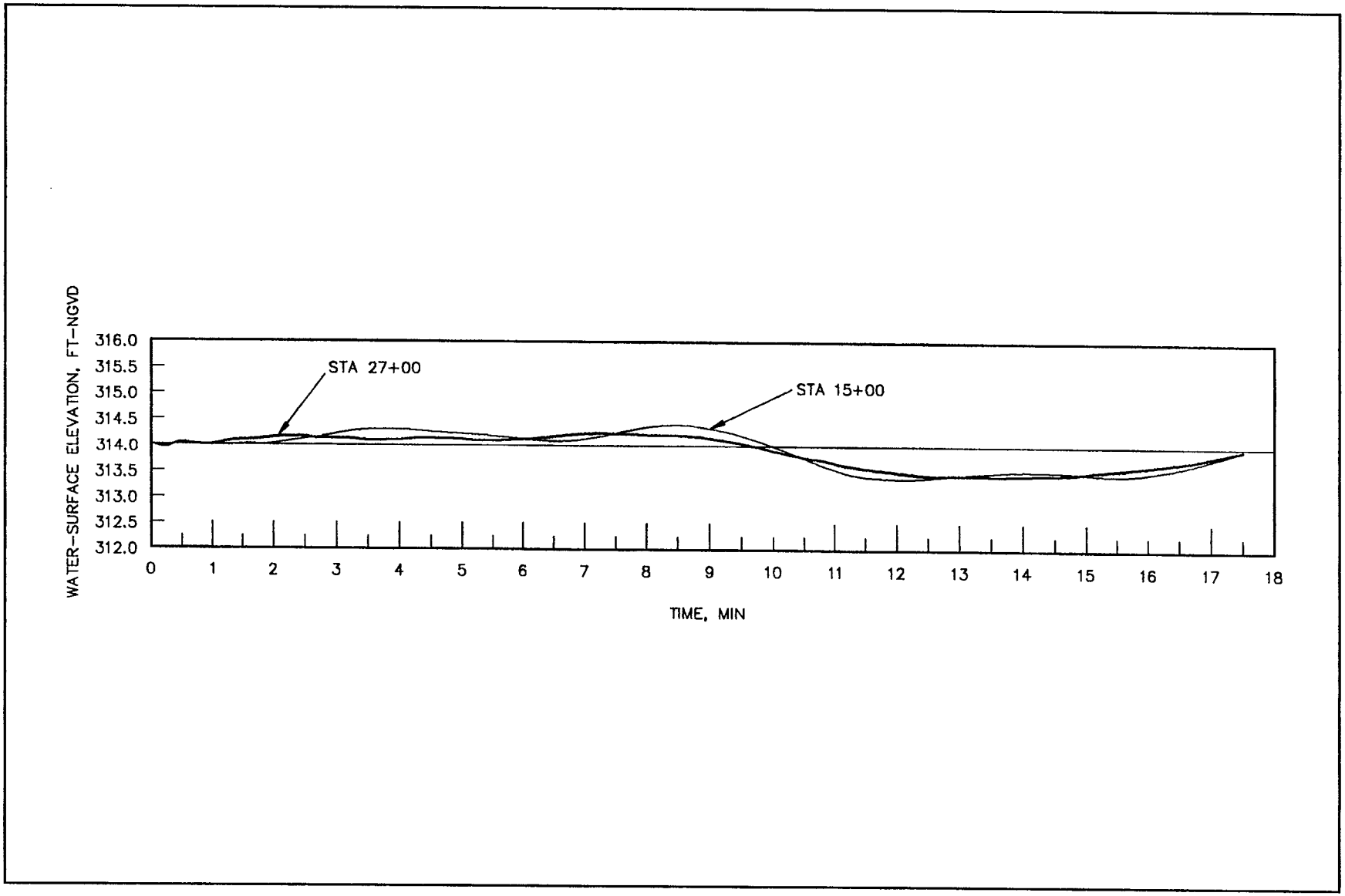

Figure 23. Water-surface elevations, sta 15+00 and 27+00, headwater el 359, tailwater el 302, 6-min valve, landside discharge channel alternative

Table 1
Emptying Valve Hydrograph, 1.5-min Emptying Valve, Interlaced Lateral Discharge Alternative, Headwater El 357, Tailwater El 304.2

Time, sec	Total Discharge, cfs
0	0
2	175.7
4	371.6
6	577.5
8	804.4
10	1013.1
12	1284.5
14	1519.2
16	1789.6
18	2086.7
20	2312
22	2577.7
24	2944.4
26	3254.6
28	3558.5
30	3886.5
32	4231.4
34	4649.6
36	5076.3
38	5509.5
40	5941.8
42	6399.5
44	6868.1
46	7335.3
48	7818.7
50	8320.7
52	8846.3
54	9379.8
46	9914.3
58	10422.6

Table 1 (Continued)

Time, sec	Total Discharge, cfs
60	10907
62	11369.5
64	11818
66	12257.2
68	12674.1
70	13056.1
72	13395.8
74	13704.3
76	13981.3
78	14227.2
80	14433.5
82	14601.4
84	14750.3
86	14883.3
88	14991.1
90	15059.7
92	15082.6
94	15073.8
96	15054.6
98	15039.2
100	15032.8
102	15032.4
104	15030.8
106	15021.1
108	14999.8
110	14967.8
112	14928.9
114	14888.6
116	14850.9
118	14817.7
120	14788.5
122	14761.1

Table 1 (Continued)

Time, sec	Total Discharge, cfs
124	14732.8
126	14701.9
128	14667.9
130	14631.7
132	14594.9
134	14558.8
136	14524.3
138	14491.6
140	14459.9
142	14428.4
144	14396.3
146	14363.1
148	14328.9
150	14294
152	14259
154	14224.2
156	14189.8
158	14155.7
160	14121.8
162	14087.8
164	14053.6
166	14019.3
168	13985
170	13950.8
172	13916.8
174	13883
176	13849.4
178	13815.8
180	13782.1
182	13748.1
184	13714
186	13679.7

Table 1 (Continued)

Time, sec	Total Discharge, cfs
188	13645.4
190	13611.2
192	13577.3
194	13543.7
196	13510.2
198	13476.9
200	13443.6
202	13410.1
204	13376.5
206	13342.8
208	13308.8
210	13274.8
212	13240.7
214	13206.5
216	13172.2
218	13137.9
220	13103.6
222	13069.3
224	13035
226	13000.8
228	12966.7
230	12932.7
232	12898.8
234	12865
236	12831.2
238	12797.4
240	12763.5
242	12729.6
244	12695.5
246	12661.4
248	12627.3
250	12593.3

Table 1 (Continued)

Time, sec	Total Discharge, cfs
252	12559.3
254	12525.5
256	12491.8
258	12458.2
260	12424.6
262	12391.1
264	12357.5
266	12323.8
268	12290.1
270	12256.2
272	12222.3
274	12188.2
276	12154.1
278	12119.9
280	12085.7
282	12051.4
284	12017.2
286	11983
288	11948.8
290	11914.7
292	11880.6
294	11846.6
296	11812.7
298	11778.8
300	11744.9
302	11711.1
304	11677.2
306	11643.2
308	11609.2
310	11575.2
312	11541.2
314	11507.2

Table 1 (Continued)

Time, sec	Total Discharge, cfs
316	11473.3
318	11439.4
320	11405.6
322	11371.8
324	11338.1
326	11304.5
328	11270.8
330	11237.1
332	11203.4
334	11169.6
336	11135.7
338	11101.8
340	11067.8
342	11033.7
344	10999.6
346	10965.4
348	10931.2
350	10897.1
352	10862.9
354	10828.7
356	10794.6
358	10760.6
360	10726.5
362	10692.5
364	10658.6
366	10624.7
368	10590.8
370	10556.8
372	10522.9
374	10489
376	10455
378	10421.1

Table 1 (Continued)

Time, sec	Total Discharge, cfs
380	10387.1
382	10353.1
384	10319.2
386	10285.3
388	10251.4
390	10217.6
392	10183.8
394	10150.1
396	10116.3
398	10082.6
400	10048.8
402	10015
404	9981.2
406	9947.3
408	9913.4
410	9879.4
412	9845.4
414	9811.3
416	9777.2
418	9743.1
420	9708.9
422	9674.8
424	9640.7
426	9606.6
428	9572.5
430	9538.5
432	9504.5
434	9470.5
436	9436.5
438	9402.6
440	9368.6
442	9334.7

Table 1 (Continued)

Time, sec	Total Discharge, cfs
444	9300.7
446	9266.8
448	9232.9
450	9198.9
452	9164.9
454	9131
456	9097.1
458	9063.1
460	9029.2
462	8995.4
464	8961.5
466	8927.7
468	8893.9
470	8860.1
472	8826.3
474	8792.5
476	8758.7
478	8724.9
480	8691
482	8657.1
484	8623.1
486	8589.1
488	8555.1
490	8521
492	8487
494	8452.9
496	8418.8
498	8384.7
500	8350.6
502	8316.5
504	8282.5
506	8248.4

Table 1 (Continued)

Time, sec	Total Discharge, cfs
508	8214.4
510	8180.4
512	8146.4
514	8112.5
516	8078.5
518	8044.5
520	8010.6
522	79.76.6
524	7942.7
526	7908.7
528	7874.8
530	7840.8
532	7806.9
534	7772.9
536	7739
538	7705.1
540	7671.2
542	7637.3
544	7603.5
546	7569.6
548	7535.8
550	7502
552	7468.1
554	7434.3
556	7400.7
558	7366.6
560	7332.7
562	7298.7
564	7264.8
566	7230.8
568	7196.8
570	7162.8

Table 1 (Continued)

Time, sec	Total Discharge, cfs
572	7128.7
574	7094.7
576	7060.6
578	7026.6
580	6992.5
582	6958.4
584	6924.4
586	6890.3
588	6856.3
590	6822.3
592	6788.3
594	6754.3
596	6720.3
598	6686.3
600	6652.3
602	6618.3
604	6584.4
606	6550.4
608	6516.4
610	6482.4
612	6448.5
614	6414.5
616	6380.6
618	6346.6
620	6312.7
622	6278.8
624	6244.8
626	6210.9
628	6177.1
630	6143.2
632	6109.3
634	6075.4

Table 1 (Continued)

Time, sec	Total Discharge, cfs
636	6041.6
638	6007.7
640	5973.8
642	5939.9
644	5906
646	5872.1
648	5838.2
650	5804.2
652	5770.3
654	5736.3
656	5702.3
658	5668.3
660	5634.2
662	5600.2
664	5566.1
666	5532.1
668	5498
670	5464
672	5429.9
674	5395.9
676	5361.8
678	5327.8
680	5293.8
682	5259.7
684	5225.7
686	5191.7
690	5157.7
692	5123.7
694	5089.6
696	5021.6
698	4987.6
700	4953.6

Table 1 (Continued)	
Time, sec	Total Discharge, cfs
702	4919.6
704	4885.6
706	4851.7
708	4817.
710	4783.7
712	4749.7
714	4715.8
716	4681.8
718	4647.9
720	4614
722	4580.1
724	4546.1
726	4512.2
728	4478.3
730	4444.4
732	4410.5
734	4376.6
736	4342.6
738	4308.7
740	4274.7
742	4240.7
744	4206.7
746	4172.7
748	4138.7
750	4104.7
752	4070.6
754	4036.6
756	4002.5
758	3968.4
760	3934.3
762	3900.3
764	3866.2

Table 1 (Continued)	
Time, sec	Total Discharge, cfs
766	3832.1
768	3798
770	3763.9
772	3729.8
774	3695.7
776	3661.6
778	3627.5
780	3593.4
782	3559.2
784	3525.1
786	3491
788	3456.9
790	3422.8
792	3388.7
794	3354.6
796	3320.5
798	3286.4
800	3252.3
802	3218.2
804	3184.1
806	3150
808	3115.9
810	3081.8
812	3047.8
814	3013.7
816	2979.6
818	2945.5
820	2911.5
822	2877.4
824	2843.4
826	2809.3
828	2775.2

Table 1 (Continued)

Time, sec	Total Discharge, cfs
830	2741.1
832	2707
834	2672.9
836	2638.8
838	2604.7
840	2570.6
842	2536.4
844	2502.2
846	2468
848	2433.8
850	2399.6
852	2365.3
854	2331
856	2296.7
858	2262.4
860	2228.1
862	2193.7
864	2159.4
866	2125
868	2090.6
870	2056.1
872	2021.7
874	1987.2
876	1952.7
878	1918.2
880	1883.7
882	1849.1
884	1814.6
886	1780
888	1745.4
890	1710.7
892	1676

Table 1 (Concluded)

Time, sec	Total Discharge, cfs
894	1641.4
896	1606.6
898	1571.9
900	1537.1
902	1502.2
904	1467.3
906	1432.3
908	1397.3
910	1362.2
912	1327.1
914	1291.9
916	1256.7
918	1221.4
920	1186.1
922	1150.6
924	1115.1
926	1079.4
928	1043.5
930	1007.7
932	971.8

Table 2
Emptying Valve Hydrograph, 11.7-min Emptying Valve, Interlaced Lateral Discharge Alternative, Headwater El 357, Tailwater El 304.2

Time, sec	Total Discharge, cfs
0	0
2	24.3
4	43.3
6	67.6
8	91.5
10	114.6
12	138.2
14	161.2
16	184.6
18	207.6
20	230.8
22	251.5
24	270
26	292.9
28	323.2
30	363.2
32	383.7
34	405.1
36	433.2
38	466.2
40	494
42	515.9
44	545.9
46	582.1
48	612.7
50	639.4
52	670.3
54	706.2
46	733.5
58	760.9

Table 2 (Continued)	
Time, sec	Total Discharge, cfs
60	793.5
62	825.2
64	845.8
66	865.2
68	887.7
70	910.8
72	940.1
74	973.5
76	1010.3
78	1051.9
80	1099.1
82	1148.1
84	1178.6
86	1206.6
88	1240.4
90	1275.5
92	1314.2
94	1355.5
96	1381.6
98	1403
100	1428.6
102	1454.4
104	1482.4
106	1513.2
108	1550.2
110	1590.8
112	1633.9
114	1681
116	1732.2
118	1772.5
120	1801.4
122	1832.1

Table 2 (Continued)

Time, sec	Total Discharge, cfs
124	1865.3
126	1900.3
128	1936.8
130	1974.7
132	2014.2
134	2055.5
136	2099.4
138	2140.4
140	2164.7
142	2185.8
144	2212.5
146	2239.8
148	2268
150	2296.4
152	2325.1
154	2354
156	2383.6
158	2414.3
160	2446.4
162	2480.3
164	2516
166	2553.7
168	2593.3
170	2634.9
172	2678.4
174	2723.9
176	2772.5
178	2830.2
180	2894.6
182	2962.5
184	3013.4
186	3044

Table 2 (Continued)

Time, sec	Total Discharge, cfs
188	3074.2
190	3108.5
192	3144.2
194	3180.4
196	3216.3
198	3251.7
200	3287
202	3322.6
204	3359.3
206	3397.6
208	3437.9
210	3480.4
212	3525
214	3571.6
216	3620.2
218	3670.7
220	3723.1
222	3774.4
224	3813.8
226	3847.6
228	3884.7
230	3923.6
232	3963.8
234	4004.6
236	4045.9
238	4087.7
240	4130.3
242	4174
244	4219.1
246	4266
248	4320
250	4380.2

Table 2 (Continued)

Time, sec	Total Discharge, cfs
252	4442.6
254	4507.5
256	4575.4
258	4646.7
260	4704.3
262	4747.6
264	4792
266	4840.2
268	4890.7
270	4942.2
272	4993.8
274	5045.4
276	5097.1
278	5149.7
280	5203.7
282	5259.7
284	5318
286	5378.9
288	5442.5
290	5508.7
292	5574.6
294	5627.5
296	5671.4
298	5717.7
300	5767.2
302	5818.5
304	5870.6
306	5922.7
308	5974.9
310	6027.3
312	6080.7
314	6135.3

Table 2 (Continued)

Time, sec	Total Discharge, cfs
316	6191.7
318	6252.9
320	6319.8
322	6389.7
324	6461.9
326	6520.2
328	6565
330	6610.8
332	6660.9
334	6714.1
336	6768.8
338	6823.5
340	6877.6
342	6931.4
344	6985.5
346	7040.5
348	7069.9
350	7155.2
352	7215.4
354	7277.6
356	7332.9
358	7380.3
360	7427.9
362	7478.1
364	7530.7
366	7584.7
368	7639.2
370	7693.8
372	7748.4
374	7803.6
376	7859.8
378	7917.3

Table 2 (Continued)

Time, sec	Total Discharge, cfs
380	7976.5
382	8037.4
384	8100.1
386	8155.7
388	8203.3
390	8251.3
392	8302.7
394	8356.8
396	8412.6
398	8468.9
400	8525.1
402	8581.2
404	8637.8
406	8695.4
408	8754.3
410	8814.8
412	8877.2
414	8934.6
416	8983.1
418	9027.8
420	9073.7
422	9122.5
424	9173.7
426	9225.8
428	9277.7
430	9329
432	9379.8
434	9430.7
436	9482.2
438	9535
440	9589.2
442	9639.8

Table 2 (Continued)

Time, sec	Total Discharge, cfs
444	9681.1
446	9716.5
448	9751.6
450	9789.1
452	9829.2
454	9870.5
456	9911.6
458	9951.8
460	9991.4
462	10030.7
464	10070.1
466	10110
468	10150.9
470	10189.7
472	10223
474	10252.5
476	10281.6
478	10312.2
480	10344.6
482	10378
484	10411.4
486	10444.2
488	10476.1
490	10507.6
492	10539
494	10570.9
496	10603.5
498	10633.2
500	10657.7
502	10679.2
504	10700.5
506	10723

Table 2 (Continued)

Time, sec	Total Discharge, cfs
508	10747
510	10771.8
512	10796.5
514	10820.4
516	10843.3
518	10865.6
520	10887.8
522	10910.3
524	10933.3
526	10952
528	10964.1
530	10973.1
532	10982
534	10992.3
536	11004.2
538	11016.7
540	11028.7
542	11039.3
544	11048.4
546	11056.4
548	11064
550	11071.8
552	11079.8
554	11085.7
556	11088.7
558	11090.2
560	11091.6
562	11093.4
564	11095.7
566	11098.1
568	11100.2
570	11101.6

Table 2 (Continued)	
Time, sec	Total Discharge, cfs
572	11102.3
574	11102.4
576	11102.4
578	11102.4
580	11102
582	11099.3
584	11094.1
586	11087.8
588	11081.4
590	11075.6
592	11070.2
594	11064.9
596	11059.1
598	11052.5
600	11044.9
602	11036.5
604	11027.7
606	11018.9
608	11009.6
610	10997.9
612	10983.5
614	10967.9
616	10952.1
618	10936.9
620	10922.1
622	10907.4
624	10892.1
626	10876
628	10859
630	10841.2
632	10823
634	10804.8

Table 2 (Continued)

Time, sec	Total Discharge, cfs
636	10786.8
638	10768.6
640	10750.1
642	10731.3
644	10712.2
646	10693
648	10673.6
650	10654.2
652	10634.6
654	10615
656	10595.2
658	10575.3
660	10555.2
662	10535
664	10514.7
666	10492.8
668	10468.6
670	10443.1
672	10417.3
674	10391.8
676	10366.9
678	10342.3
680	10317.5
682	10292.2
684	10266
686	10239.2
688	10211.9
690	10184.5
692	10157.3
694	10129.6
696	10100.2
698	10069

Table 2 (Continued)

Time, sec	Total Discharge, cfs
700	10036.9
702	10004.5
704	9972.5
706	9940.7
708	9909.1
710	9877.2
712	9844.8
714	9811.7
716	9778.1
718	9744.3
720	9710.5
722	9676.9
724	9643.5
726	9610.2
728	9576.9
730	9543.3
732	9509.6
734	9475.6
736	9441.6
738	9407.5
740	9373.5
742	9339.6
744	9305.8
746	9271.9
748	9238.1
750	9204.2
752	9170.3
754	9136.3
756	9102.4
758	9068.4
760	9034.6
762	9000.7

Table 2 (Continued)

Time, sec	Total Discharge, cfs
764	8966.8
766	8932.9
768	8899
770	8865
772	8831
774	8797
776	8763
778	8729
780	8695
782	8661
784	8627
786	8593.1
788	8559.1
790	8525.1
792	8491.2
794	8457.3
796	8423.4
798	8389.5
800	8355.6
802	8321.7
804	8287.8
806	8253.8
808	8219.9
810	8185.9
812	8152
814	8118
816	8084
818	8050
820	8016
822	7982
824	7984
826	7914.1

Table 2 (Continued)	
Time, sec	Total Discharge, cfs
828	7880.1
830	7846.2
832	7812.3
834	7778.3
836	7744.4
838	7710.5
840	7676.6
842	7642.6
844	7608.7
846	7574.7
848	7540.8
850	7506.8
852	7472.8
854	7438.8
856	7404.8
858	7370.8
860	7336.8
862	7302.8
864	7268
866	7234
868	7200.9
870	7167
872	7133
874	7099.1
876	7065.1
878	7031.2
880	6997.3
882	6963.4
884	6929.4
886	6895.5
888	6861.6
890	6827.6

Table 2 (Continued)	
Time, sec	Total Discharge, cfs
892	6793.7
894	6759.7
896	6725.7
898	6691.7
900	6657.7
902	6623.8
904	6589.8
906	6555.8
908	6521.8
910	6487.8
912	6453.9
914	6419.9
916	6386
918	6352
920	6318.1
922	6284.2
924	6250.2
926	6216.3
928	6182.3
930	6148.3
932	6114.4
934	6080.4
936	6046.4
938	6012.4
940	5978.4
942	5944.4
944	5910.4
946	5876.4
948	5842.4
950	5808.4
952	5774.5
954	5740.5

Table 2 (Continued)	
Time, sec	Total Discharge, cfs
956	5706.5
958	5672.5
960	5638.6
962	5604.6
964	5570.7
966	5536.7
968	5502.8
970	5468.8
972	5434.9
974	5400.9
976	5366.9
978	5333
980	5299
982	5265
984	5231
986	5197
988	5163
990	5129
992	5095
994	5061
996	5027
998	4993
1000	4959.1
1002	4925.1
1004	4891.1
1006	4857.1
1008	4823.1
1010	4789.2
1012	4755.2
1014	4721.2
1016	4687.2
1018	4653.2

Table 2 (Continued)	
Time, sec	Total Discharge, cfs
1020	4619.2
1022	4585.2
1024	4551.2
1026	4517.2
1028	4483.2
1030	4449.2
1032	4415.2
1034	4381.2
1036	4347.1
1038	4313.1
1040	4279.1
1042	4245
1044	4211
1046	4177
1048	4143
1050	4108.9
1052	4074.9
1054	4040.9
1056	4006.9
1058	3972.9
1060	3938.9
1062	3904.9
1064	3870.9
1066	3836.8
1068	3802.8
1070	3768.8
1072	3734.8
1074	3700.7
1076	3666.7
1078	3632.6
1080	3598.6
1082	3564.5

Table 2 (Continued)

Time, sec	Total Discharge, cfs
1084	3530.4
1086	3496.4
1088	3462.3
1090	3428.2
1092	3394.2
1094	3360.1
1096	3326
1098	3291.9
1100	3257.8
1102	3223.8
1104	3189.7
1106	3155.6
1108	3121.5
1110	3087.4
1112	3053.3
1114	3019.2
1116	2985.1
1118	2951
1120	2916.8
1122	2882.7
1124	2848.5
1126	2814.4
1128	2780.2
1130	2746
1132	2711.8
1134	2677.6
1136	2643.4
1138	2609.2
1140	2575
1142	2540.8
1144	2506.6
1146	2472.3

Table 2 (Continued)

Time, sec	Total Discharge, cfs
1148	2438.1
1150	2403.8
1152	2369.6
1154	2335.3
1156	2301
1158	2266.8
1160	2232.5
1162	2198.2
1164	2163.8
1166	2129.5
1168	2095.1
1170	2060.8
1172	2026.4
1174	1992
1176	1957.6
1178	1923.1
1180	1888.7
1182	1854.2
1184	1819.7
1186	1785.2
1188	1750.6
1190	1716.1
1192	1681.5
1194	1646.8
1196	1612.2
1198	1577.5
1200	1542.8
1202	1508
1204	1473.1
1206	1438.3
1208	1403.3
1210	1368.2

Table 2 (Concluded)	
Time, sec	**Total Discharge, cfs**
1212	1333.1
1214	1298
1216	1262.7
1218	1227.5
1220	1192.1
1222	1156.7
1224	1121.1
1226	1085.4
1228	1049.5
1230	1013.6
1232	977.6
1234	941.5

Table 3
Hydrograph and Stages at Sta 26+20, 1.5-min Emptying Valve, Headwater EL 359, Tailwater El 302, Landside Discharge Channel Alternative

Time, sec	Total Discharge, cfs	Stage, feet
0	0.00	302.0
2	0	302.0
4	0	302.0
6	0	302.0
8	0	302.0
10	0	302.0
12	0	302.0
14	0	302.0
16	0	302.0
18	0	302.0
20	2E-06	302.0
22	1E-05	302.0
24	9E-05	302.0
26	0.0006	302.0
28	0.003	302.0
30	0.0146	302.0
32	0.0635	302.0
34	0.2495	302.0
36	0.8874	302.0
38	2.8645	302.0
40	8.4071	302.0
42	22.473	302.0
44	54.791	302.0
46	121.94	302.0
48	247.78	302.0
50	459.14	302.0
52	774.23	302.0
54	1185.9	302.0
56	1653.2	302.0
58	2119	301.9

Table 3 (Continued)

Time, sec	Total Discharge, cfs	Stage, feet
60	2550.6	301.9
62	2962.2	301.9
64	3389.8	301.8
66	3848.4	301.8
68	4328.6	301.7
70	4830.3	301.7
72	5372.5	301.6
74	5964.4	301.5
76	6597	301.3
78	7268.5	301.2
80	7986.2	301.0
82	8742.8	300.7
84	9519.5	300.4
86	10317	300.0
88	11153	299.6
90	12027	298.9
92	12912	297.9
94	13784	295.7
96	14003	295.9
98	14538	296.3
100	14790	296.5
102	15211	296.7
104	15475	296.9
106	15815	297.2
108	16047	297.3
110	16306	297.5
112	16503	297.6
114	165.15	297.8
116	16889	297.9
118	17062	298.0
120	17204	298.1

Table 3 (Continued)

Time, sec	Total Discharge, cfs	Stage, feet
122	17339	298.2
124	17447	298.3
126	17541	298.3
128	17614	298.4
130	17686	298.4
132	17759	298.5
134	17833	298.5
136	17894	298.6
138	17935	298.6
140	17952	298.6
142	17953	298.6
144	17945	298.6
146	17934	298.6
148	17923	298.6
150	17912	298.6
152	17898	298.6
154	17882	298.6
156	17861	298.6
158	17837	298.5
160	17810	298.5
162	17780	298.5
164	17745	298.5
166	17704	298.5
168	17658	298.4
170	17606	298.4
172	17551	298.3
174	17494	298.3
176	17436	298.3
178	17377	298.2
180	17318	298.2
182	17258	298.2

Table 3 (Continued)

Time, sec	Total Discharge, cfs	Stage, feet
184	17196	298.1
186	17133	298.1
188	17070	298.0
190	17006	298.0
192	16943	297.9
194	16880	297.9
196	16819	297.9
198	16758	297.8
200	16699	297.8
202	16640	297.7
204	16582	297.7
206	16524	297.7
208	16467	297.6
210	16410	297.6
212	16353	297.5
214	16297	297.5
216	16240	297.5
218	16185	297.4
220	16130	297.4
222	16075	297.3
224	16021	297.3
226	15968	297.3
228	15916	297.2
230	15864	297.2
232	15813	297.2
234	15762	297.1
236	15711	297.1
238	15661	297.1
240	15611	297.0
242	15561	297.0
244	15512	297.0

Table 3 (Continued)		
Time, sec	Total Discharge, cfs	Stage, feet
246	15464	296.9
248	15416	296.9
250	15369	296.9
252	15323	296.8
254	15277	296.8
256	15231	296.8
258	15186	296.7
260	15141	296.7
262	15096	296.7
264	15052	296.6
266	15008	296.6
268	14965	296.6
270	14922	296.5
272	14880	296.5
274	14838	296.5
276	14796	296.5
278	14755	296.4
280	14714	296.4
282	14673	296.4
284	14633	296.3
286	14593	296.3
288	14554	296.3
290	14515	296.3
292	14476	296.2
294	14438	296.2
296	14400	296.2
298	14362	296.1
300	14324	296.1
302	14287	296.1
304	14249	296.1
306	14212	296.0

Table 3 (Continued)

Time, sec	Total Discharge, cfs	Stage, feet
308	14176	296.0
310	14139	296.0
312	14102	296.0
314	14066	295.9
316	14029	295.9
318	13992	295.9
320	13955	295.9
322	13919	295.8
324	13882	295.8
326	13846	295.8
328	13810	295.7
330	13775	295.7
332	13740	295.7
334	13705	295.7
336	13670	295.6
338	13633	295.8
340	13562	296.4
342	13479	296.7
344	13430	296.9
346	13363	297.1
348	13302	297.2
350	13248	297.3
352	13182	297.5
354	13132	297.6
356	13068	297.7
358	13018	297.8
360	12959	297.8
362	12907	297.9
364	12853	298.0
366	12798	298.1
368	12746	298.1

Table 3 (Continued)

Time, sec	Total Discharge, cfs	Stage, feet
370	12692	298.2
372	12641	298.3
374	12588	298.3
376	12537	298.4
378	12486	298.5
380	12436	298.5
382	12386	298.6
384	12337	298.6
386	12289	298.7
388	12240	298.7
390	12193	298.8
392	12145	298.8
394	12098	298.8
396	12051	298.9
398	12005	298.9
400	11959	299.0
402	11913	299.0
404	11866	299.0
406	11819	299.1
408	11773	299.1
410	11726	299.2
412	11679	299.2
414	11631	299.2
416	11584	299.3
418	11536	299.3
420	11488	299.3
422	11439	299.4
424	11391	299.4
426	11342	299.4
428	11294	299.5
430	11245	299.5

Table 3 (Continued)

Time, sec	Total Discharge, cfs	Stage, feet
432	11196	299.5
434	11147	299.6
436	11097	299.6
438	11047	299.6
440	10997	299.7
442	10947	299.7
444	10898	299.7
446	10848	299.7
448	10799	299.8
450	10750	299.8
452	10700	299.8
454	10650	299.9
456	10598	299.9
458	10543	299.9
460	10482	300.0
462	10413	300.0
464	10337	300.0
466	10256	300.1
468	10174	300.1
470	10095	300.1
472	10023	300.2
474	9954.7	300.2
476	9889.3	300.2
478	9826.3	300.3
480	9765.1	300.3
482	9703.1	300.3
484	9636.7	300.4
486	9565.3	300.4
488	9492.3	300.4
490	9422	300.4
492	9355.9	300.5

Table 3 (Continued)

Time, sec	Total Discharge, cfs	Stage, feet
494	9294.1	300.5
496	9236	300.5
498	9181.5	300.5
500	9129.7	300.6
502	9080	300.6
504	9032.9	300.6
506	8990.6	300.6
508	8955.9	300.6
510	8930.9	300.6
512	8916.3	300.6
514	8910.5	300.6
516	8909.5	300.6
518	8906.5	300.6
520	8894.2	300.7
522	8867.2	300.7
524	8824.6	300.7
526	8770.5	300.7
528	8712	300.7
530	8654.5	300.7
532	8599.1	300.8
534	8543.4	300.8
536	8485.9	300.8
538	8428.7	300.8
540	8376.9	300.8
542	8332.9	300.8
544	8294.7	300.9
546	8257.2	300.9
548	8217.2	300.9
550	8174.9	300.9
552	8132.7	300.9
554	8092.3	300.9

Table 3 (Continued)

Time, sec	Total Discharge, cfs	Stage, feet
556	8054.3	300.9
558	8018.9	300.9
560	7986.3	301.0
562	7955.9	301.0
564	7927.5	301.0
566	7900.6	301.0
568	7875.4	301.0
570	7851.3	301.0
572	7827.8	301.0
574	7804.8	301.0
576	7782.3	301.0
578	7760.6	301.0
580	7740.4	301.0
582	7721.8	301.0
584	7704.7	301.0
586	7688.2	301.0
590	7651.2	301.1
592	7628.7	301.1
594	7603.3	301.1
596	7576	301.1
598	7547.7	301.1
600	7519.1	301.1
602	7490.1	301.1
604	7460.2	301.1
606	7428.7	301.1
608	7395	301.1
610	7358.8	301.1
612	7320	301.1
614	7279	301.2
616	7236.2	301.2
618	7191.9	301.2

Table 3 (Continued)

Time, sec	Total Discharge, cfs	Stage, feet
620	7146.7	301.2
622	7101.1	3-1.2
624	7055.9	301.2
626	7012.2	301.2
628	6971.1	301.2
630	6933.8	301.2
632	6900.9	301.2
634	6872.8	301.3
636	6849	301.3
638	6828.7	301.3
640	6810.4	301.3
642	6792.3	301.3
644	6773	301.3
646	6750.9	301.3
648	6725.5	301.3
650	6696.2	301.3
652	6663.3	301.3
654	6627.3	301.3
656	6588.9	301.3
658	6548.6	301.3
660	6507.3	301.3
662	6465.3	301.3
664	6422.8	301.4
666	6379.6	301.4
668	6335.5	301.4
670	6290.2	301.4
672	6243.5	301.4
674	6195.8	301.4
676	6147.4	301.4
678	6098.9	301.4
680	6050.7	301.4

Table 3 (Continued)		
Time, sec	Total Discharge, cfs	Stage, feet
682	6003	301.4
684	5955.9	301.5
686	5909.7	301.5
688	5864.3	301.5
690	5819.7	301.5
692	5775.8	301.5
694	5732.4	301.5
696	5689.5	301.5
698	5647.2	301.5
700	5605.6	301.5
702	5564.7	301.5
704	5524.5	301.5
706	5484.7	301.5
708	5445.2	301.6
710	5405.9	301.6
712	5366.6	301.6
714	5327.5	301.6
716	5288.6	301.6
718	5249.9	301.6
720	5211.2	301.6
722	5172.3	301.6
724	5132.9	301.6
726	5092.6	301.6
728	5051	301.6
730	5007.7	301.6
732	4962.6	301.6
734	4915.4	301.6
736	4866.2	301.6
738	4815.3	301.7
740	4763.1	301.7
742	4710.2	301.7

Table 3 (Continued)

Time, sec	Total Discharge, cfs	Stage, feet
744	4657.3	301.7
746	4605.2	301.7
748	4554.6	301.7
750	4506.1	301.7
752	4460.1	301.7
754	4416.8	301.7
756	4376.2	301.7
758	4338	301.7
760	4301.7	301.7
762	4266.8	301.7
764	4232.7	301.7
766	4198.9	301.7
768	4165	301.7
770	4130.7	301.7
772	4096.1	301.8
774	4060.9	301.8
776	4025.4	301.8
778	3989.4	301.8
780	3952.8	301.8
782	3915.5	301.8
784	3877.5	301.8
786	3838.5	301.8
788	3798.5	301.8
790	3757.6	301.8
792	3716	301.8
794	3673.8	301.8
796	3631.4	301.8
798	3589	301.8
800	3546.9	301.8
802	3505.3	301.8
804	3464.2	301.8

Table 3 (Continued)

Time, sec	Total Discharge, cfs	Stage, feet
806	3423.7	301.8
808	3383.8	301.8
810	3344.4	301.8
812	3305.5	301.8
814	3267	301.8
816	3228.9	301.8
818	3191.1	301.9
820	3153.8	301.9
822	3117	301.9
824	3080.7	301.9
826	3045	301.9
828	3010.1	301.9
830	2975.9	301.9
832	2942.5	301.9
834	2909.8	301.9
836	2877.6	301.9
838	2845.7	301.9
840	2813.6	301.9
842	2781.1	301.9
844	2747.7	301.9
846	2713	301.9
848	2676.8	301.9
850	2639	301.9
852	2599.4	301.9
854	2558.2	301.9
856	2515.5	301.9
858	2471.8	301.9
860	2427.4	301.9
862	2382.7	301.9
864	2338.1	301.9
866	2294.1	301.9

Table 3 (Concluded)

Time, sec	Total Discharge, cfs	Stage, feet
868	2251	301.9
870	2208.7	301.9
872	2167.6	301.9
874	2127.5	301.9
876	2088.5	301.9
878	2050.3	301.9
880	2012.8	301.9
882	1976	301.9
884	1939.7	301.9
886	1903.7	301.9
888	1867.9	301.9
890	1832.2	302.0
892	1796.2	302.0
894	1759.9	302.0
896	1722.9	302.0
898	1685.2	302.0
900	1646.5	302.0
902	1606.8	302.0
904	1566	302.0
906	1524.4	302.0
908	1481.9	302.0
910	1438.9	302.0
912	1395.5	302.0
914	1351.8	302.0
916	1308	302.0
918	1264.2	302.0
920	1220.4	302.0
922	1176.7	302.0

Table 4
Hydrograph and Stages at Sta 26+20, 1.5-min Emptying Valve, Headwater El 359, Tailwater EL 314, Landside Discharge Channel Alternative

Time, sec	Total Discharge, cfs	Stage, feet
0	0	314.0
2	0	314.0
4	0	314.0
6	0	314.0
8	0	314.0
10	0	314.0
12	0	314.0
14	0	314.0
16	2.5701E-06	314.0
18	1.4875E05	314.0
20	0.00010724	314.0
22	0.0006851	314.0
24	0.00388801	314.0
26	0.0194718	314.0
28	0.08675722	314.0
30	0.3452752	314.0
32	1.231922	314.0
34	3.951802	314.0
36	11.42364	314.0
38	29.81327	314.0
40	70.34557	314.0
42	150.2311	314.0
44	290.6227	314.0
46	509.6554	314.0
48	811.3852	314.0
50	1176.976	314.0
52	1568.432	314.0
54	1948.892	314.0
56	2305.967	314.0
58	2654.913	314.0

Table 4 (Continued)

Time, sec	Total Discharge, cfs	Stage, feet
60	3016.962	314.0
62	3397.985	314.0
64	3792.553	313.9
66	4203.528	313.9
68	4645.935	313.9
70	5130.179	313.9
72	5653.517	313.9
74	6214.077	313.9
76	6822.334	313.8
78	7488.36	313.8
80	8204.276	313.7
82	8951.315	313.7
84	9723.485	313.6
86	10533.33	313.6
88	11389.62	313.5
90	12277.82	313.4
92	13169.74	313.3
94	14042.73	313.2
96	14879.88	313.1
98	15666.27	313.0
100	16399.73	312.9
102	17092.11	312.7
104	17749.46	312.6
106	18362.52	312.5
108	18920.27	312.4
110	19422.11	312.3
112	19874.85	312.2
114	20283.29	312.1
116	20644.92	312.0
118	20953.43	311.9
120	21205.87	311.8

Table 4 (Continued)		
Time, sec	Total Discharge, cfs	Stage, feet
122	21402.79	311.8
124	21543.27	311.7
126	21625.8	311.7
128	21658.55	311.7
130	21665.29	311.7
132	21675.88	311.7
134	21707.16	311.7
136	21751.3	311.7
138	21785.11	311.7
140	21792.48	311.7
142	21774.12	311.7
144	21735.16	311.7
146	21676.99	311.7
148	21599.58	311.7
150	21500.17	311.7
152	21375.61	311.8
154	21226.32	311.8
156	21055.36	311.9
158	20866.89	311.9
160	20663.64	312.0
162	20445.76	312.0
164	20213.55	312.1
166	19969.5	312.1
168	19717.09	312.2
170	19459.34	312.3
172	19198.6	312.3
174	18936.76	312.4
176	18674.16	312.4
178	18409.35	312.5
180	18140.34	312.5
182	17866.13	312.6

Table 4 (Continued)

Time, sec	Total Discharge, cfs	Stage, feet
184	17587.51	312.7
186	17306.71	312.7
188	17026.22	312.8
190	16747.62	312.8
192	16471.21	312.8
194	16196.01	312.9
196	15919.79	312.9
198	15639.69	313.0
200	15353.54	313.0
202	15060.67	313.1
204	14761.4	313.1
206	14455.62	313.1
208	14142.28	313.2
210	13820.17	313.2
212	13488.79	313.3
214	13148.76	313.3
216	12802.1	313.3
218	12452.58	313.4
220	12105.58	313.4
222	11767.31	313.5
224	11443.6	313.5
226	11138.6	313.5
228	10853.67	313.5
230	10587.02	313.6
232	10334.44	313.6
234	10090.84	313.6
236	9852.238	313.6
238	9616.955	313.6
240	9385.33	313.7
242	9158.299	313.7
244	8936.149	313.7

Table 4 (Continued)

Time, sec	Total Discharge, cfs	Stage, feet
246	8718.41	313.7
248	8505.159	313.7
250	8298.689	313.7
252	8103.81	313.8
254	7926.276	313.8
256	7770.491	313.8
258	7638.222	313.8
260	7529.284	313.8
262	7443.203	313.8
264	7379.898	313.8
266	7338.828	313.8
268	7318.033	313.8
270	7314.333	313.8
272	7324.143	313.8
274	7343.966	313.8
276	7370.825	313.8
278	7402.939	313.8
280	7440.018	313.8
282	7482.745	313.8
284	7532	313.8
286	7588.497	313.8
288	7653.066	313.8
290	7727.165	313.8
292	7812.928	313.8
294	7912.609	313.8
296	8028.009	313.8
298	8160.181	313.7
300	8309.322	313.7
302	8474.886	313.7
304	8655.85	313.7
306	8850.931	313.7

Table 4 (Continued)

Time, sec	Total Discharge, cfs	Stage, feet
308	9058.375	313.7
310	9275.27	313.7
312	9496.85	313.7
314	9716.598	313.6
316	9927.487	313.6
318	10124.02	313.6
320	10304.04	313.6
322	10469.34	313.6
324	10624.39	313.6
326	10774.21	313.5
328	109.22.4	313.5
330	11070.47	313.5
332	11218.28	313.5
334	11364.77	313.5
336	11508.2	313.5
338	11645.99	313.5
340	11775.04	313.5
342	11892.48	313.4
344	11996.5	313.4
346	12086.6	313.4
348	12163.3	313.4
350	12227.68	313.4
352	12281.07	313.4
354	12324.66	313.4
356	12359.31	313.4
358	12385.66	313.4
360	12404.31	313.4
362	12415.87	313.4
364	12420.79	313.4
366	12419.14	313.4
368	12410.52	313.4

Table 4 (Continued)

Time, sec	Total Discharge, cfs	Stage, feet
370	12394.22	313.4
372	12369.46	313.4
374	12335.55	313.4
376	12291.99	313.4
378	12238.33	313.4
380	12174.04	313.4
382	12098.59	313.4
384	12011.59	313.4
386	11912.96	313.4
388	11803.13	313.5
390	11683	313.5
392	11553.93	313.5
394	11417.52	313.5
396	11275.49	313.5
398	11129.59	313.5
400	10981.51	313.5
402	10832.83	313.5
404	10684.9	313.6
406	10538.74	313.6
408	10394.89	313.6
410	10253.29	313.6
412	10113.31	313.6
414	9973.869	313.6
416	9833.57	313.6
418	9691.017	313.6
420	9545.062	313.7
422	9395.026	313.7
424	9240.815	313.7
426	9082.917	313.7
428	8922.288	313.7
430	8760.189	313.7

Table 4 (Continued)		
Time, sec	Total Discharge, cfs	Stage, feet
432	8597.986	313.7
434	8436.99	313.7
436	8278.334	313.7
438	8122.902	313.8
440	7971.307	313.8
442	7823.898	313.8
444	7680.82	313.8
446	7542.085	313.8
448	7407.655	313.8
450	7277.509	313.8
452	7151.672	313.8
454	7030.22	313.8
456	6913.262	313.8
458	6800.937	313.8
460	6693.419	313.8
462	6590.946	313.8
464	6493.837	313.8
466	6402.497	313.8
468	6317.397	313.9
470	6239.042	313.9
472	6167.92	313.9
474	6104.467	313.9
476	6049.005	313.9
478	6001.696	313.9
480	5962.474	313.9
482	5930.997	313.9
484	5906.616	313.9
486	5888.404	313.9
488	5875.234	313.9
490	5865.921	313.9
492		

Table 4 (Continued)		
Time, sec	Total Discharge, cfs	Stage, feet
494	5854.785	313.9
496	5851.655	313.9
498	5849.921	313.9
500	5849.907	313.9
502	5852.28	313.9
504	5857.959	313.9
506	5867.987	313.9
508	5883.375	313.9
510	5904.934	313.9
512	5933.113	313.9
514	5967.902	313.9
516	6008.79	313.9
518	6054.818	313.9
520	6104.699	313.9
522	6156.972	313.9
524	6210.179	313.9
526	6263.019	313.9
528	6314.445	313.9
530	6363.718	313.8
532	6410.393	313.8
534	6454.262	313.8
536	6495.286	313.8
538	6533.516	313.8
540	6569.035	313.8
542	6601.929	313.8
544	6632.261	313.8
546	6660.074	313.8
548	6685.375	313.8
550	6708.133	313.8
552	6728.255	313.8
554	6745.579	313.8

Table 4 (Continued)

Time, sec	Total Discharge, cfs	Stage, feet
556	6759.863	313.8
558	6770.803	313.8
560	6778.061	313.8
562	6781.311	313.8
564	6780.288	313.8
566	6774.833	313.8
568	6764.919	313.8
570	6750.668	313.8
572	6732.328	313.8
574	6710.243	313.8
576	6684.791	313.8
578	6656.313	313.8
580	6625.047	313.8
582	6591.071	313.8
584	6554.277	313.8
586	6514.372	313.8
588	6470.924	313.8
590	6423.422	313.8
592	6371.364	313.8
594	6314.333	313.9
596	6252.075	313.9
598	6184.552	313.9
600	6111.964	313.9
602	6034.745	313.9
604	5953.529	313.9
606	5869.097	313.9
608	5782.301	313.9
610	5693.99	313.9
612	5604.94	313.9
614	5515.795	313.9
616	5427.033	313.9

Table 4 (Continued)

Time, sec	Total Discharge, cfs	Stage, feet
618	5338.948	313.9
620	5251.662	313.9
622	5165.147	313.9
624	5079.26	313.9
626	4993.789	313.9
628	4908.497	313.9
630	4823.156	313.9
632	4737.584	313.9
634	4651.661	313.9
636	4565.347	313.9
638	4478.688	313.9
640	4391.821	313.9
642	4304.971	313.9
644	4218.442	313.9
646	4132.603	313.9
648	4047.863	313.9
650	3964.642	313.9
652	3883.338	313.9
654	3804.295	313.9
656	3727.776	313.9
658	3653.951	314.0
660	3582.89	314.0
662	3514.585	314.0
664	3448.967	314.0
666	3385.948	314.0
668	3325.458	314.0
670	3267.476	314.0
672	3212.053	314.0
674	3159.319	314.0
676	3109.47	314.0
678	3062.74	314.0

Table 4 (Continued)

Time, sec	Total Discharge, cfs	Stage, feet
680	3019.362	314.0
682	2979.52	314.0
684	2943.309	314.0
686	2910.703	314.0
688	2881.536	314.0
690	2855.512	314.0
692	2832.22	314.0
694	2811.18	314.0
696	2791.884	314.0
698	2773.853	314.0
700	2756.686	314.0
702	2740.089	314.0
704	2723.904	314.0
706	2708.107	314.0
708	2692.799	314.0
710	2678.173	314.0
712	2664.482	314.0
714	2651.998	314.0
716	2640.969	314.0
718	2631.585	314.0
720	2623.95	314.0
722	2618.061	314.0
724	2613.798	314.0
726	2610.929	314.0
728	2609.114	314.0
730	2607.927	314.0
732	2606.88	314.0
734	2605.46	314.0
736	2603.154	314.0
738	2599.494	314.0
740	2594.083	314.0

Table 4 (Concluded)

Time, sec	Total Discharge, cfs	Stage, feet
742	2586.622	314.0
744	2576.924	314.0
746	2564.912	314.0
748	2550.611	314.0
750	2534.118	314.0
752	2515.577	314.0
754	2495.139	314.0
756	2472.932	314.0
758	2449.038	314.0
760	2423.477	314.0
762	2396.214	314.0
764	2367.164	314.0
766	2336.219	314.0
768	2303.273	314.0
770	2268.248	314.0
772	2231.111	314.0
774	2191.893	314.0
776	2150.679	314.0
778	2107.607	314.0
780	2062.844	314.0
782	2016.564	314.0
784	1968.924	314.0
786	1920.044	314.0
788	1869.989	314.0
790	1818.767	314.0
792	1766.326	314.0
794	1712.57	314.0
796	1657.374	314.0
798	1600.608	314.0
800	1542.158	314.0

Table 5
Hydrograph and Stages at Sta 26+20, 6-min Emptying Valve, Headwater El 359, Tailwater El 302, Lanside Discharge Channel Alternative

Time, sec	Total Discharge, cfs	Stage, feet
0	0.00	302.0
2	0	302.0
4	0	302.0
6	0	302.0
8	0	302.0
10	0	302.0
12	0	302.0
14	0	302.0
16	0	302.0
18	0	302.0
20	4.7793E-07	302.0
22	3.1424E-06	302.0
24	2.1375E-05	302.0
26	0.00012973	302.0
28	0.00069445	302.0
30	0.00334921	302.0
32	0.01452084	302.0
34	0.05676994	302.0
36	0.2006171	302.0
38	0.6420375	302.0
40	1.863379	302.0
42	4.909262	302.0
44	11.7485	302.0
46	25.5475	302.0
48	50.48649	302.0
50	90.68285	302.0
52	148.1404	302.0
54	220.5676	302.0
56	300.9068	302.0
58	380.1743	302.0

Table 5 (Continued)

Time, sec	Total Discharge, cfs	Stage, feet
60	452.7185	302.0
62	519.8619	302.0
64	588.0554	302.0
66	662.6149	302.0
68	743.0439	302.0
70	824.6349	302.0
72	904.0706	302.0
74	982.2689	302.0
76	1061.704	302.0
78	1142.69	302.0
80	1223.829	302.0
82	1305.742	302.0
84	1393.071	302.0
86	1492.086	302.0
88	1605.712	302.0
90	1729.985	302.0
92	1855.399	302.0
94	1973.395	301.9
96	2083.36	301.9
98	2193.718	301.9
100	2315.606	301.9
102	2454.626	301.9
104	2607.702	301.9
106	2766.529	301.9
108	2922.777	301.9
110	3071.019	301.9
112	3210.418	301.9
114	3345.338	301.8
116	3481.111	301.8
118	3616.974	301.8
120	3746.75	301.8

Table 5 (Continued)

Time, sec	Total Discharge, cfs	Stage, feet
122	3869.528	301.8
124	3995.885	301.8
126	4138.977	301.7
128	4301.425	301.7
130	4474.812	301.7
132	4650.235	301.7
134	4824.212	301.7
136	4993.595	301.6
138	5149.691	301.6
140	5282.091	301.6
142	5388.838	301.6
144	5481.111	301.5
146	5576.836	301.5
148	5688.853	301.5
150	5817.425	301.5
152	5952.904	301.5
154	6085.781	301.4
156	6213.664	301.4
158	6338.299	301.4
160	6459.741	301.4
162	6578.189	301.3
164	6699.549	301.3
166	6833.009	301.3
168	6981.971	301.2
170	7140.614	301.2
172	7299.106	301.2
174	7448.829	301.1
176	7583.698	301.1
178	7702.162	301.0
180	7810.455	301.0
182	7920.761	301.0

Table 5 (Continued)

Time, sec	Total Discharge, cfs	Stage, feet
184	8042.235	300.9
186	8172.766	300.9
188	8300.81	300.9
190	8415.98	300.8
192	8516.877	300.8
194	8609.297	300.8
196	8700.765	300.7
198	8798.362	300.7
200	8907.412	300.7
202	9027.736	300.6
204	9152.079	300.6
206	9271.135	300.5
208	9380.677	300.5
210	9483.647	300.4
212	9587.123	300.4
214	9698.262	300.3
216	9819.975	300.3
218	9946.927	300.2
220	10067.43	300.2
222	10173.34	300.1
224	10268.12	300.1
226	10363.39	300.0
228	10468.71	300.0
230	10586.12	299.9
232	10711.75	299.8
234	10839.02	299.8
236	10962.22	299.7
238	11081.01	299.6
240	11201.84	299.5
242	11332.38	299.5
244	11474.21	299.4

Table 5 (Continued)

Time, sec	Total Discharge, cfs	Stage, feet
246	11620.79	299.2
248	11761.22	299.1
250	11886.48	299.0
252	11995.48	298.9
254	12096.39	298.9
256	12200.73	298.8
258	12314.75	298.7
260	12435.14	298.5
262	12551.27	298.4
264	12652.69	298.3
266	12737.27	298.2
268	12813.71	298.1
270	12895.1	298.0
272	12988.88	297.8
274	13091.86	297.7
276	13193.51	297.5
278	13284.44	297.3
280	13364.05	297.1
282	13441.12	296.9
284	13526.26	296.6
286	13574.78	296.7
288	13632.16	296.7
290	13683.46	296.8
292	13732.38	296.8
294	13772.27	296.8
296	13812.49	296.9
298	13853.18	296.9
300	13899.55	296.9
302	13945.88	297.0
304	13989.75	297.0
306	14025.64	297.0

Table 5 (Continued)		
Time, sec	Total Discharge, cfs	Stage, feet
308	14055.5	297.1
310	14082.23	297.1
312	14111.71	297.1
314	14145	297.1
316	14180.51	297.2
318	14213.48	297.2
320	14241.36	297.2
322	14264.4	297.2
324	14286.33	297.2
326	14310.43	297.3
328	14337.68	297.3
330	14365.89	297.3
332	14391.85	297.3
334	14413.14	297.3
336	14430	297.3
338	14444.86	297.4
340	14460.54	297.4
342	14477.83	297.4
344	14495.02	297.4
346	14509.04	297.4
348	14517.63	297.4
350	14520.99	297.4
352	14521.76	297.4
354	14523.23	297.4
356	14527.21	297.4
358	14533.05	297.4
360	14538.52	297.4
362	14541.46	297.4
364	14541.32	297.4
366	14539.26	297.4
368	14536.92	297.4

Table 5 (Continued)

Time, sec	Total Discharge, cfs	Stage, feet
370	14535.05	297.4
372	14533.04	297.4
374	14529.35	297.4
376	14522.42	297.4
378	14511.74	297.4
380	14498.44	297.4
382	14484.82	297.4
384	14472.8	297.4
386	14462.43	297.4
388	14451.62	297.4
390	14437.45	297.4
392	14418.24	297.3
394	14394.77	297.3
396	14369.72	297.3
398	14345.91	297.3
400	14324.64	297.3
402	14305.2	297.3
404	14285.58	297.2
406	14264	297.2
408	14240.11	297.2
410	14214.9	297.2
412	14189.68	297.2
414	14165.08	297.1
416	14140.95	297.1
418	14116.74	297.1
420	14091.83	297.1
422	14065.87	297.1
424	14038.94	297.0
426	14011.44	297.0
428	13983.82	297.0
430	13956.25	297.0

Table 5 (Continued)

Time, sec	Total Discharge, cfs	Stage, feet
432	13928.63	297.0
434	13900.71	296.9
436	13872.25	296.9
438	13843.17	296.9
440	13813.61	296.9
442	13783.82	296.8
444	13754.05	296.8
446	13724.4	296.8
448	13694.83	296.8
450	13665.23	296.8
452	13635.49	296.7
454	13605.58	296.7
456	13575.58	296.7
458	13545.64	296.7
460	13507.37	296.7
462	13453.82	296.9
464	13399.35	297.0
466	13347.7	297.2
468	13295.73	297.3
470	13245.23	297.4
472	13194.74	297.5
474	13145.18	297.6
476	13095.86	297.7
478	13047	297.7
480	12998.27	297.8
482	12949.67	297.9
484	12901.23	298.0
486	12852.92	298.0
488	12804.95	298.1
490	12757.28	298.2
492	12710.05	298.2

Table 5 (Continued)

Time, sec	Total Discharge, cfs	Stage, feet
494	12663.04	298.3
496	12616.35	298.3
498	12569.89	298.4
500	12523.78	298.4
502	12477.93	298.5
504	12432.43	298.5
506	12387.24	298.6
508	12342.36	298.6
510	12297.71	298.7
512	12253.32	298.7
514	12209.18	298.8
516	12165.3	298.8
518	12121.66	298.8
520	12078.25	298.9
522	12034.92	298.9
524	11991.5	299.0
526	11947.81	299.0
528	11903.82	299.0
530	11859.57	299.1
532	11815	299.1
534	11770.58	299.1
536	11725.81	299.2
538	11680.76	299.2
540	11635.4	299.2
542	11589.76	299.3
544	11543.84	299.3
546	11497.67	299.3
548	11451.29	299.4
550	11404.69	299.4
552	11357.83	299.4
554	11310.7	299.5

Table 5 (Continued)

Time, sec	Total Discharge, cfs	Stage, feet
556	11263.26	299.5
558	11215.51	299.5
560	11167.52	299.6
562	11119.35	299.6
564	11071.13	299.6
566	11022.94	299.7
568	10974.8	299.7
570	10926.61	299.7
572	10878.04	299.7
574	10828.43	299.8
576	10776.7	299.8
578	10721.43	299.8
580	10661.37	299.9
582	10596.16	299.9
584	10526.88	299.9
586	10455.95	300.0
588	10385.92	300.0
590	10318.24	300.0
592	10252.89	300.1
594	10189.38	300.1
596	10127.42	300.1
598	10066.57	300.2
600	10005.45	300.2
602	9942.322	300.2
604	9876.649	300.3
606	9809.745	300.3
608	9743.626	300.3
610	9679.602	300.3
612	9618.054	300.4
614	9558.984	300.4
616	9502.284	300.4

Table 5 (Continued)

Time, sec	Total Discharge, cfs	Stage, feet
618	9447.693	300.4
620	9395.043	300.5
622	9344.754	300.5
624	9298.025	300.5
626	9256.454	300.5
628	9221.392	300.5
630	9193.364	300.5
632	9171.606	300.6
634	9153.787	300.6
636	9136.175	300.6
638	9114.469	300.6
640	9085.205	300.6
642	9047.146	300.6
644	9001.747	300.6
646	8952.182	300.6
648	8901.36	300.7
650	8850.372	300.7
652	8798.626	300.7
654	8745.571	300.7
656	8692.251	300.7
658	8640.994	300.8
660	8593.509	300.8
662	8549.421	300.8
664	8506.811	300.8
666	8464.031	300.8
668	8420.844	300.8
670	8378	300.8
672	8336.226	300.9
674	8295.784	300.9
676	8256.699	300.9
678	8219.002	300.9

Table 5 (Continued)

Time, sec	Total Discharge, cfs	Stage, feet
680	8182.757	300.9
682	8148.036	300.9
684	8114.898	300.9
686	8083.296	300.9
688	8052.978	300.9
690	8023.587	301.0
692	7994.875	301.0
694	7966.838	301.0
696	7939.683	301.0
698	7913.702	301.0
700	7889.078	301.0
702	7865.723	301.0
704	7843.246	301.0
706	7821.059	301.0
708	7798.497	301.0
710	7774.956	301.0
712	7750.078	301.0
714	7723.868	301.0
716	7696.607	301.0
718	7668.621	301.1
720	7640.086	301.1
722	7610.943	301.1
724	7580.872	301.1
726	7549.406	301.1
728	7516.148	301.1
730	7480.93	301.1
732	7443.804	301.1
734	7404.945	301.1
736	7364.59	301.1
738	7323.013	301.1
740	7280.559	301.2

Table 5 (Continued)

Time, sec	Total Discharge, cfs	Stage, feet
742	7237.734	301.2
744	7195.253	301.2
746	7153.982	301.2
748	7114.795	301.2
750	7078.41	301.2
752	7045.24	301.2
754	7015.306	301.2
756	6988.235	301.2
758	6963.317	301.2
760	6939.618	301.2
762	6916.122	301.2
764	6891.889	301.3
766	6866.178	301.3
768	6838.51	301.3
770	6808.67	301.3
772	6776.67	301.3
774	6742.694	301.3
776	6707.037	301.3
778	6670.039	301.3
780	6632.007	301.3
782	6593.149	301.3
784	6553.534	301.3
786	6513.102	301.3
788	6471.738	301.4
790	6429.371	301.4
792	6386.044	301.4
794	6341.932	301.4
796	6297.275	301.4
798	6252.322	301.4
800	6207.28	301.4
802	6162.321	301.4

Table 5 (Continued)		
Time, sec	Total Disharge, cfs	Stage, feet
804	6117.593	301.4
806	6073.208	301.4
808	6029.223	301.4
810	5985.633	301.5
812	5942.399	301.5
814	5899.497	301.5
816	5856.945	301.5
818	5814.802	301.5
820	5773.129	301.5
822	5731.948	301.5
824	5691.233	301.5
826	5650.921	301.5
828	5610.942	301.5
830	5571.244	301.5
832	5531.801	301.5
834	5492.605	301.5
836	5453.64	301.6
838	5414.848	301.6
840	5376.108	301.6
842	5337.231	301.6
844	5297.965	301.6
846	5258.023	301.6
848	5217.116	301.6
850	5174.98	301.6
852	5131.416	301.6
854	5086.313	301.6
856	5039.68	301.6
858	4991.668	301.6
860	4942.571	301.6
862	4892.813	301.6
864	4842.904	301.7

Table 5 (Continued)

Time, sec	Total Discharge, cfs	Stage, feet
866	4793.388	301.7
868	4744.777	301.7
870	4697.494	301.7
872	4651.836	301.7
874	4607.95	301.7
876	4565.833	301.7
878	4525.341	301.7
880	4486.229	301.7
882	4448.187	301.7
884	4410.889	301.7
886	4374.042	301.7
888	4337.41	301.7
890	4300.829	301.7
892	4264.196	301.7
894	4227.446	301.7
896	4190.525	301.7
898	4153.37	301.7
900	4115.896	301.8
902	4078.006	301.8
904	4039.6	301.8
906	4000.603	301.8
908	3960.983	301.8
910	3920.768	301.8
912	3880.039	301.8
914	3838.926	301.8
916	3797.588	301.8
918	3756.186	301.8
920	3714.867	301.8
922	3673.748	301.8
924	3632.9	301.8
926	3592.361	301.8

Table 5 (Continued)

Time, sec	Total Discharge, cfs	Stage, feet
928	3552.13	301.8
930	3512.195	301.8
932	3472.537	301.8
934	3433.147	301.8
936	3394.033	301.8
938	3355.222	301.8
940	3316.757	301.8
942	3278.7	301.8
944	3241.126	301.8
946	3204.114	301.9
948	3167.733	301.9
950	3132.029	301.9
952	3096.999	301.9
954	3062.59	301.9
956	3028.682	301.9
958	2995.096	301.9
960	2961.597	301.9
962	2927.914	301.9
964	2893.762	301.9
966	2858.866	301.9
968	2822.993	301.9
970	2785.977	301.9
972	2747.738	301.9
974	2708.293	301.9
976	2667.754	301.9
978	2626.314	301.9
980	2584.221	301.9
982	2541.756	301.9
984	2499.197	301.9
986	2456.8	301.9
988	2414.775	301.9

Table 5 (Concluded)

Time, sec	Total Discharge, cfs	Stage, feet
990	2373.275	301.9
992	2332.394	301.9
994	2292.172	301.9
996	2252.607	301.9
998	2213.665	301.9
1000	2175.293	301.9
1002	2137.426	301.9
1004	2099.989	301.9
1006	2062.896	301.9
1008	2026.044	301.9
1010	1989.309	301.9
1012	1952.551	301.9
1014	1915.616	301.9
1016	1878.351	301.9
1018	1840.615	302.0
1020	1802.3	302.0
1022	1763.336	302.0
1024	1723.705	302.0
1026	1683.432	302.0
1028	1642.586	302.0
1030	1601.257	302.0
1032	1559.549	302.0
1034	1517.555	302.0
1036	1475.354	302.0
1038	1433	302.0
1040	1390.518	302.0
1042	1347.917	302.0
1044	1305.197	302.0
1046	1262.354	302.0
1048	1219.402	302.0
1050	1176.371	302.0

Table 6
Computed Hawser Forces, Headwater El 357, Tailwater El 304.2, Interlaced Lateral Discharge Alternative

Excavation Plan	Valve Opening Time, min	Water-Surface Differential, ft		Computed Longitudinal Hawser Force, tons	
		Sta 17+00 and 23+00	Sta 17+00 and 27+00	Sta 17+00 and 23+00	Sta 17+00 and 27+00
Minimum	1.5	-0.74	-1.19	21.3	34.2
	11.7	0.10	-0.16	2.9	4.6
Moderate	1.5	-0.59	-0.99	17.0	28.5
	11.7	0.09	-0.14	2.6	4.0

Table 7
Computed Hawser Forces, Landside Discharge Channel Alternative

Headwater El	Tailwater El	Valve Opening Time, min	Water-Surface Differential, ft		Computed Longitudinal Hawser Force, tons	
			Sta 17+00 and 23+00	Sta 15+00 and 27+00	Sta 17+00 and 23+00	Sta 15+00 and 27+00
359	302	1.5	0.70	1.32	20.1	37.9
359	314	1.5	0.37	0.88	10.6	25.3
359	302	6.0	-0.09	0.22	2.6	6.3

REPORT DOCUMENTATION PAGE

Form Approved
OMB No. 0704-0188

1. AGENCY USE ONLY *(Leave blank)*	2. REPORT DATE	3. REPORT TYPE AND DATES COVERED
	April 1998	Final report

4. TITLE AND SUBTITLE
Application of a Two-Dimensional Model of Hydrodynamics to the Lower Approach of the New Kentucky Lock, Tennessee River, Kentucky; Numerical Model Investigation

5. FUNDING NUMBERS

6. AUTHOR(S)
Richard L. Stockstill, John E. Hite, Jr.

7. PERFORMING ORGANIZATION NAME(S) AND ADDRESS(ES)
U.S. Army Engineer Waterways Experiment Station
3909 Halls Ferry Road
Vicksburg, MS 39180-6199

8. PERFORMING ORGANIZATION REPORT NUMBER
Technical Report CHL-98-9

9. SPONSORING/MONITORING AGENCY NAME(S) AND ADDRESS(ES)
U.S. Army Engineer District, Nashville
P.O. Box 1070
Nashville, TN 37202-1070

10. SPONSORING/MONITORING AGENCY REPORT NUMBER

11. SUPPLEMENTARY NOTES
Available from National Technical Information Service, 5285 Port Royal Road, Springfield, VA 22161.

12a. DISTRIBUTION/AVAILABILITY STATEMENT
Approved for public release; distribution is unlimited.

12b. DISTRIBUTION CODE

13. ABSTRACT ***(Maximum 200 words)***

Because the existing Kentucky Lock, located on the Tennessee River, is operating at capacity, an additional 1,200-ft-long by 110-ft-wide lock is projected to be necessary to satisfy future capacity requirements. The new lock features a through-the-sill intake that carries flow to a multiport filling and emptying system. Two alternatives for the lock discharge outlet system were proposed by the U.S. Army Engineer District, Nashville. One plan used an interlaced lateral system located in the lower lock approach. The other plan had a landside channel that discharged downstream of the lower approach guide wall.

The two-dimensional (2D), depth-averaged flow model, HIVEL2D, was used to simulate the unsteady velocities and water-surface elevations in the lower lock approach resulting from lock emptying operations. The HIVEL2D model was chosen for this study because it provides numerically stable solutions for advection-dominated flow containing large gradients in the flow variables. The HIVEL2D code was modified to allow specification of time-dependent inflow boundary conditions. Simulations of the flow conditions in the lower lock approach for the proposed 1,200-ft lock were performed to evaluate the interlaced lateral and landside channel discharge alternatives. Adverse flow conditions (large streamwise and

(Continued)

14. SUBJECT TERMS
Finite element
Kentucky Lock
Locks (Waterways)
Numerical models
Tennessee River
Two-dimensional
Unsteady flow

15. NUMBER OF PAGES
144

16. PRICE CODE

17. SECURITY CLASSIFICATION OF REPORT	18. SECURITY CLASSIFICATION OF THIS PAGE	19. SECURITY CLASSIFICATION OF ABSTRACT	20. LIMITATION OF ABSTRACT
UNCLASSIFIED	UNCLASSIFIED		

13. (Concluded).

cross-stream water-surface gradients) in the lower approach may prohibit tows from mooring in this area during lock discharges.

The landside and interlaced lateral discharge alternatives were evaluated by comparing water-surface differentials at selected locations. The hawser forces a tow and barge arrangement will experience are directly related to the water-surface slope on which the vessel rests. These locations were in the vicinity of the bow and stern of various moored barge arrangements.

The simulation results with the interlaced lateral discharge system indicate with the minimum excavation plan and the fast (1.5 min) valve, large longitudinal water-surface slopes exist in the lower approach. A 3×3 barge arrangement would experience hawser forces greater than 20 tons, and a 3×5 barge arrangement would experience hawser forces grater than 34 tons. The water-surface slopes resulting from the 11.7-min valve and minimum excavation were greatly reduced from those observed with the fast valve. A 3×3 and a 3×5 barge arrangement would probably experience hawser forces less than 5 tons with the 11.7-min emptying valve.

Evaluation of the interlaced lateral design with the moderate excavation plan showed that the water-surface slopes computed for the 1.5- and 11.7-min valve were slightly less than those computed with the minimum excavation plan as one would expect given the same boundary conditions. The surge produced by the lock discharge is essentially independent of the bed elevation, although the greater depths resulting form the moderate excavation would coincide with slower velocities.

The results from the simulations with the landside discharge channel alternative support the results obtained with the interlaced lateral discharge alternative. A slower emptying valve reduces the water-surface slopes in the lower lock approach for the same headwater and tailwater combination. A higher tailwater elevation helps reduce the hawser forces, but the slower valve is where the most reduction in hawser force can be achieved. Discharging a lock immediately downstream from the lower miter gates with an interlaced lateral is generally less expensive, but requires extreme caution when operating the emptying valves. Slower valve operations and lock emptying times will be required for this type discharge system versus one that discharges away from the lower approach.